DEVELOPMENT OF ACETYLCHOLINE-BINDING PROTEIN (ACHBP) AS A BIOSENSOR FOR SEROTONIN LIGANDS

BY

Yeganeh Ataian

A Dissertation Submitted in Partial Fulfillment of the Requirements

for the Degree of

Doctor of Philosophy

in

Biochemistry and Molecular Biology

University of Alaska Fairbanks

May 2018

APPROVED:

Dr. Marvin Schulte, Committee Co-Chair
Dr. Lawrence Duffy, Committee Co-Chair
Dr. Thomas Kuhn, Committee Member
Dr. Abel Bult-Ito, Committee Member
Dr. Thomas Green, Chair
Department of Chemistry and Biochemistry
Dr. Anupma Prakash, Interim Dean
College of Natural Science and Mathematics
Dr. Michael Castellini, *Dean of the Graduate School*

Abstract

Acetylcholine-binding protein (AChBP) is a water-soluble novel protein with a high sequence similarity (15-30% identity) to ligand-gated ion channel (LGIC) receptors. The crystal structure of AChBP is used to study the extracellular domain of the pentameric LGICs such as nicotinic acetylcholine receptors (nAChRs) and 5-hydroxytryptamine type 3 receptors (5-HT_3Rs); and homology models have been developed to study receptor-ligand interactions. The 5-HT_3 serotonin receptors are potential therapeutic targets for multiple nervous system disorders such as alcohol and drug dependence, anxiety, depression, schizophrenia, sleep, cognition, memory, and chemotherapy-induced and post-operative nausea and vomiting. Therefore, the ligands that target the 5-HT_3Rs are considered powerful therapeutic agents. As such, 5-HT_3 serotonin receptors have been the targets of drug discovery efforts. The main objective of the current protein engineering project was to develop a soluble serotonin-binding protein using AChBP, which would mimic the specificity of the native 5-HT_3 serotonin receptor. Once developed, this soluble protein would be used as a model to design an array of receptors, which could be placed on biosensors for high-throughput drug screening (HTDS).

The results of site-directed mutagenesis of AChBP demonstrated that mutation of certain AChBP residues to its equivalent in serotonin resulted in an increased affinity of AChBP for serotonin ligands, and that each individual mutation increased the affinity of AChBP to a certain degree. It indicates that this approach is going in the right direction but multiple mutations will probably be needed to get to an AChBP whose affinity is equivalent to wild-type serotonin. In addition, the most significant changes appeared to be in the C-loop as it produced the largest increase in affinity of AChBP for serotonin agonists. The results also support the proposed C-loop closure model for the receptor, and based on data presented here, a new alignment of the C-loop is suggested.

Table of Contents

Page

Title Page i

Abstract iii

Table of Contents v

List of Figures ix

List of Tables xi

Acknowledgements xiii

Chapter 1: Introduction 1

1.1 Ligand-gated Ion Channels (LGICs) 1
1.2 Health and Diseases Related to Cys-loop LGICs 4
1.3 The Drug Discovery and Development Process 5
1.4 Basic Steps and Different Methods of Drug Discovery 7
1.4.1 Traditional Approaches to HTDS 9
1.4.2 Modern Approaches to HTDS: Biosensors 10
1.5 Development of Sensor Proteins for Small Molecules 14
1.5.1 Periplasmic Proteins 14
1.5.2 Intact Receptors in a Synthetic Membrane 15
1.5.3 Human Proteins without Transmembrane Components 15
1.6 Approaches of Developing Soluble Binding Domains 17
1.7 Hypothesis and Specific Aim 19

Chapter 2: Materials and Methods 21

2.1 Construction of the AChBP 21
2.2 Amplification of the AChBP 21
2.3 Stable Expression of the AChBP 22
2.4 Purification of the AChBP 23

2.5 Analysis of the AChBP 24
2.6 Storage of the AChBP 25
2.7 Pharmacological Characterization of the AChBP 26
2.8 Data Analysis for the AChBP 27
2.9 Mutation of the AChBP 28

Chapter 3: Expression and Validation of the AChBP as a Viable Biosensor Protein 31

3.1 Acetylcholine-binding Protein (AChBP) 31
3.2 Engineering of the AChBP 33
3.3 Production and Purification of the AChBP 35
3.4 Yield Increase of the AChBP 36
3.5 Storage of the AChBP 37
3.6 Biosensor Platform for the AChBP 38
3.6.1 The SPA Bead Concentration 39
3.6.2 Counting by the Scintillation Counter 42
3.6.3 The SPA Bovine Serum Albumin (BSA) Concentration 42
3.6.4 The SPA Protein Concentration 43
3.7 Functionality of the AChBP 44
3.7.1 The AChBP Binding Assay 46
3.7.2 The AChBP Competition Assays 47
3.8 Evaluation of the AChBP as a Sensor Protein Using a Microcantilever Biosensor Platform 51
3.9 Conclusion 52

Chapter 4: Mutation of the AChBP 55

4.1 Introduction 55
4.2 Experimental Approach 58
4.2.1 Chimeric Approach: α7-Binding Protein Studies 58
4.2.2 Site-directed Mutagenesis Approach 61
4.3 Selection of the AChBP Amino Acid Mutation 63
4.4 Methods 70

4.5 Functionality of the AChBP Mutants 71
4.5.1 The AChBP Mutant Binding Assay 71
4.5.2 The AChBP Mutant Competition Assay 72
4.6 Results 72
4.6.1 Mutants that Did Not Interact with Granisetron 73
4.6.2 Mutants that Interacted with Granisetron and Different Ligands 77
4.7 Summary 88

Chapter 5: Discussion 91

5.1 Introduction 91
5.2 The AChBP Mutant Data 92
5.3 New Mutant Constructs 94
5.4 Future Directions 95
5.4.1 Mutations 95
5.4.2 Optimizing Results 96
5.4.3 Acetylcholine-binding Protein from Other Species 97
5.4.4 Development of other LGIC Binding Proteins 98
5.4.5 Biosensor Platforms 99
5.4.6 Protein Expression 100
5.4.7 Protein Expression Systems 102
5.5 General Summary and Closing Remarks 103

References 105

List of Figures

Page

Figure 1.1: Ligand-gated Ion Channel, Nicotinic Acetylcholine Receptor Structure ... 2

Figure 1.2: Schematic of Cys-loop LGIC ... 3

Figure 1.3: The Drug Development Process and Timeline ... 6

Figure 1.4: Schematic of Surface Plasmon Resonance ... 11

Figure 1.5: Schematic of the Microcantilever Mechanism ... 12

Figure 1.6: Schematic of the Scintillation Proximity Assay ... 13

Figure 3.1: X-Ray Structure of Acetylcholine-binding Protein (AChBP) in Complex with Nicotine and Carbamycholine ... 32

Figure 3.2: p3XFLAG-CMV-9 Expression Vector ... 34

Figure 3.3: DNA Sequence ... 35

Figure 3.4: Polyacrylamide Gel Electrophoresis of the AChBP ... 37

Figure 3.5: The SPA Bead Concentration ... 41

Figure 3.6: Measurement of Radioactivity Level Using the Scintillation Counter ... 43

Figure 3.7: Bovine Serum Albumin (BSA) Titration Test ... 44

Figure 3.8: The SPA Protein Titration Test ... 45

Figure 3.9: Kd for the AChBP ... 48

Figure 3.10A: dTC Inhibition Assay ... 49

Figure 3.10B: Ach Inhibition Assay ... 49

Figure 3.10C: 5HT Inhibition Assay ... 50

Figure3.10D: mCPBG Inhibition Assay ... 51

Figure 3.10E: 2-Me-5HT Inhibition Assay ... 51

Figure 4.1: Sequence Alignment of Binding Loops in the AChBP and 5-HT_3 Receptors ... 57

Figure 4.2: Polyacrylamide Gels of α7-Binding Protein ... 60

Figure 4.3: Results of Binding Assays for Different Mutants ... 78

List of Tables

Page

Table 4.1: Mutants 65

Table 4.2: Mutant Data 74

Table 4.3: Alternative Sequence Alignment of the C-loop for the AChBP and 5-HT_3 Receptors 83

Acknowledgements

I would like to express the deepest appreciation to my mentor and committee chair, Dr. Marvin Schulte, who has the attitude, knowledge and substance of a genius. He continually and convincingly conveyed a spirit of adventure, enthusiasm and excitement in regard to scientific research and scholarship. Without his guidance, patience, support, positive attitude and persistent help, this Dissertation would not have been possible.

I am grateful to my committee members, Dr. Thomas Kuhn, Dr. Abel Bult-Ito, and Dr. Lawrence Duffy, as well as my honorary committee member Ms. Mary van Muelken, for their time, personal and professional guidance, encouragement and advice throughout my time at the University of Alaska Fairbanks. I have been very fortunate to have committee members who cared so much about me as an individual, as well as my research and academic career.

Nobody has been more important to me in the pursuit of my goal than the members of my family. Completing this research and Dissertation would have been impossible were it not for the loving support of my late husband, Robert, and our wonderful children, Milaud and Didar. After Robert's sudden and unexpected passing, it was our children who stood by me and carried me until I was able to find my footing and stand on my own again. They gave me hope and provided me with unending inspiration and courage for which I owe them a debt of gratitude.

This Dissertation is a milestone in my academic career due to my personal circumstances, and I have been extremely lucky to have so many people who cared, supported and guided me throughout my journey. Thank you to all of you for making this an unforgettable experience for me.

Chapter 1: Introduction

1.1 Ligand-gated Ion Channels (LGICs)

Living cells are surrounded by membranes which are involved in the interaction of the cell with its environment. Ion channels are located within the membrane of most cells and many intracellular organelles. They are often described as narrow tunnels that allow only ions of certain size and/or charge to pass through and be transported across the membrane; a characteristic called 'selective permeability.' However, some channels are permeable to passage of ions that share a common charge, such as positive (cation) or negative (anion). In many ion channels, passage through the ion pore is controlled by a 'gate' which may be opened or closed in response to chemical or electrical signals, temperature, etc. (1).

Ion channels are broadly divided into voltage-gated and ligand-gated ion channels. Ligand-gated ion channels (LGICs) or ionotropic receptors are transmembrane ion channel proteins which open in response to binding of a ligand, such as a neurotransmitter, to allow passage of ions such as Na^+, Ca^{2+}, K^+, and Cl^- through the membrane; thus mediating cell-cell communication and cellular excitability. LGICs are the fundamental signaling molecules in neurons, and are consist of three domains: the extracellular amino-terminal domain containing the ligand-binding site, the hydrophobic transmembrane-domain containing the ion channel, and the intracellular domain (Figure 1.1). LGICs are divided into three superfamilies based on their structure and function: ATP-gated channels, ionotropic glutamate receptors, and cysteine-loop (cys-loop) receptors (2).

The cys-loop receptors have a disulfide bond between two cysteine residues (13 amino acids apart) in the N-terminal extracellular domain. Mutation of these cysteines or elimination of disulfide bond produces a non-functional protein. Cys-loop receptors are composed of five protein subunits that form a pentameric arrangement around a central pore. Individual subunits have three domains: a) a large extracellular amino-terminal domain which is contains mostly β-sheets. This domain contains the N-and-C terminal residues, a small M2-M3 region, and a ligand-biding site. The binding sites are

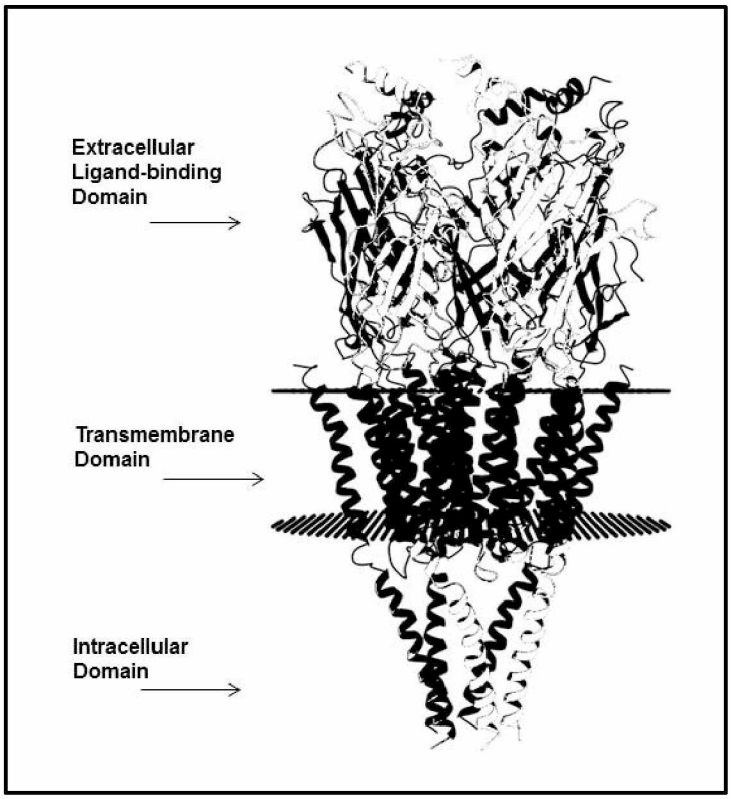

Figure 1.1: Ligand-gated Ion Channel, Nicotinic Acetylcholine Receptor Structure. Ribbon structure shows different domains of a ligand-gated ion channel. Protein Data Bank (PDB) file 2BG9.

composed of six loops of amino acids referred to as A-F, and each subunit contributes three loops on each of its two interfaces. The neurotransmitters bind at the interface between subunits in the extracellular, N-terminal, ligand binding domain; b) four transmembrane regions (M1-M4) of α-helices which form the ion channel (ion pore), and are involved in ion-selectivity. The pore is primarily formed by the M2 helices; and c) an intracellular domain of α-helices that contains a large M3-M4 region. The intracellular (or cytoplasmic) domain interacts with the interior of the cell, relaying the signal which can depolarize or hyperpolarize the cell (Figure 1.2).

In cys-loop receptors, the ion channels open in response to binding of a specific ligand molecule to the extracellular domain of the receptor protein (3,4). Ligand binding causes a conformational change in the structure of the channel protein that leads to the opening of the ion pore, and subsequent ion flux across membrane and into or out of

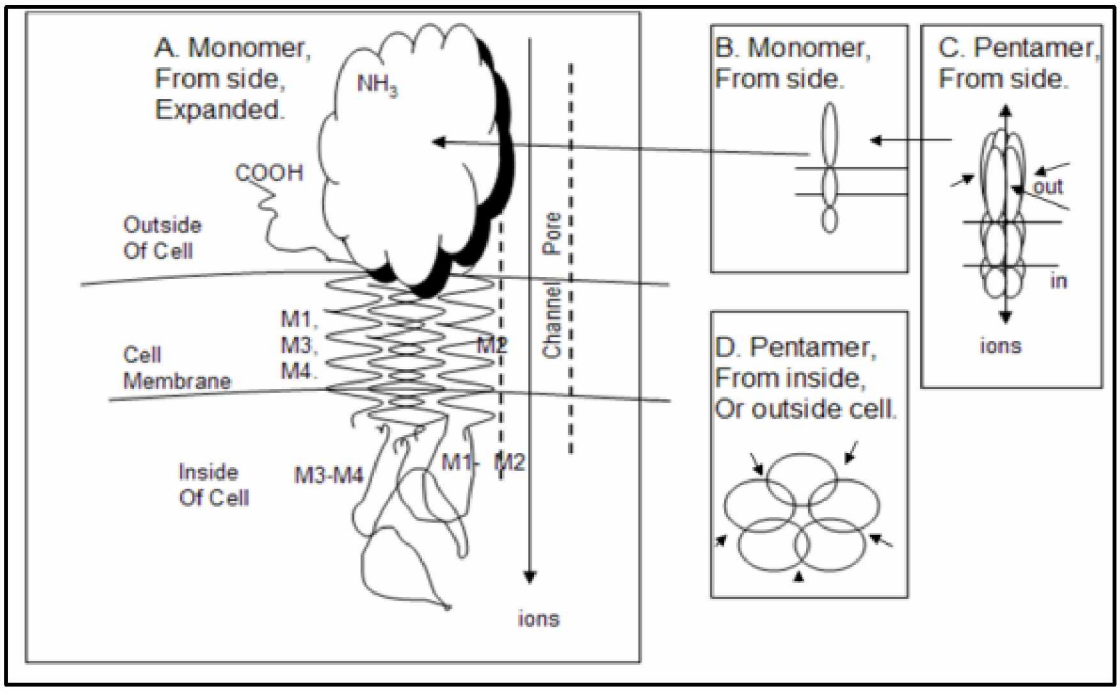

Figure 1.2: Schematic of Cys-loop LGIC. A: Side view of a single subunit. B,C, D: Side and top views of the pentamer. Arrows in C-and-D indicate potential ligand binding sites.

the cell. Ion flux is passive; thus Ions pass through channels down their electrochemical gradient without the input of metabolic energy (e.g. ATP or active transport mechanisms). The flow of charged ions represents an electrical current that changes the voltage across the membrane, which can be transmitted rapidly over long distances and trigger downstream effects (1). Channel activity is terminated when the channel closes or when it enters a desensitized (non-conducting) state (5).

Members of the cys-loop LGIC are divided into four different subfamily of receptors based on their endogenous agonist/ligand: nicotinic acetylcholine (nACh), glycine, γ-aminobutyric acid (GABA), and 5-hydroxytryptamine type 3 (5-HT_3) (1). These receptors can be further subdivided with respect to the type of ion they conduct: GABA and glycine are anion-selective channels that conduct Cl^- ions, thus producing neural inhibition, and are commonly referred to as inhibitory channels; whereas nACh and 5-HT_3 receptors are cation-selective channels that conduct Na^+, Ca^{2+} and K^+ ions, producing neural excitation and are referred to as excitatory channels (6).

The 5-HT_3 receptors differ in structure and mechanism from the other serotonin receptor subtypes (types 1, 2 and 4), which are all G-protein-coupled receptors (7-10). The 5-HT_3 receptors are expressed in the nervous system in regions involved in the cognition, anxiety, seizure (11), addiction, GI motility (12), emesis and nausea (13). The pharmacology of the 5-HT_3 receptors varies among species, and evidence for different subtypes within a single species was first noted in 1993 by Bonhaus et al. (14). Recent studies show that different 5-HT_3 receptor subtypes (3A, 3B) are transcribed and located in different areas of the nervous system (8). Information regarding receptor heterogeneity and its localization is very important to understand involvement of the 5-HT_3 receptor in normal physiology of the nervous system, as well as its role in different diseases (15). To determine subunit composition of individual receptors requires ligands that have the ability to discriminate between different subtypes of the 5-HT_3 receptor (16).

The 5-HT_3 receptors are most closely related by homology to the nACh receptor, and site-directed mutagenesis studies have focused on regions of the 5-HT_3 receptor amino terminal homologous to the nACh receptor binding loops A-F (17). Mutagenesis studies on the murine (mouse) 5-HT_3 receptor have identified a number of amino acid residues that are important for binding of agonists and competitive antagonists to the 5-HT_3 receptor (18,19), and key amino acids have been identified in loops-B (20), loop-C (18) and loop-E (21). The 5-HT_3 receptor is discussed in more detail in Chapter 4.

1.2 Health and Diseases Related to Cys-loop LGICs

Cys-loop receptors are involved in a wide range of physiological processes as they mediate both excitatory and inhibitory neurotransmission (22). These receptors are crucial to the function of the peripheral and central nervous systems, and have been implicated in learning and memory, fluid balance, appetite control, regulation of blood flow, and pain (22). The malfunction of cys-loop LGICs is linked to various diseases and disorders such as muscular dystrophies (23), central neurological disorders (e.g. autism and attention deficit hyperactivity) (24,25), neurodegenerative diseases (e.g. Alzheimer's, Parkinson's) (26-29), neuropsychiatric disorders (e.g. anxiety, epilepsy, schizophrenia, depression) (30,31), and nicotine, drug and alcohol addiction (32,33).

Clearly, cys-loop receptors cover a wide spectrum of functions, ranging from muscle contraction to cognitive functions, which in turn makes them important drug targets for the treatment of nervous system disorders and diseases. Therefore, drug discovery strategies require an in-depth understanding of the ligand binding sites, and structure-function relationships between the receptor and ligand/drug.

1.3 The Drug Discovery and Development Process

Developing a new drug from concept to therapeutic agent is a very complex process (34,35), which includes drug discovery and screening, pre-clinical trials using non-human subjects (work on animals such as rats), toxicity studies, clinical trials using human subjects, and approval by Food and Drug Administration (FDA). This process can take an average of 15 years and cost in excess of US$1 billion per new pharmaceutical drug (Figure 1.3) (34).

The first step of developing a pharmaceutical drug is drug discovery and screening (pharmacodynamics). The process of drug discovery begins by targeting a medical condition or disease that lacks a suitable therapeutic intervention. The initial research often occurs in academia, and generates data to develop a hypothesis that the activation or inhibition of a pathway or receptor protein will have therapeutic effect on the condition or disease. Once the target (e.g. pathway, gene or receptor protein) is identified, an intensive search to find or produce a drug begins (36,37). New drugs are typically identified in 'natural products' or produced using 'combinatorial chemistry' (38).

Natural products are organic compounds from marine and terrestrial organisms, including terrestrial plants, microorganisms, vertebrates and invertebrates, that may have played an important role in preventing and treating human diseases for thousands of years, or may be the result of extensive screening of natural materials (39,40). These natural products can serve as compounds of interest both in their natural state and/or through synthetic modifications (41,42). Combinatorial chemistry is the method of synthesizing many different substances at the same time (43). The result is production of thousands of new molecules / compounds, called 'libraries', which have to

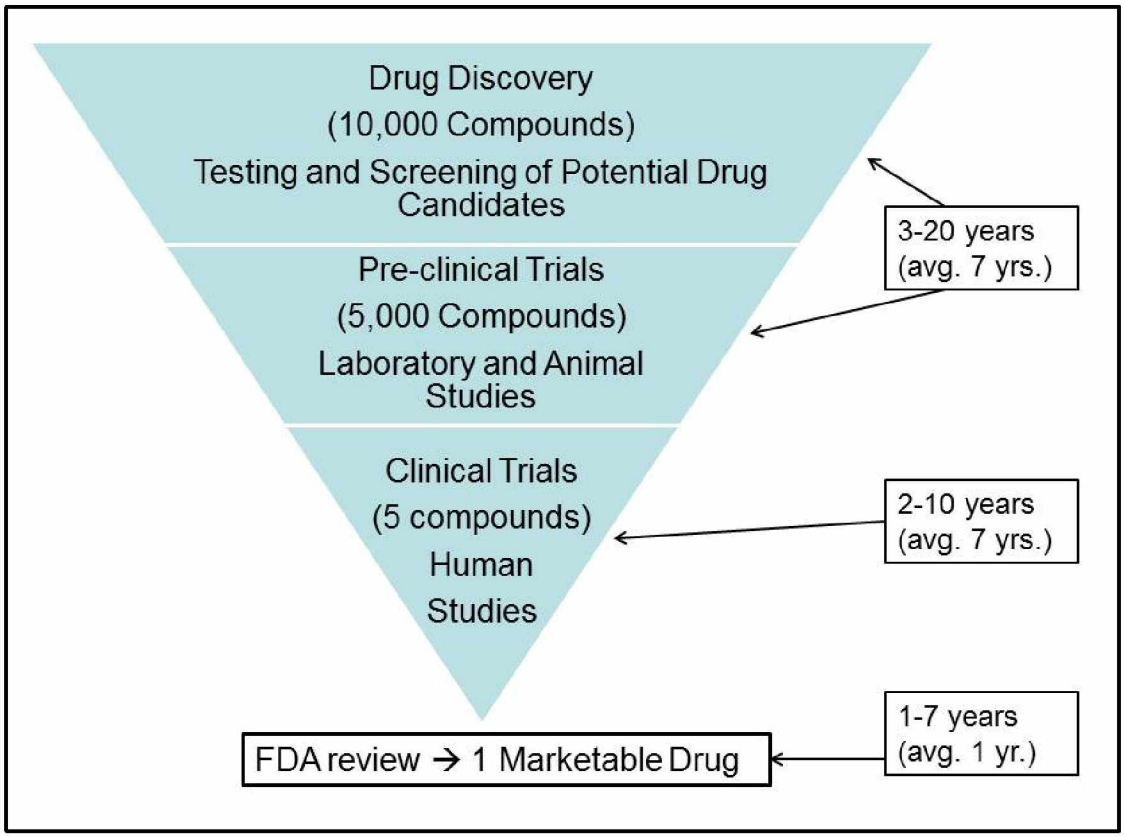

Figure 1.3: The Drug Development Process and Timeline. Drug discovery is the first stage of drug development process where thousands of potential drug candidates are tested and screened. In the second stage, preclinical trial, the 'lead compounds' are tested on animals and screened further. Clinical trial is the third stage where the drug is tested on humans. Information from all studies is received by FDA, and if satisfied, product license is issued and the drug is marketed. Information to develop the figure was obtained from: https://www.fda.gov/drugs/developmentapprovalprocess/

be screened and identified (44,45).

Potential drug candidates, whether discovered in academic or pharmaceutical / biotech research labs, are rigorously tested and screened for their interaction with the target and for off target interactions that may produce side effects or toxicity. Many drug candidates fail at this stage since they do not work, do not interact with the target, are not highly selective or are not safe. After careful review of the results (46,47), 'lead compounds' are chosen for early testing or 'pre-clinical' trials on animals.

Tufts Center for the Study of Drug Development (csdd.tufts.edu) has published numerous studies estimating the cost of developing new pharmaceutical drugs. In 2001, the cost was estimated at US$802 million; in 2010, the research and development

cost of each new drug was estimated about US$1.8 billion; in 2014, the estimated cost of developing a prescription drug that gains market approval was estimated at US$2.6 billion (48) ; and in 2016, the cost was found to have averaged US$2.9 billion per new pharmaceutical drug (49,50).

Drug discovery and screening is the area of research in the drug development process that takes the most amounts of time and money. The timeframe can range from 3-20 years, and costs can range between several million to tens of millions of dollars (51). The drug discovery process is often a difficult, lengthy, expensive, and inefficient process despite of many advances in technology. In addition, an incomplete knowledge of the specific receptor type and subtype involved in different diseases and disorders presents many challenges in developing therapeutic approaches since it requires receptor-selective or subtype-selective drugs.

The process of drug discovery starts with thousands of compounds as potential drug candidates; however, only a small number of compounds look promising and undergo further study after early testing (52). On average, only 5 in every 5,000 compounds that make it as the 'lead compound' to the 'pre-clinical trial' stage becomes an approved compound/drug to be tested on humans (Figure 1.3), and only 1 of those 5 drugs that progress to human 'clinical trials' is approved by the FDA as a marketable drug (53). Clearly, developing subtype-selective drugs is hindered by the high cost, as well as inability to rapidly evaluate candidate compounds on multiple receptor subtypes. Therefore, the length of time required for drug discovery and screening, as well as its associated expenses to develop a marketable drug, calls for new approaches and technologies -- approaches that enable the researchers to either discover or produce new drugs for many receptor subtypes quickly, efficiently and economically.

1.4 Basic Steps and Different Methods of Drug Discovery

Following the identification of potential drug candidates, vigorous testing and screening of these compounds are needed to study their interaction with the target and identify potential drug candidates. A drug discovery method which is widely used in both academic laboratories and in the pharmaceutical industry is called high-throughput drug screening (HTDS). HTDS uses automation (robots, liquid handling devices,

sensitive detectors, and data processing/control software) to quickly screen the entire libraries of chemicals against the target (54,55). It allows researchers to rapidly screen libraries containing millions of compounds, with molecular weight of <300 Da and identify the molecules that interact with the drug target to select lead compounds (56). This information provides a starting point for drug design and/or understanding the interaction and/or role of a particular biochemical process. Another important function of HTDS is to show how selective the compounds are for the chosen target since the ultimate goal is to find a molecule which will only interact with the chosen target, and no other related targets.

It should be noted that HTDS is an expensive method, and requires highly specialized and expensive instrumentations. Therefore, other approaches to drug discovery have been pursued to screen smaller libraries, namely fragment-based drug discovery (57,58) and protein-directed dynamic combinatorial chemistry (59,60). These methods use libraries that are composed of a few thousand compounds with molecular weight HTDS of around 200 Da. The ligands used in the process are small and bind to the target with a weak binding affinity in millimolar range (HTDS requires nanomolar binding affinity). The promising ligand-target complexes are then studied through X-ray crystallography (61,62) and suggested modification(s) are generated and applied to produce lead compounds with a higher affinity for the target (63-65). When compared to HTDS, these methods have the advantage of efficient screening as well as generating a library that covers a large chemical space.

Another important drug discovery method is *de novo* drug design which utilizes computer software, and involves the design of molecules that are complementary in charge and shape to the binding site of target with which they interact and bind to. There can be different approaches to this method, for example, 'virtual high throughput screening' (45,47,66), where screening of potential drugs are accomplished using computer-generated models of the target and docking of virtual libraries to a drug target. Another approach, namely 'computer-aided drug design' (67,68), uses virtual screening of libraries of small molecules to identify compounds whose structure are most likely to bind and interact with a target. Once the lead compounds are identified, molecular modeling (69) and molecular dynamics stimulations (70,71) are used to improve the

potency, selectivity and physiochemical properties of the potential lead molecules or drugs.

1.4.1 Traditional Approaches to HTDS

Scientists in academic labs and small biotechnology companies have traditionally used high-throughput screening method of drug discovery in receptor-binding assays and functional assays. These are cell-based assays that investigate the effect of a given treatment (e.g. drug) on living cells. Receptor-binding assays (RBAs) are typically used to study membrane proteins/receptors (72). RBAs are competitive inhibition assays using a known radiolabeled drug (derived from chemical or natural product libraries), to examine the interaction of a drug/ligand with receptor/target. RBAs typically use filter-based separation methods to obtain data for bound versus free drug/ligand fractions and obtain quantitative binding parameters such as K_m and B_{max}, to determine minimal effective drug concentrations (73). RBAs are not only used for identification of lead compounds, but also for characterization of drug candidates (e.g. drug stability, mechanism of action, potency and purity). Although RBA has been developed for HTDS, it is an expensive method which requires living cells and radioactive materials (72-74).

A second approach to drug screening employs functional assays. Functional assays (e.g. automated oocytes and patch clamp), are electrophysiology methods that are used to study the functional activity of a target. These assays involve biological organisms and the data reflect the effect of receptor activation or its block rather than direct measures of receptor interaction as with RBAs. This causes the system intrinsically more complex in composition or behavior, or both, making the reading and interpretation of the assay(s) more difficult (75,76). Functional assays are expensive to perform, and are considered medium HTDS, since experiments are intrinsically slower to perform as they require live cells and membrane preparations. Functional assays do provide information not provided by receptor assays, but would ideally be performed once an appropriate HTDS assay has identified a smaller subset of the library as a viable option (76).

1.4.2 Modern Approaches to HTDS: Biosensors

In addition to traditional approaches to HTDS, there are more recent innovations in high-throughput methods and instruments that have become powerful analytical tools because they can measure the activity and binding of very diverse classes of drug targets. These are called 'sensor surfaces or biosensors'. Biosensors are analytical devices composed of an immobilized biological material (e.g. antibody, cells) which can specifically interact with an analyte (e.g. drug) to produce signals (e.g. electrical, physical, chemical, etc.) that can be measured. Examples of biosensors are: surface plasmon resonance (77), microcantilever (78), and scintillation proximity assay (79).

Surface plasmon resonance (SPR) is a rapid, non-radioactive, and chip-based technology developed by Biacore Inc. (www.biacore.com), which relies on plasmon resonance (77,80). Plasmon resonance refers to the excitation of surface plasmon by light. Surface plasmons are electromagnetic waves that propagate along a metal surface, and molecules binding to the surface interact with the waves, altering its properties. The SPR is composed of as sensor chip, a flow cell or channel, a light source, a prism, and a detector. The sensor chip is a gold-coated glass chip, which is sandwiched between a flow channel (containing buffer and ligand solution), and a glass prism. The chip is coated with coupling reagents that attach the desired protein or small molecules to the chip surface. As ligands in solution buffer flow through the channels, they bind to the molecules on the chip surface. Protein and ligand binding results in alteration of chip surface properties, which lead to changes in surface plasmon waves. The end result is a change in the angle of reflection of light. The SPR Biacore instrument monitors and measures this angle and its changes, which correspond to the ligand binding to the protein or small molecule on the gold surface of the chip. Therefore, SPR measures changes in molecular weight over time. For the Biacore SPR instruments, the detection limit for ligands binding to the chip is about 180 KD, thus in general, the lower molecular weight molecule is attached to the chip and the higher molecular weight molecule is placed in the flow channel with buffer (Figure 1.4).

Microcantilevers (MCs) are chip-based sensor devices that can detect changes in cantilever bending or vibrational frequency (78,81). In MC, the biosensor protein is

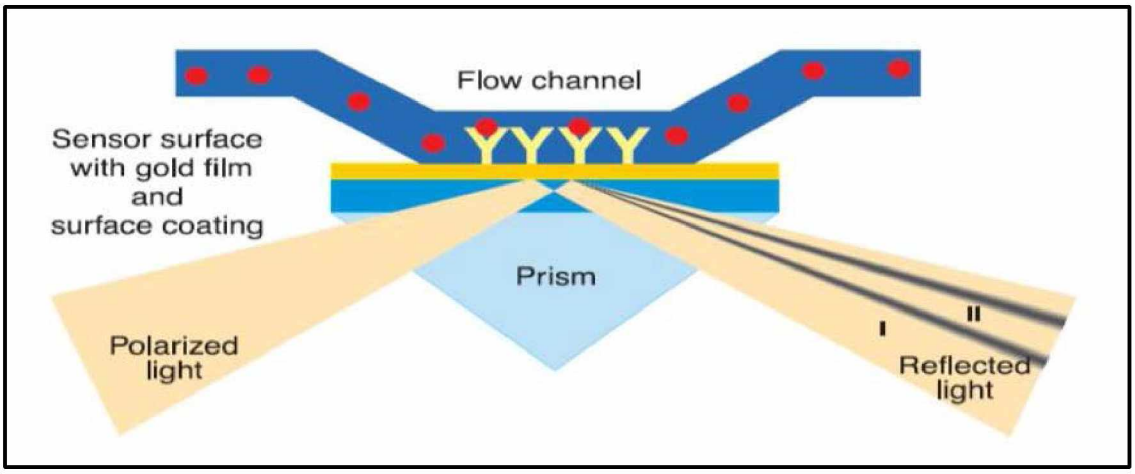

Figure 1.4: Schematic of Surface Plasmon Resonance. The properties of the gold surface changes as molecules bind to the chip surface, leading to changes in surface plasmon waves. This causes a change in the angle of reflection of light which is detected and measured in resonance units (RU). Picture adapted from Biacore TN1 handbook.

bound to a chip on one side of the cantilever, and the ligand is run over the chip. The biosensor protein and ligand can have different forms of molecular interaction such as electrostatic attraction, repulsion, conformational change, etc., which results in the cantilever surface expanding or contracting on the side containing the receptor in response to ligand binding. The expansion or contraction of only one side causes the cantilever to deflect and bend up or down. This deflection is detected as a change in position of the reflected light hitting the detector which can be measured using optical techniques or piezoelectric effects. The information from the detector is sent to a computer for analysis (Figure 1.5).

Scintillation proximity assay (SPA) is a bead-based technology used to study radioligand binding (79,82). SPA utilizes microscopic size SPA beads coated with a scintillant. Protein of interest is typically bound to the bead surface and then exposed to a radioligand. The scintillant emits light when it is stimulated by the interaction of radiolabeled molecules and their binding to the surface of the bead. The SPA technique relies on the process of radioactive decay during which the radioligand releases a beta particle. The beta particle, when close to the beads, causes the scintillant coating of the bead to emit photon/light. This signal is detected by scintillation counter and analyzed

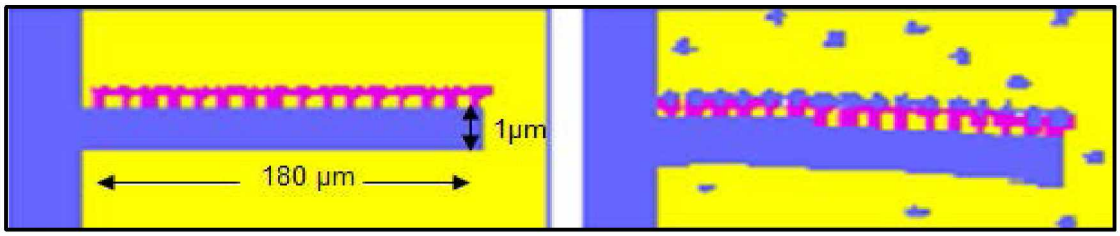

Figure 1.5: Schematic of the Microcantilever Mechanism. At left, the protein is bound to one side of the microcantilever. At right, the ligand binds to the protein and causes the surface to expand (as shown) or contract on one side only, resulting in bending which is detected optically or piezoelectrically. Information obtained from our collaborator, Dr. Hai-Feng (81).

using GraphPad Prism software. Incorporation of scintillant into the bead eliminates the filtration step since only radioligand bound at close proximity to the bead can excite the scintillant, and trigger the bead to emit light (Figure 1.6).

The biosensors mentioned above, namely, surface plasmon resonance (SPR), microcantilever (MC), and scintillation proximity assay (SPA) clearly have many advantages and at the same time their own limitations. SPR is a label-free binding assay that can detect binding of non-labeled compounds, as well as non-competitive ligands, which makes it a good candidate for screening libraries of non-labelled compounds and natural products. In addition, SPR can provide association and dissociation constants (on-and-off rates). However, this method is not designed to study low molecular weight compounds since it relies on molecular weight detection; therefore, to investigate any compound below 120 KD requires another type of biosensor (80).

MC is a label-free detection method which is low-cost, and is capable of rapid screening of multiple receptors and mass production. MC has a high sensitivity level and can differentiate between agonist versus antagonist binding (81). This biosensor is relatively new and requires further study, adjustment and tuning.

SPA is a high-throughput binding assay that requires a small quantity of protein and is able to evaluate binding of competitive ligands. This is a low-cost assay without any molecular weight limitations for compounds which is ideal for working with and detecting small molecules. SPA differs from the traditional receptor-binding assay as it

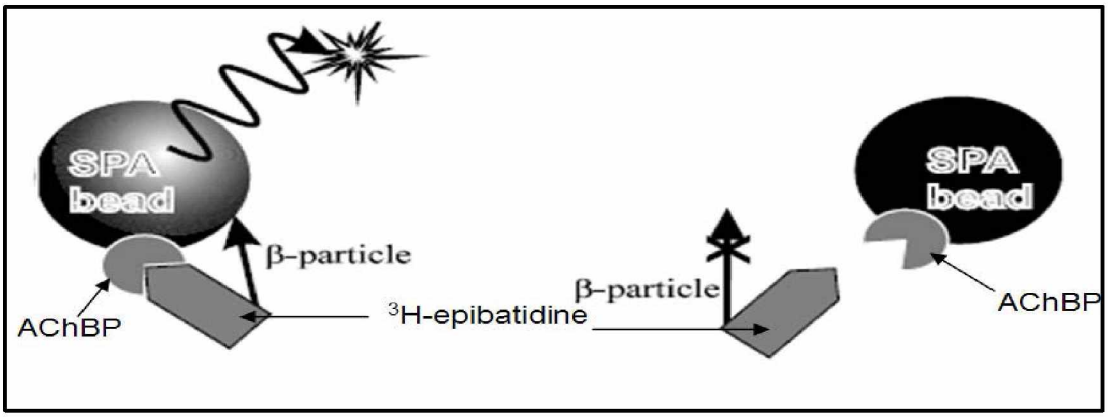

Figure 1.6: Schematic of the Scintillation Proximity Assay. At left, the radioligand emits B-particles and when it is bound and in close proximity to the bead, it causes the scintillant coating of the bead to emit a photon, which is detected by the counter. At right, unbound radioligand is not close to the bead and does not excite the scintillant. Picture adapted from SPA handbook (GE/Amersham Biosciences).

does not require a separation of free and bound radioligand (79). Therefore, it represents a convenient method to assay a wide range of molecular interactions in a homogenous system. In addition, elimination of the filtration step permits automation and high-throughput assay development. SPA has the disadvantage of requiring the use of radioligand for direct determination of K_d although it can be used to determine an indirect inhibition constant (K_i) for non-labeled compounds when used with a selective radioligand. SPA cannot be used to detect binding of non-competitive ligands. SPA technology does provide a rapid and sensitive method which is routinely used for drug screening where ligand-binding affinity and high-throughput is required.

The ultimate goal of any biosensor technology is to develop a platform which is able to detect and identify different molecules with high sensitivity and accuracy at a reasonable price. And the ideal system for the drug discovery is one in which the biosensor can use <1 mg of drug and identify every receptor that it binds. Therefore, in order to perform high-throughput drug screening, a 'specific sensor protein' is needed which can rapidly and reversibly detect binding of potential lead compounds. The current problem with all the biosensors is the lack of this appropriate 'specific sensor protein.' Biosensor applications typically require pure protein capable of being immobilized intact on a sensor bead or surface. This is a particularly large problem with the ubiquitous membrane-bound proteins as they are challenging to purify, and when

purified in lipid or detergent, they are difficult to immobilize or may be inactive (1). Ideally, a receptor would be solubilized, purified and covalently attached to a sensor surface, then used over and over again to screen large numbers of compounds.

1.5 Development of Sensor Proteins for Small Molecules

Studying the mechanism by which proteins fold into their correct three-dimensional structure, as well as their interaction with other proteins or small molecules has been the focus of intense research as it is the segue to developing particular or specific sensor proteins. Here, we will focus on three approaches that address development of sensor proteins for small molecules, namely: periplasmic proteins, intact receptors in synthetic membranes, and human proteins without transmembrane components.

1.5.1 Periplasmic Proteins

Periplasmic proteins are present in the periplasm of bacteria. The periplasm is a gel-like fluid in the space between outer membrane and inner, or cytoplasmic, membrane in both gram-positive and gram-negative bacteria (83,84). The periplasm contains a number of proteins (e.g. proteases, nucleases, phosphatases, etc.) that carry out different functions. For example, some periplasmic proteins are involved in folding, electron transport, substrate hydrolysis, and degradation of large molecules (e.g. large proteins, nucleic acid, etc.) into smaller and transportable sizes (85) .

Other type of periplasmic proteins, called periplasmic-binding proteins (PBPs), are secreted by bacteria, and are involved in nutrient binding and transport (86). PBPs bind to different molecules (e.g. sugars, ions, amino acids, etc.) in the environment, and transport them into the periplasm. Once in the periplasm, PBPs bind to cytoplasmic membrane-bound proteins and release their bound molecule. The nutrient molecule is then transported into the cytoplasm, and PBP is secreted back into the bacterial surroundings (87). Clearly, a number of proteins of interest in biotechnology are present in the bacterial periplasm, such as PBP. The PBP has been recognized as a biosensor molecule/protein due to its small size, and its ability to recognize and transport different molecules into the periplasm by coupling with them (88).

Advantages of this approach are: a) proteins are widely available, and b) proteins have broad ligand specificity. In addition, some modeling has been done that shows proteins can be mutated for different ligand selectivity (89). The main disadvantage of this approach is use of bacterial protein. Based on current receptor modeling, it is assumed that the bacterial proteins can be mutated for specific ligand selectivity or respond to certain drugs; however, they may not respond to unknown drugs the same as a human receptor since the modeling is based on bacterial proteins.

1.5.2 Intact Receptors in a Synthetic Membrane

Another technology for drug discovery is use of intact receptors in a synthetic membrane. In this method, artificial or synthetic membranes are used to model the properties of native membrane, and provide an isolation or separation environment (90,91). The intact receptor is prepared by using a detergent purification system, and it is then inserted into the artificial membrane bilayer. The main advantage of this method is the ability to use human proteins, thus the response to certain drugs should be similar to human receptors. However, this technology has many disadvantages in regard to protein production, insertion and stability. For instance, it is very difficult to prepare intact receptor proteins as proteins are known to lose their structure and/or activity when purified with detergent (1). In addition, attempting to insert a receptor protein into the synthetic membrane, without losing protein activity and stability, introduces its own challenges. Furthermore, producing a synthetic lipid membrane system with all its components and characteristics is a daunting task that has not yet been achieved since membranes adapt their composition in response to environmental cues, and cells use lipid remodeling to carry out specific tasks (e.g. signaling, division) or respond to their environment and maintain membrane homeostasis (1).

1.5.3 Human Proteins without Transmembrane Components

A new approach to address development of sensor proteins for small molecules is use of human proteins without transmembrane (TM) components (92). Cell membranes are composed of lipid bilayers which provide the structure of the membrane. A number of proteins are inserted into this hydrophobic environment that

allow for many of the interactions that occur within and between cells, such as cell signaling, division, movement of specific molecules into and out of the membrane, etc. (92).

The two main categories of membrane proteins are integral proteins and peripheral proteins. Peripheral proteins are temporarily attached to integral proteins or to the lipid bilayer by hydrophobic, electrostatic, and other non-covalent interactions. This type of interaction can be disrupted by the change in pH. On the other hand, integral membrane proteins are permanently bound to the membrane. They are classified as integral monotopic proteins if they are attached to only one side of the membrane, and transmembrane proteins if they span across the entire lipid bilayer or membrane (1). The transmembrane proteins are composed of one or more segments that are permanently embedded within the lipid bilayer, and their amino acid residues contain hydrophobic side chains that interact with the hydrophobic interior of phospholipid bilayer. These stretches of approximately 25 hydrophobic residues that pass across the membrane are known as transmembrane domains (TMDs). TMDs are not only involved in anchoring the integral proteins to the membrane, but also in forming ion channels, enzymatic sites, or transporters (6,22).

Transmembrane proteins account for the majority of membrane proteins, and they can only be dissociated from the membrane using detergent, non-polar solvents, and denaturing agents (1). Therefore, removing transmembrane proteins from their native surrounding, as well as removing the transmembrane domains may lead to destabilization of the protein, which is the main disadvantage and challenge of developing human protein analogs using removal of the transmembrane component approach (1). However, there are many advantages to this method; for example, most ligands bind to the extracellular domain of a protein, and the majority of proteins have a large extracellular domain (e.g. LGIC). Therefore, there is an excellent possibility that this approach would work. In addition, these proteins can be produced, purified and characterized easily, and due to their stability, they can also be stored, shipped, and manufactured. Furthermore, this approach uses the binding domain of a human protein which means its response to unknown drugs would be the same as a human receptor (92).

1.6 Approaches of Developing Soluble Binding Domains

Drug screening approaches, particularly chip-based systems used in HTDS, are greatly facilitated by the use of soluble proteins. Unfortunately, this is often not a viable option for receptor proteins such as ligand-gated ion channel (LGIC) receptors that are principal targets for a large class of therapeutic drugs. A solution to this problem would be to engineer the desired protein(s) using a soluble homolog of the receptor as a lead molecule. For LGICs, nature has provided an ideal candidate in the acetylcholine-binding protein (AChBP) (93,94).

The AChBP is a water-soluble protein secreted by glial cells in the central nervous system of the fresh water snail, *Lymnaea stagnalis*, where it specifically binds to acetylcholine (ACh) and inactivates it at the synapse (95,96). Other AChBP proteins have been discovered in other snail species as well (97,98). The AChBPs are structurally homologous to the amino terminal domain of LGIC receptors with a relatively high sequence identity (15-30%) in the extracellular ligand-binding domain (20,99). Like the nACh receptor, the AChBP has a tertiary structure consisting of five identical subunits (210 amino acids each), and assembles in a homo-pentameric form (93,99). Unlike the nACh receptor and other LGICs, the AChBPs lack the transmembrane domain, making them soluble homologs rather than integral membrane proteins. Since they are soluble proteins, crystal structures of the AChBPs have been resolved to 1.8A^{o} (100,101). These crystal structures have been used extensively in developing homology models of the N-terminal, ligand-binding domain of cys-loop LGIC receptors (nAChR, GABA, glycine, and 5-HT_3) (93,99). More recent structures of the LGICs themselves have corroborated the structural similarity of the AChBPs and the validity of these homology models (102,103). In addition, site-directed mutagenesis and affinity labeling experiments on the AChBP have shown conservation of residues involved in the ligand-binding site and receptor-binding function of LGIC in general, and nicotinic receptors in particular (101,104). For example, the AChBP binds to the agonists and competitive antagonists of the nicotinic ACh receptor (e.g. nicotine, ACh, bungarotoxin, epibatidine, and tubocurarine), and the crystal structure of these complex binding sites have provided insight into the ligand-binding domain of nicotinic ACh receptors (101,105).

The application of the AChBPs as cys-loop LGIC receptor models is further supported by experiments showing that the *Lymnaea stagnalis* AChBP can be functionally coupled to the transmembrane region of a 5-HT_3 serotonin receptor, and trigger opening of the ion channel (106). Clearly, similarities between the AChBPs and LGICs binding domains make them ideal candidates for the study and modeling of cys-loop LGIC receptors and their interactions with various ligands and drugs.

As a model system, an AChBP needs to be modified so it can be placed on a biosensor surface and used as a biosensor molecule capable of detecting different classes of ligands. There are two different approaches for modification of an AChBP and development of a soluble binding domain: mutagenesis and chimera construction. Chimera experiments executed by several labs have encountered numerous problems, and in general have not yet been very successful (107,108). However, there have been some results when mutagenesis was used in conjunction with chimera construction, where the ligand was able to recognize and bind to the chimera if the AChBP residues were also mutated to their counterpart in the cys-loop LGIC receptor (106). On the other hand, mutagenesis introduces its own problems, namely the fact that the AChBPs are snail proteins. Therefore, data only provide information about the snail protein, and any information about the human protein could only be inferred. This is insufficient for drug screening where a modified protein would be required to mimic the endogenous receptor protein binding site with a high degree of fidelity.

Taken together, it appears that although the AChBPs are good models of cys-loop LGIC receptors, more information about similarities and differences between the AChBP and LGIC receptors are needed before the AChBP can be modified and used as a biosensor molecule. One of the best ways to investigate similarities and differences is through mutagenesis where a binding site that is similar between the AChBP and LGIC receptor superfamily is developed. This task could potentially be accomplished through systematic site-directed mutagenesis designed to alter and hone the selectivity of an AChBP to favor specific LGIC receptor ligands.

The end result of this work will be the development or engineering of a soluble biosensor molecule similar to a human receptor protein that can be used in biosensor applications (e.g. SPR, MC, SPA) including high-throughput screening of small

molecules (e.g. drugs). An engineered soluble receptor analog suitable for biosensor use would allow screening of a wide range of natural products and synthetic drugs in a much shorter period of time. As the cost of drug discovery is about 1/3 of the cost of developing a drug (https://www.fda.gov/drugs/developmentapprovalprocess/), this would represent a large cost savings. Such proteins would also find important uses in detection of bioweapons or bedside drug screenings as these receptors are important receptors for toxic compounds as well (109).

1.7 Hypothesis and Specific Aim

The overarching goal of this Dissertation is to explore the AChBP as a potential biosensor molecule, and use it as a template for development of a soluble binding protein suitable for high-throughput biosensor devices. The target receptor protein is the serotonin type 3 (5-HT_3) receptor, important in central nervous system disorders and the anti-emetic class of therapeutic agents.

We hypothesize that the AChBP can be modified by site-directed mutagenesis to mimic the ligand selectivity and specificity of the 5-HT_3 serotonin receptor. The specific aim of this Dissertation is to engineer a soluble serotonin-binding protein using the AChBP, which will mimic the specificity of native 5-HT_3 serotonin protein. This will be approached in a sequential manner as follows:

1) Develop stable cell lines and expression of the *Lymnaea* AChBP and evaluate its pharmacology using SPA (Chapter 3).
2) Create mutations of the AChBP consistent with the 5-HT_3 receptor ligand interactions designed to improve interactions of the AChBP with serotonin ligands (Chapter 4).
3) Create double mutations to determine if the selectivity for serotonin ligands can be enhanced (Chapter 4).
4) Using the data from 2-and-3 above, produce a new model and suggest new mutations to further enhance selectivity for serotonin ligands (Chapter 5).

Chapter 2: Materials and Methods

2.1 Construction of the AChBP

The AChBP used in this project was custom synthesized by GeneArt Inc. (Germany), using an AChBP cDNA sequence identical to the molluscan snail *Lymnaea stagnalis* (Figure 3.3, Source: http://www.uniprot.org/uniprot/P58154). The following modifications to the AChBP sequence were made to provide for ease of purification and attachment to sensor surfaces:

a) An N-terminal FLAG tag was added by insertion of the synthetic AChBP gene into a p3xFLAG-CMV-9 expression vector (Sigma, Figure 3.2). The p3-Flag epitope tag is used with an anti-FLAG antibody for detection, characterization, and immobilization of the protein.
b) A C-terminal 6X His tag was added to the vector to facilitate rapid protein purification. This tag is used for immobilization of the protein on nickel and copper-containing surfaces such as the SPA beads.
c) A pre-protrypsin leader peptide preceding the FLAG tag was added for ease of protein recovery from cell culture. This allows for secretion of the AChBP into the extracellular medium surrounding the cell culture.
d) The expression vector also contains ampicillin-resistant and G418-resistant genes for clonal selection of stable transfectants in both bacterial and mammalian cell lines (HEK-293 cell lines). This provides rapid development of sable cell lines for protein production.

2.2 Amplification of the AChBP

XL-1 blue supercompetent *E.Coli* cells were transformed with the AChBP/ p3xFLAG-CMV-9 DNA using standard protocol and reagents (Stratagene). DNA was purified using Mini-prep and Maxi-prep (Qiagen), and the presence of the insert (vector DNA) was verified by restriction digest and agarose gel electrophoresis. The process of transformation and verification required over one week time for a single DNA sample (for the AChBP and each mutant DNA afterward). The DNA was sequenced by

commercial sequencing (Sequetech Corp, Mountain View, CA, http://datasytem.sequetech.com).

2.3 Stable Expression of the AChBP

The AChBP/p3xFLAG-CMV-9 plasmid DNA prepared by Maxi-prep, and verified by Sequetech, was transfected into HEK-293 cells (Human embryonic kidney cells, ATCC), to develop stably transfected cell lines that secrete an AChBP containing an N-terminal FLAG epitope tag and a C-terminal poly-His tag into the extracellular medium surrounding the growing HEK-293 cell culture.

Prior to transfection, a kill curve (dose response curve) for HEK-293 cells was established using antibiotic G418 (BD Biosciences). Untransfected HEK-293 cells were plated at a 10^6 cells/cm^2 cell density and placed in DMEM media (ATCC) supplemented with 10% Fetal Bovine Serum (Invitrogen), 2% Penicillin/Streptomycin (Invitrogen), and G418 antibiotic (Sigma-Aldrich) at varying concentrations. Cells were incubated at 37 ºC in a humidified atmosphere of 5% CO_2 in a growth chamber / CO_2 incubator. The optimal concentration of an antibiotic is considered to be that which results in 90% cell death (when cells become round and fail to adhere to the dish) in one week, and 100% cell death within two weeks. Based on these criterions, the optimal G418 concentration was determined to be 0.4 mg/ml. This concentration of the G418 antibiotic was sufficient to kill all HEK-293 cells that did not contain p3xFLAG-CMV-9 vector.

Stable transfections were performed using the SuperFect reagent kit and protocol (Qiagen). Cells were maintained in DMEM media (ATCC) supplemented with 10% Fetal Bovine Serum (Invitrogen), and 2% Penicillin/Streptomycin (Invitrogen) for 48 hours after transfections. Medium was then replaced with fresh supplemented DMEM and 0.4 mg/ml G418 antibiotic. Cells were incubated at 37 ºC in a humidified atmosphere of 5% CO_2 in a Growth chamber / CO_2 incubator. Cells recovered very slowly, and over one month of incubation and change of medium (twice a week) was required before sufficient cells were obtained to allow splitting of cells and its propagation (the same applied for each subsequent mutant DNA).

Cells were split into new flasks when 90-95% confluent (an average of once a week). The culture medium was removed and cells were washed with 10-ml of warm

Dulbecco's phosphate buffered saline (ATCC) at 37 ºC in a water bath, and then re-suspended in 10-ml of fresh DMEM (plus 10% Fetal Bovine Serum, 2% Penicillin/Streptomycin, and 0.4 mg/ml G418 antibiotic) by repeated up-and-down pipetting. Typically, 0.5-ml of the cell suspension was transferred to a new flask and diluted with 24.5 of fresh warm DMEM growth media. After several passes, the surviving cells were determined to contain a stable copy of the AChBP/p3xFLAG-CMV-9 plasmid. Stable cell lines actively secrete an AChBP containing a C-terminal poly-His tag and an N-terminal FLAG epitope tag into the culture medium.

The process of cell splitting and growth of stable cell lines required an average of one month (for the AChBP and each mutant DNA afterward) before stable cells could be transferred to large flasks suitable for large scale protein production. Once cells were split and transferred to large cell culture dishes (VWR) that could hold 100-120 ml of media, the cell culture media was collected at 90-95% cell confluency (an average of twice a week), for protein purification.

2.4 Purification of the AChBP

Culture medium from flasks containing the AChBP/HEK-293 cells was collected every 2-3 days. The AChBP was purified from the cell culture medium using a Dynamax machine with Nickel-EDTA His-Select Columns (Sigma) with the following modifications to Sigma's protocol: a) addition of salts to the collected medium at the concentrations of 50mM sodium phosphate (monobasic, Na_2HPO_4), 0.3M sodium chloride (NaCl), and 10mM imidazole; b) adjustment of medium pH to 8.0 using 1M sodium hydroxide (NaOH), and; c) filtration of medium through 0.2-µm cellulose acetate filters. Addition of imidazole served to decrease non-specific protein binding to the affinity column resulting in a highly pure final product, and NaCl was used to increase the ionic strength of the solution.

Purification is based on the binding of a 6X His tag incorporated into the AChBP to the highly selective His-Select affinity resin. Therefore, the Nickel-EDTA His-Select Columns were equilibrated before and after the protein purification with 10-ml/column of a media-free equilibration buffer, 50mM Na_2HPO_4, 0.3M NaCl, 10mM imidazole, and adjusted with sodium hydroxide to pH of 8.0. Adjusted culture medium was placed on

ice for the duration of the protein purification process, and then loaded onto equilibrated Nickel-EDTA His-Select Columns at a flow rate of 4ml/min for protein purification at room temperature.

The bound protein was eluted with elution buffer (50mM Na_2HPO_4, 0.3M NaCl, 250mM imidazole) with pH of 8.0. This buffer has a higher concentration of imidazole since imidazole acts as a competitor for binding to the AChBP. Elution was performed in the following manner: pre-wash (0:00-1:00 minute), Elution-1 (1:00-4:00 minutes), Elution-2 (4:00-5:00 minutes), Elution-3 (5:00-6:00 minutes), with most of the AChBP appearing in the second fraction. The second fraction was used for all the experiments, and other fractions were discarded. The process of medium adjustment, equilibration before and after purification, and protein purification takes 12-15 hours (for the AChBP and each mutant), depending on the volume of the culture medium. At this point, the purified protein (with imidazole) can be stored or used to verify presence of the protein by performing gel electrophoresis. Since His-Select columns enables purification of the AChBP in one-step from the AChBP/HEK-293 cells, the purified protein can also be directly transferred to sensor surfaces such as the scintillation proximity assay (SPA).

Eluted protein requires further purification, namely imidazole removal, to perform Lowry assay since imidazole interferes with protein quantification. Free imidazole was removed by passing the eluted protein (plus imidazole) through 10kD-MW Cutoff MicroSep centrifugal filters (Pall Life Science), and centrifuging at 7500 rpm for 40 minutes. Three washes of 3-4 ml PBS/wash with centrifugation at 7500 rpm for 40 minutes each were performed to remove excess imidazole. The protein was then removed from the filter by addition of 1-ml PBS.

2.5 Analysis of the AChBP

The His-Select purified and imidazole-free protein was analyzed by Lowry assay (Sigma), and polyacrylamide gel electrophoresis (PAGE) using standard methods (BioRad). Purification of the AChBP from the 0.4 mg/ml G418 cell line typically produced more than 1-mg of protein per liter of culture media as determined by Lowry assay. Therefore, this method produces sufficient protein for evaluation of the AChBP

and the AChBP-derivatives using SPA, which was our standard method for evaluating the binding interactions.

The purity and the molecular weight of denatured and native AChBP and the AChBP-derivatives were characterized using PAGE under non-denaturing and denaturing conditions using standard methods. Precast 7.5%, to 12% tris-HCl gels (BioRad) were pre-run at 200V for 20-minutes before they were loaded with 4-µg of the protein samples and Kaleidoscope protein standard (BioRad) and ran for another 40-60 minutes at 120V. Gels were stained with Coomassie Brilliant Blue at room temperature by shaking for 1-2 hours, followed by de-staining with dH_2O for 30-minutes. The AChBP was identified as the 37kD band under denatured conditions, and as the 150kD under non-denaturing conditions. These results showed that the protein was expressed as a pentamer, as expected. The AChBP in samples was also visually estimated to be highly pure. No bands of similar molecular weight were observed in a control, un-transfected HEK-293 culture media sample (Figure 3.4).

2.6 Storage of the AChBP

In order to facilitate storage and increase stability of the AChBP, we lyophilized the purified AChBP protein, and then reconstitute it. The eluted AChBP in PBS was aliquoted into 200-µl portions and placed in 2-ml micro-centrifuge tubes. The tubes were spun, uncapped, under vacuum in a rotatory evaporator (Savant Instruments, DNA Speed Vac) at room temperature for 2.5-3 hours until dry. The samples were then refrigerated at 2-8 ºC for up to 12-months. The dried samples were rehydrated and tested immediately after drying, as well as 6-months and 12-months after drying, using PAGE or SPA assays, and then compared to samples before drying. The results showed no differences in protein composition or binding characteristics (data presented in Chapter 3.5). The stability of the AChBP protein for long-term storage and the fact that it can be easily dried and reconstituted, and transported are added benefits that should facilitate the AChBP-related experiments.

2.7 Pharmacological Characterization of the AChBP

To determine if the binding characteristics of the mutated proteins were intact, we utilized a Scinitillation Proximity Assay (SPA) using the serotonin antagonist [^{3}H]-granisetron. SPA also utilizes PVT Copper His-tag SPA beads, where the copper on the beads bind to the 6X His tag engineered into the C-terminal of the AChBP (110). Scintillant is integrated into the bead matrix, thus the bead fluoresce only when a radioisotope is in close proximity to it, and molecules not in close proximity to the bead do not fluoresces and do not contribute to the signal (Figure 1.6). Since only bound molecules produce a signal, no filtration or other separation technique is necessary to distinguish bound from unbound ligand. This enables rapid analysis of binding data, as well as the use of low affinity ligands. In addition, SPA enables rapid evaluation of radioligand binding characteristics with minimal amounts of protein. We used this technique for pharmacological characterization of the AChBP, and as our standard method of evaluating the binding interactions for the AChBP and AChBP-derivatives.

SPA assays were performed in 200 µl reaction vessels containing protein, radioligand, and SPA beads. For the AChBP binding assays, the protein concentration was held constant and the [^{3}H]-granisetron was added in variable concentrations. The protein (the AChBP and AChBP-derivatives) was added to anti-His SPA beads (GE/Amersham Biosciences), at a concentration of 10 nM per well. The SPA beads were diluted with phosphate-buffered saline (PBS) and Bovine Serum Albumin (BSA, Sigma; 5 mg/ml) to a final concentration of 0.2 mg/ml per well before they were added to protein. BSA was added to decrease non-specific binding. The protein/bead mixture was incubated at ~21 º C (room temperature) for a minimum of 1-hour. Then, six different concentrations of radioligand, [^{3}H]-granisetron, increasing by approximately three-fold intervals from 0-to-300 nM (0, 3, 10, 30, 100, and 300 nM) were added to the protein/bead mixture. The mixtures in the reaction vessels were incubated at ~21 º C (room temperature) on a shaker with low speed for a minimum of 2-hours before counting. Non-specific binding was determined in the presence of 1-M acetylcholine since it strongly binds to the AChBP, and subtracted from the total binding.

For competition assays, the [^{3}H]-granisetron concentration was held constant and used as the radioligand in competitive binding, and the competing ligand was

added in variable concentrations. The purpose of theses assays was to determine the affinity (K_i value) of compounds that were not available in radiolabeled form. Therefore, the K_d value of the [^{3}H]-granisetron for the AChBP and AChBP-derivatives (using10nM of protein, 5 mg/ml BSA, 0.25 mg/ml SPA beads, and 6-different concentrations of [^{3}H]-granisetron), were calculated using one-site binding model and GraphPad Prism software. This K_d value was used as [^{3}H]-granisetron concentration in the assays. For competition assays, 8-12 concentrations of competing ligand, increasing by approximately three-fold intervals from 0-to-3000 μM, were added to the protein/bead mixture. These assays were carried out using the same concentration of protein and reagents, and in the similar manner as the binding assays.

Radioactivity level was measured by counting the samples for a minimum of 4-hours using a 1450 Microbeta Plus liquid scintillation counter (Perkin-Elmer). Each count is taken over one minute per sample and then averaged. This is considered one round of counting, which is repeated every 15 minutes. Therefore, each sample well is counted many times (at every 15-minute interval) depending on the length of time a scintillation counter is running. The optimal output occurred 2-3 hours after the samples had been placed in the scintillation counter for counting. Longer time periods likely resulted in a settling of the SPA beads, producing uneven counting and higher background noise. Shorter periods produced highly unstable readings, likely due to pre-equilibrium conditions. The results from 5-rounds of plate reading were averaged and used for analysis. K_d and K_i values were determined from this information using non-linear fitting and GraphPad Prism software. The data reported in this Dissertation resulted from the average of at least four experiments.

2.8 Data Analysis for the AChBP

The equilibrium binding constant or dissociation constant (K_d) for the [^{3}H]-granisetron radioligand was calculated directly from a plot of radioligand concentration versus fraction bound. Data was analyzed using GraphPad Prism software. The K_d value was calculated using the simple one-site binding model shown below:

$$Y = B_{max} * X / K_d + X$$

where X is the [^{3}H]-granisetron radioligand concentration, Y is the amount of bound ligand in counts per minute (CPM), K_d is the binding affinity, and B_{max} is the calculated maximal binding.

Competition assays determine the IC_{50} value (in nM or μM), which represents the concentration of a ligand/drug that is required for 50% inhibition. The IC_{50} of cold (non-radioactive) ligands for the inhibition of [^{3}H]-granisetron was determined by using the sigmoidal dose-response equation below and GraphPad Prism software:

$$Y = B_{max} / (1 + 10^{([\log(IC50)-X] * n)})$$

where X is the logarithm of the concentration of cold ligand, Y is the response in count per minute (CPM), and n is the Hill-slope.

The K_i value shows the concentration of the drug that binds to half of available receptor binding sites. K_i was calculated using the Cheng-Prusoff equation:

$$K_i = IC_{50} / (1+L/K_d)$$

2.9 Mutation of the AChBP

The AChBP, custom synthesized by GeneArt Inc. (Germany), was mutated with single and double amino acid substitutions from equivalent positions in the 5-hydroxytryptamine type 3 receptor (5-HT_3R) sequences. The goal was to construct a serotonin-binding protein by modification of the AChBP residues to recognize serotonin ligands, as well as synthesize and purify these mutated proteins in quantities usable for biosensor applications. The construction of a serotonin-binding protein would enable the development of a molecular biosensor for serotonin.

The AChBP amino acids for single-site and double-site mutations were determined as explained in Chapter 4. Oligos to mutate amino acids were designed using the DNA Strider program, quality checked with Basilisk (a Mac emulator), and ordered through The Midland Certified Reagent Co., Inc. Once oligos arrived, mutations were constructed utilizing the QuickChange II Site-Directed Mutagenesis kit (Stratagene's), which is designed for rapid and efficient incorporation of insertions, deletions and substitutions into double-stranded DNA. We used the standard methods and protocol of the kit with the following modifications: 50 ng of AChBP DNA and a pair of designed oligos for a specific mutation were used for each Polymerace Chain

Reaction (PCR). The PCR machine was programmed for 18 cycles of denaturation for 1-minute at 95 ºC, annealing for 1-minute at 60-65 ºC (it was always 10 ºC less than oligo's temperature), and extension for 9-minutes at 68 ºC. The PCR products in each test tube was treated with 1- µl of DpnI restriction enzyme (20,000 units/ml), and incubated for 1-hour at 37 ºC to digest methylated parental DNA.

XL-1 blue supercompetent *E.Coli* cells were transformed with 4- µl of DpnI-treated DNA using standard protocol and reagents (Stratagene). DNA was purified using Mini-prep and Maxi-prep (Qiagen), and the presence of the insert was verified by restriction digest and agarose gel electrophoresis. The verified mutant DNA was sent to Sequetech for commercial sequencing (Sequetech Corp, Mountain View, CA, http://datasytem.sequetech.com).

Once presence of the DNA substitution was verified by Sequetech, the mutated DNA was transfected into HEK-293 cells to develop stably transfected cell lines that secrete a mutated AChBP protein into the extracellular medium in a manner similar to that used to produce the wild-type AChBP and explained in Chapter 2.3. The mutant DNA was then purified, analyzed, stored, and pharmacologically characterized using SPA. It should be noted that the construction, development, amplification, expression and testing of each mutant receptor took approximately one year.

Chapter 3: Expression and Validation of the AChBP as a Viable Biosensor Protein

3.1 Acetylcholine-binding Protein (AChBP)

Research into ligand-gated ion channel (LGIC) structure has been greatly facilitated by the discovery of the acetylcholine-binding protein (AChBP) in the great pond snail, *Lymnaea Stagnalis* (99). Two additional homologs of this protein have also been identified in the freshwater snail *Bulinus truncates* (98), and sea hare *Aplysia californica* (111). The AChBP protein in these molluscs is secreted by glia cells, and its role is postulated to involve regulation of synaptic function through binding and inhibition of acetylcholine (96,99). It is also hypothesized that the AChBP could help defend snails against nicotinic toxins, which are common in aquatic species, by binding to the toxins before they reach the receptors (96,99). Sequence alignment of the AChBP shows a high similarity to the extracellular, N-terminal ligand-binding domains of various cys-loop LGICs, and specifically the nicotinic acetylcholine (nACh) receptor (93,95,101,102,105), and sequence analysis suggests that this protein may have evolved as a result of a nACh receptor truncation in ancestral snails (96).

Structural data for the AChBP confirms much of what has been reported from previous studies on LGIC receptors. Like LGICs, this protein assembles in a pentameric form, and the binding site of the AChBP is composed of the same structural loops (or pockets) hypothesized for the LGIC family of receptors (99). Within these loops, amino acid side chains and the protein backbone make contacts with nicotine (or other orthosteric ligands) (95,99). The AChBP, like the nACh receptor, contains a crucial cys-cys loop that is involved in structuring the ligand-binding domain, as well as conserved residues at the ACh binding site (95,99,104). In addition, the AChBP binds to nACh receptor agonists and antagonists including Ach (112), nicotine (101), α-bungarotoxin (100), and epibatidine (111).

The AChBP has a high sequence homology (15-30%) with the amino terminal domain of LGIC receptors (20,99). The water-soluble nature of the AChBP and its similarity in structure to LGICs has enabled the determination of a high resolution crystal structure (2.7 A) of the AChBP (Figure 3.1), that has been used as a template for

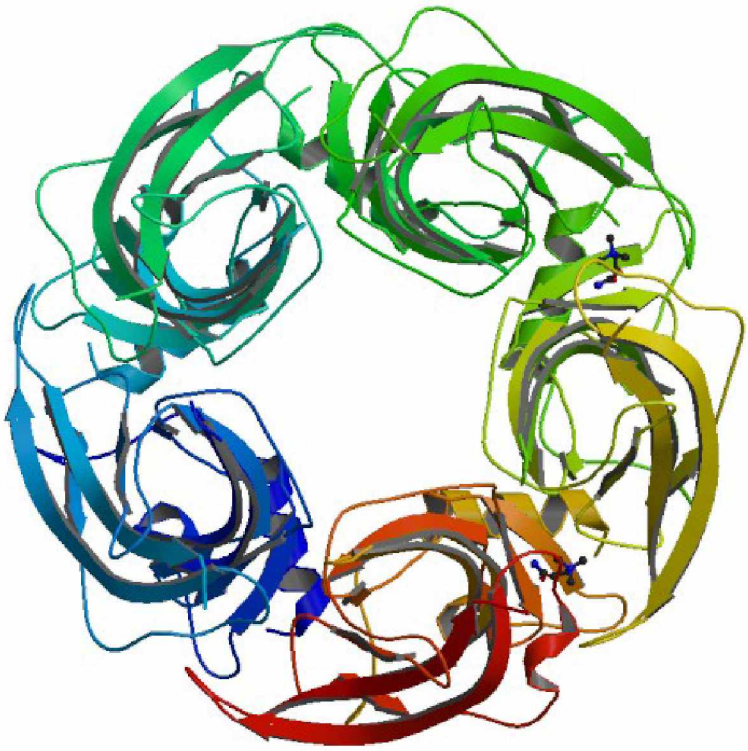

Figure 3.1: X-Ray Structure of Acetylcholine-binding Protein (AChBP) in Complex with Nicotine and Carbamycholine. From *Lymnaea Stagnalis* (Great Pond Snail), at 2.5 A resolution, from Protein Data Bank (PDB) file 1UV6.

homology modeling of N-terminal binding domains of cys-loop LGICs (93,95). Models of LGIC receptor binding sites have been developed based on the AChBP crystal structure to study and analyze receptor-ligand interactions. These models have been further refined using site-directed mutagenesis methods (97,107,113-115).

The similarity of the AChBP binding site to LGIC binding domains also raises the possibility that the AChBP could be used to mimic LGIC receptors, acting as a potential lead molecule for a family of biosensor proteins. In addition, since the AChBP is a soluble protein that is easily expressed and purified (112,113), it is an ideal biosensor molecule that can be easily attached to biosensor surfaces. It is also possible that the AChBP protein can be modified to detect different classes of ligands for different receptors (94).

This chapter describes exploration and development of the AChBP protein as a sensor protein, as well as evaluation of its structure, functionality and stability.

3.2 Engineering of the AChBP

The AChBP was custom synthesized to specifications that facilitate the proposed engineering and biosensor applications of this project using commercial AChBP DNA from the great pond snail, *Lymnaea stagnalis*. In order to rapidly develop stable cell lines for protein production, the synthetic AChBP gene was inserted into the p3xFLAG-CMV-9 expression vector (Figure 3.2). The vector contains ampicillin resistant genes for selection in bacterial cell lines; neomycin resistant genes, which confer resistant to the antibiotic G418, for use in selecting transfected mammalian cell lines (HEK-293); and an MCS (multiple cloning site) on its C-terminal. In addition, some modifications to the AChBP sequence were made to provide for ease of purification and/or attachment to sensor surfaces, such as a C-terminal 6X His tag and an N-terminal FLAG tag.

The C-terminal 6X His tag allows the protein to bind to metals such as copper and nickel to facilitate rapid protein purification. This tag can also be used for protein immobilization on nickel containing surfaces such as the scintillation proximity assay (SPA) beads. The N-terminal FLAG tag was added to provide a secondary option for purification using an anti-FLAG antibody for protein detection and characterization, as well as its immobilization. The vector also contains a pre-protrypsin leader peptide preceding the FLAG tag to allow for secretion of the AChBP into the extracellular medium, and provide for ease of recovery of the protein. A similar N-terminal FLAG and C-terminal 6X His AChBP was previously expressed and used by Hansen et al. (116). Both tags were shown to be accessible and used for purification, and do not seem to interfere with normal binding (96). Thus, the FLAG and His tags do not appear to affect the AChBP/ligand binding. A comparison of sequence data between the AChBP DNA and the p3xFLAG-CMV-9 expression vector/AChBP indicated that the vector was created as indicated above (Figure 3.3).

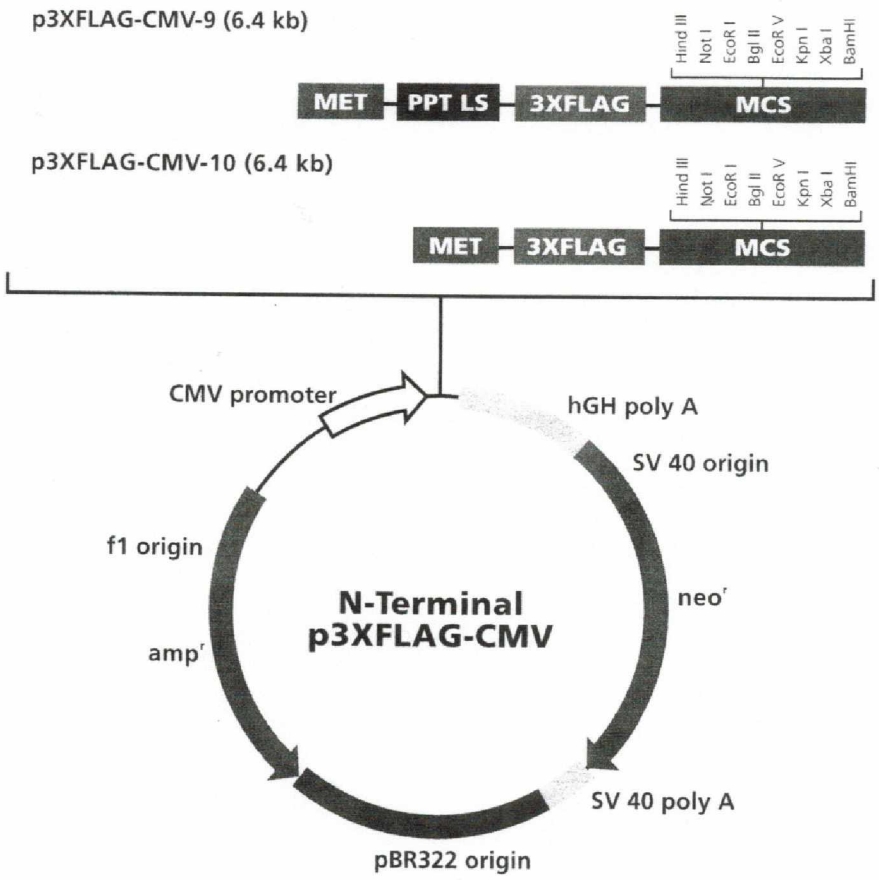

Multiple Cloning Site

(p3XFLAG-CMV-9* and p3XFLAG-CMV-10)

	3XFLAG Peptide Sequence														
Met*	Asp	Tyr	Lys	Asp	His	Asp	Gly	Asp	Tyr	Lys	Asp	His	Asp	Ile	
ATG	GAC	TAC	AAA	GAC	CAT	GAC	GGT	GAT	TAT	AAA	GAT	CAT	GAC	ATC	
TAC	CTG	ATG	TTT	CTG	GTA	CTG	CCA	CTA	ATA	TTT	CTA	GTA	CTG	TAG	

3XFLAG Peptide Sequence															
Asp	Tys	Lys	Asp	Asp	Asp	Asp	Lys								
GAT	TAC	AAG	GAT	GAC	GAT	GAC	AAG	CTT	GCG	GCC	GCG	AAT	TCA	TCG	ATA
CTA	ATG	TTC	CTA	CTG	CTA	CTG	TTC	GAA	CGC	CGG	CGC	TTA	AGT	AGC	TAT

Not I, EcoR I, Hind III

Bgl II		EcoR V			Kpn I			Xba I			Bam HI			
GAT	CTG	ATA	TCG	GTA	CCA	GTC	GAC	TCT	AGA	GGA	TCC	CGG	GTG	
CTA	GAC	TAT	AGC	CAT	GGT	CAG	CTG	AGA	TCT	CCT	AGG	CCC	CAC	

*For pFLAG-CMV-9, the Met-preprotrypsin leader sequence (PPT LS) precedes the FLAG coding sequence.

Figure 3.2: p3XFLAG-CMV-9 Expression Vector. The AChBP gene was inserted into this vector.

A. The AChBP DNA Sequence:

sp|P58154|ACHP_LYMST Acetylcholine-binding protein
OS=Lymnaea stagnalis PE=1 SV=1 Source: http://www.uniprot.org/uniprot/P58154

MRRNIFCLAC LWIVQACLSL DRADILYNIR QTSRPDVIPT QRDRPVAVSV SLKFINILEV
NEITNEVDVV FWQQTTWSDR TLAWNSSHSP DQVSVPISSL WVPDLAAYNA ISKPEVLTPQ
LARVVSDGEV LYMPSIRQRF SCDVSGVDTE SGATCRIKIG SWTHHSREIS VDPTTENSDD
SEYFSQYSRF EILDVTQKKN SVTYSCCPEA YEDVEVSLNF RKKGRSEIL

B. Coding Sequence Obtained from the p3XFLAG-CMV-9 / AChBP Expression Vector:

M DYKDHDGDYK DHDIDYKDDD DK**RRNIFCLAC LWIVQACLSL DRADILYNIR QTSRPDVIPT QRDRPVAVSV SLKFINILEV NEITNEVDVV FWQQTTWSDR TLAWNSSHSP DQVSVPISSL WVPDLAAYNA ISKPEVLTPQ LARVVSDGEV LYMPSIRQRF SCDVSGVDTE SGATCRIKIG SWTHHSREIS VDPTTENSDD SEYFSQYSRF EILDVTQKKN SVTYSCCPEA YEDVEVSLNF RKKGRSEIL** HHHHHH

Figure 3.3: DNA Sequence. (A) is the published DNA sequence data for the AChBP, which is also shown in bold in (B). (B) is the coding region of the p3XFLAG-CMV-9/AChBP expression vector. Comparison of A-and-B shows the two sequences are 100% identical. The protein produced by the expression vector is a fusion protein with A-terminal His. This protein was verified by DNA sequencing.

3.3 Production and Purification of the AChBP

The AChBP was expressed and purified using methods outlined in Chapter 2 (Materials and Methods). Briefly, the AChBP/ p3xFLAG-CMV-9 vector was transformed into XL-1 blue supercompetent *E.Coli* cells using standard protocol and reagents (Stratagene). DNA was purified using mini-prep and maxi-prep (Qiagen), and the presence of AChBP DNA insert was verified by restriction digest and agarose gel electrophoresis. The DNA was sequenced by commercial sequencing (Sequetech Corp, Mountain View, CA, http://datasytem.sequetech.com).

The verified AChBP/p3xFLAG-CMV-9 DNA was transfected into HEK-293 cells using the SuperFect reagent kit and protocol (Qiagen). A stable cell line expressing the His-tagged AChBP in HEK-293 cells was developed which actively secreted the AChBP into the medium. Culture medium containing the AChBP protein was purified using Nickel-EDTA His-Select Columns (Sigma). This step was followed by imidazole removal via passing the protein through 10kD-MW Cutoff MicroSep centrifugal filters (Pall Life Science), centrifuging at 7500 rpm for 40 minutes, three washes of 3-4 ml PBS/wash with centrifugation at 7500 rpm for 40 minutes each, and final elution of the protein from the filter by addition of 1-ml of PBS.

Purified protein was analyzed by Lowry assay and polyacrylamide gel electrophoresis using precast tris-HCl polyacrylamide gels. Gel electrophoresis was performed under denaturing and non-denaturing conditions (Figure 3.4). The AChBP protein was identified as the 37kD single band under denatured conditions which is expected for the monomeric protein, and about 150kD under non-denatured conditions. Since the non-denatured protein was approximately 5X the size of the denatured protein, it was concluded that the AChBP protein was expressed as a pentamer. No bands of similar molecular weight were observed in the control, untransfected HEK-293 media sample. Above information are consistent with literature values for the AChBP and indicate the secreted protein assembles correctly with a pentameric structure.

3.4 Yield Increase of the AChBP

As noted in Chapter 2, the purification columns were purchased from Sigma Corporation, and the standard protocol was used in initial experiments; however, the protein yield was low (285 µg/L of media) and insufficient. The original protocol for extract preparation calls for: a) addition of salts at the concentrations of 50mM sodium phosphate (monobasic, Na_2HPO_4),0.3M sodium chloride (NaCl), and 10mM imidazole; b) adjustment of pH to 7.5 using 1M sodium hydroxide (NaOH), and; c) filtration through 0.4-µm cellulose acetate filters. Addition of imidazole to the media served to decrease non-specific protein binding to the affinity column, resulting in a higher yield and highly pure final product; and NaCl was used to increase the ionic strength of the solution.

After many experiments over an extended period of time, we modified the extract preparation protocol which resulted in a 5-fold increase in the protein yield (1,398 µg/L of media). Collected medium was treated and prepared as follows before it was introduced to the purification columns: a) addition of salts at the concentrations of 50mM sodium phosphate (monobasic, Na_2HPO_4),0.3M sodium chloride (NaCl), and 10mM imidazole; b) adjustment of pH to 8.0 using 1M sodium hydroxide (NaOH), and; c) filtration through 0.2-µm cellulose acetate filters. A higher pH helped with the complete elution of the salts, resulting in a higher protein yield; and a filter with smaller pores produced a cleaner extract to be run on the columns. These modifications resulted in

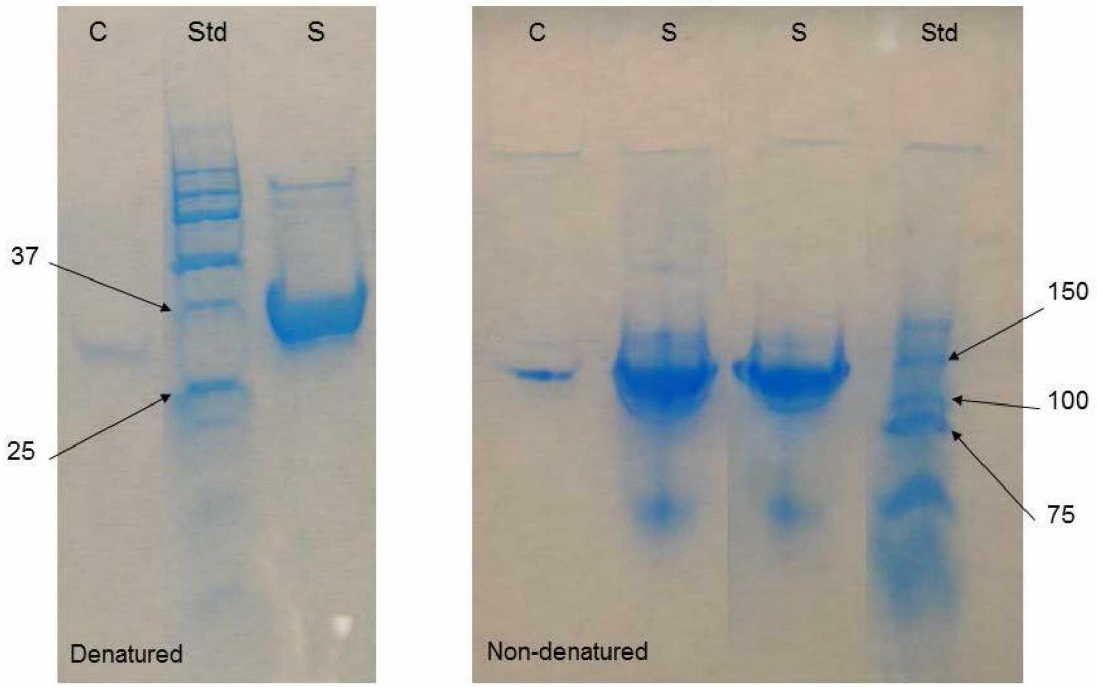

Figure 3.4: Polyacrylamide Gel Electrophoresis of the AChBP. Purity and assembly of the AChBP was determined using native and denaturing PAGE. The right hand gel shows the results of PAGE (non-denaturing conditions) and the left hand gel shows the result of separation under denaturing conditions (SDS PAGE). Gels were stained with coomassie blue stain (BioRad). The protein sample lane is indicated by S and the BioRad Kaleidoscope standard is indicated by Std. Under non-denaturing conditions, a distinct band is shown to migrate similar to the 150kD standard. Under denaturing conditions, the dominant band shifts to slightly less than 37 kD. The molecular wt of the native protein of about 150kD is consistent with the predicted molecular wt of the pentameric AChBP. The 37 kD single band in the denaturing gel is as expected for the monomeric protein. In the non-denatured protein, a smaller band is evident at around 37kD as well suggesting some unassembled monomers are present.

production of more than 1-mg of pure protein for every liter of culture media as determined by Lowry assay.

3.5 Storage of the AChBP

For a protein to be considered a biosensor, it must meet a number of criteria including the ability to produce it in sufficient quantity, ease of transportation, stability and sensitivity to different ligands. As described above, the AChBP can be produced and purified easily in sufficient quantities. Larger quantities are likely achievable using non-mammalian expression systems such as insect cells; however, the quantities

described here are sufficient for immobilization of the protein on bead or chip-based systems and so, no further enhancement was developed in this project.

Our initial data from binding assays performed over a period of time, using the same fresh AChBP were not consistent (data not shown). Hansen et al. (97) reported pentamer-dimerization of stored AChBP which might explain our declining results over an extended timeframe. We observed that imidazole appeared to improve the stability of the AChBP when stored at 2-8 ºC. As described above, imidazole is removed before the Lowry assay since it interferes with the assay. However, imidazole removal is not necessary for binding assays using the SPA biosensor since SPA is both an affinity purification step and an analysis platform. The AChBP stability in imidazole is most likely due to stabilization of the single pentamer structure and prevention of pentamer-dimerization (or clumping of proteins). Imidazole may bind to the orthosteric binding site, and is thus likely removed during the wash step after immobilization of the protein on the bead or chip surface. Previous data from our laboratory showed that presence of imidazole did not interfere with protein binding or influence binding data when used in the SPA system (113).

In order to increase the AChBP stability and facilitate its storage, a member of our laboratory attempted to dry the purified AChBP, and reconstitute it with distilled H_2O. It was shown that the AChBP was resistant to denaturation, could be easily dried and reconstituted, and its stability was greatly increased in dried samples (113).

3.6 Biosensor Platform for the AChBP

The soluble nature of the AChBP protein, its relative ease of production and purification, as well as stability in storage and transportation makes it an ideal potential biosensor protein. However, to be considered as an effective biosensor molecule, the potential protein must also function correctly and provide reasonable signal when attached to biosensor surfaces and exposed to ligands. To determine the binding characteristics of the AChBP protein, we utilized the scintillation proximity assay (SPA) as the biosensor surface and our standard method of evaluating binding interactions of the AChBP with different ligands.

The SPA is a bead-based assay which utilizes SPA beads coated with a Scintillant (82,117). The protein of interest is bound to the bead surface using antibody binding or copper chelation. The protein and bead mixture is then exposed and incubated with a radioligand. After an appropriate incubation time, the protein/bead/radioligand complex is placed in a scintillation counter to determine the amount of ligand bound in close proximity to the bead surface (Figure 1.6).

The SPA assay is conducted similar to the conventional radioligand binding assays, but it represents a technological advance over the conventional assays as it does not require filtration of the protein prior to counting. In traditional ligand-receptor binding, the filtration step is designed to separate bound and unbound ligands prior to scintillation counting; however, the scintillant incorporated into the SPA beads only responds when the radioligand is bound in close proximity to the bead. Thus, a signal is only seen when radioligand is bound, and no separation step is required. This permits a high throughput binding study to be performed.

The SPA technique enables rapid evaluation of radioligand binding characteristics with minimal amounts of protein. Since SPA does not have a filtration step, this assay can be used with lower affinity ligands as there is no danger of washing away a low affinity ligand during washing of the filters. In addition, lack of filtration step makes it easier to automate the SPA technique and develop high throughput assays. Taken together, it seems the SPA assay is well suited to a soluble protein like the AChBP or engineered AChBP derivatives. To utilize the SPA assay for the project described here, we modified the standard SPA protocol to be able to test the functionality of the AChBP. These modifications are discussed below, and all the assays reported in this section were run a minimum of four times.

3.6.1 The SPA Bead Concentration

The SPA assay protocol is described in Chapter 2. Briefly, the SPA assays were performed in 200 µl reaction vessels containing protein, radioligand, and the SPA beads. For the AChBP binding assays, the protein concentration was held constant and the [^{3}H]-granisetron was added in variable concentrations. The protein (AChBP and AChBP-derivatives) was added to anti-His SPA beads (GE/Amersham Biosciences).

The SPA beads were diluted with phosphate-buffered saline (PBS) and Bovine Serum Albumin (BSA, Sigma) before they were added to protein. BSA was added to decrease non-specific binding. The protein/bead mixture was incubated at ~21 º C (room temperature) for a minimum of 1-hour. Then, six different concentrations of radioligand, [^{3}H]-granisetron, increasing by approximately three-fold intervals were added to the protein/bead mixture. The mixtures in the reaction vessels were incubated at ~21 º C (room temperature) on a shaker with low speed for a minimum of 2-hours before counting. Non-specific binding was determined in the presence of 1-M acetylcholine since it strongly binds to the AChBP, and subtracted from the total binding.

In the SPA assay, the AChBP protein is immobilized by binding it to the beads using the incorporated 6X His tag on the C-terminal. Since scintillant is integrated into the bead matrix, no filtration is necessary for separation of bound and unbound ligand while using this system as only radioligand bound at close proximity to the bead excites the scintillant and produces a signal. This enables analysis of binding data as well as use of low affinity ligands. Thus, preparation of the beads is an essential step in the SPA assay.

Initial SPA data, using 0.5 mg/ml of beads, showed high background binding which could be attributed to a) high concentration [^{3}H]-granisetron, and thus non-specific binding of the radioligand to the beads or binding of radioligand at a secondary, low affinity sites on the AChBP protein itself; b) high concentration of the beads which can lead to non-proximity effect, (where the bead would be activated when in close proximity of a radioligand, irrespective of whether the radioligand is bound to the bead); c) low concentration BSA resulting in non-specific binding; or d) low concentration of the protein. To address non-specific binding of [^{3}H]-granisetron to the beads, the protein was pre-incubated with beads before addition of [^{3}H]-granisetron; however, this modification did not decrease the high background signal. To address the possibility of high concentration of beads, a bead-titration test (0.1-to-0.5 mg/ml of beads) was carried out to find the optimal concentration of beads. The SPA data showed there were more than enough beads at 0.3 mg/ml concentration (data not included). Further

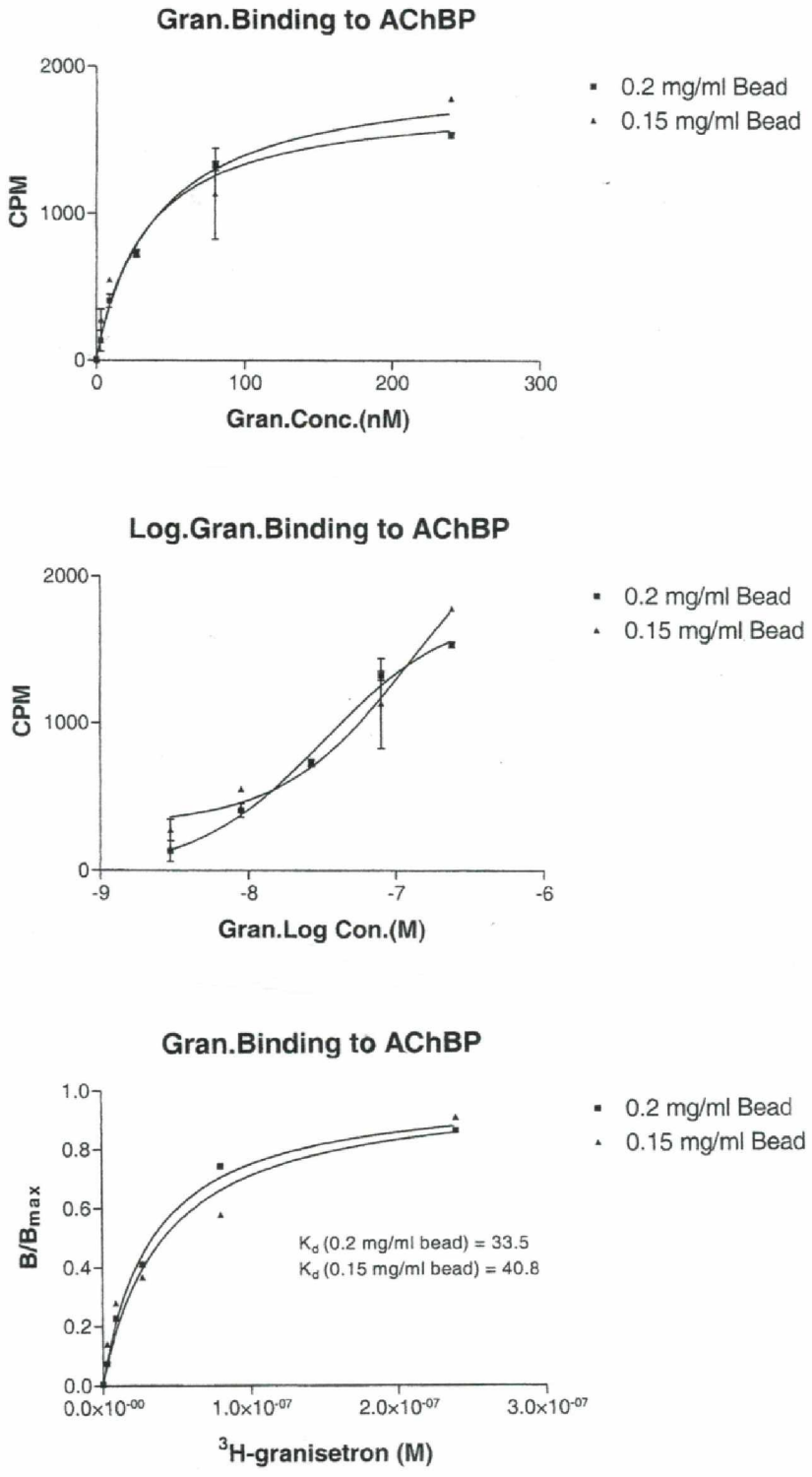

Figure 3.5: The SPA Bead Concentration. Top graph shows count per minute (CPM) vs concentration of radioligand granisetron for both 0.15-and-0.2 mg/ml of beads (continued on the next page).

Figure 3.5 (continued): Middle graph shows the same data in Log format. Bottom graph is B/B_{max} vs radioligand granisetron concentration for both 0.15-and-0.2 mg/ml of beads. CPM vs radioligand concentration placed the optimal bead concentration at 0.2 mg/ml. The bottom graph shows lower K_d (dissociation constant) for 0.2 mg/ml of beads, thus validating the result of other figures.

tests were carried out, and the results placed the optimized amount of SPA beads at 0.2 mg of beads per ml (Figure 3.5).

3.6.2 Counting by the Scintillation Counter

In the SPA assay, the protein/bead/radioligand complex is incubated at ~21 º C (room temperature) on a shaker with low speed for a minimum of 2-hours before the radioactivity level is measured using a scintillation counter. Each count is taken over one minute per sample and then averaged. This is considered one round of counting, which is repeated every 15 minutes. Therefore, each sample well is counted many times (at every 15 minutes interval) depending on the length of time a scintillation counter is running. To find the most stable results, we ran the scintillation counter for 4 hours, using the AChBP protein/SPA beads/[^{3}H]-granisetron, and evaluated the results at every one hour interval. The optimal output occurred 2-3 hours after the samples had been placed in the scintillation counter for counting. Longer time periods likely result in a settling of the SPA beads, producing uneven counting and higher background noise. Shorter periods produced highly unstable readings, likely due to pre-equilibrium conditions. Based on these data, we chose the 2-3 hour incubation period as the optimal incubation time that produced reliable, stable and reproducible results (Figure 3.6).

3.6.3 The SPA Bovine Serum Albumin (BSA) Concentration

BSA was present in all the solutions used in an SPA assay, including the bead solution and protein solution. The primary purpose of adding BSA was to decrease non-specific binding. The standard protocol for the SPA-beads called for 0.05 mg/ml of BSA. However, this concentration of BSA resulted in a very high background binding

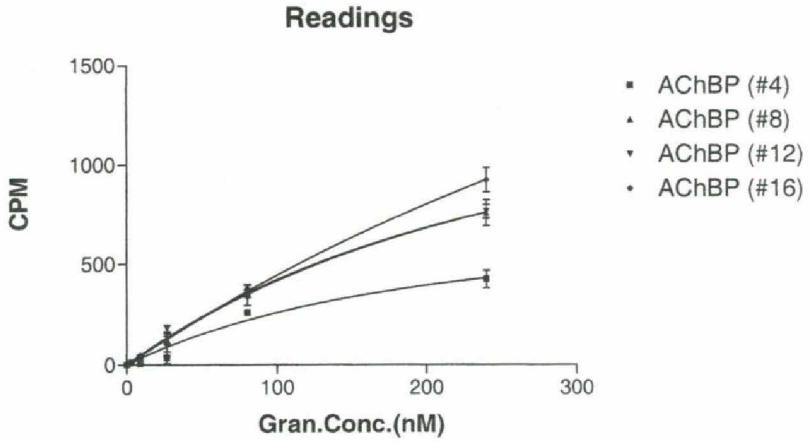

Figure 3.6: Measurement of Radioactivity Level Using the Scintillation Counter. The graph illustrates measurement of radioactivity level for 4-hours at 1-hour interval (corresponding to plate readings #4, 8, 12, and 16 respectively), using the data from samples read and counted by the Scintillation Counter. The data shows best radioactivity reading time is about 2-3 hours (plate readings #8-12) after the samples have been placed in the scintillation counter for counting.

(approximately 50% of total reading). To address high non-specific binding, a BSA-titration test (0.5-to-4.0 mg/ml) using 0.2 mg/ml of beads was performed. The results showed a 37-39% decrease in non-specific binding as the BSA concentration increased. Based on these data, it was determined that 5 mg/ml of BSA was optimal for use in these SPA assays (Figure 3.7).

3.6.4 The SPA Protein Concentration

In order to increase specific binding, the non-specific binding had to be reduced, typically through adjustment of the BSA concentration. However, at the same time, specific binding needs to be increased by optimizing the concentration of the receptor protein. The concentration of the AChBP protein used in experiments, based on previous studies and data from our lab, was 5.8 nM. A protein–titration test (1.25-to-20 nM) using 0.2 mg/ml of beads and 5 mg/ml of BSA was carried out to find the most advantageous concentration of the AChBP protein for the SPA assay in this project. The results showed an increase in specific binding as the protein concentration increased. The specific binding was most stable with a protein concentration of 10nM

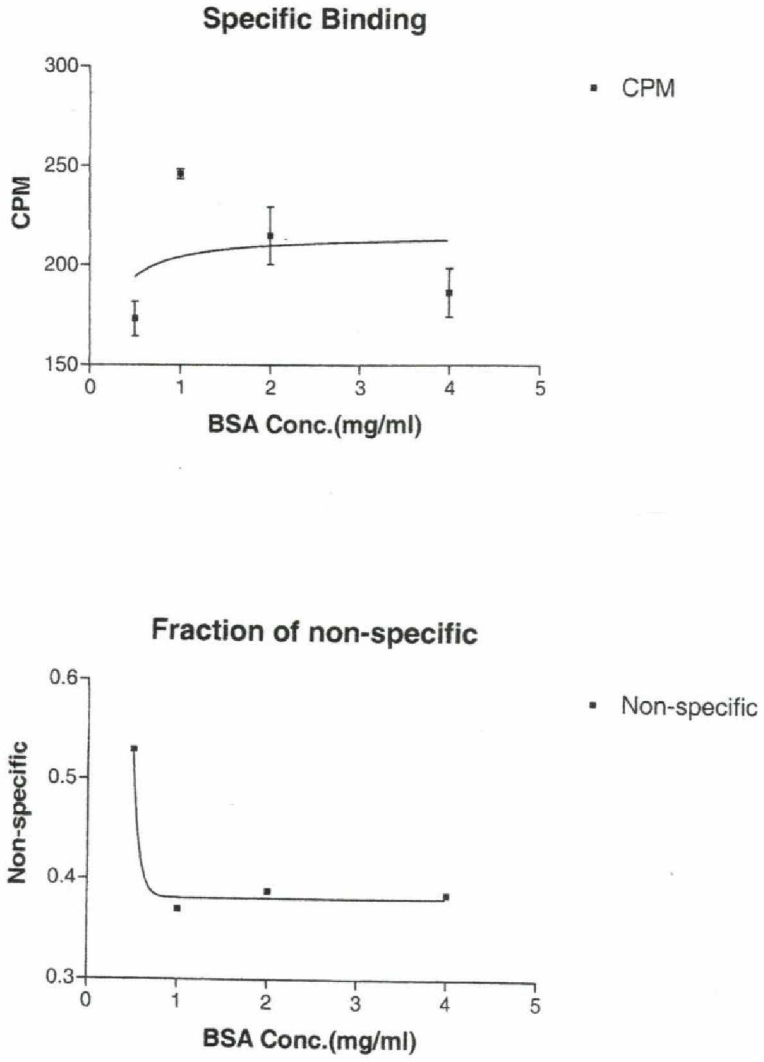

Figure 3.7: Bovine Serum Albumin (BSA) Titration Test. Different concentrations of BSA, SPA beads and radioligand granisetron were used to address high non-specific binding in SPA assay. Top graph shows an increase in specific binding, and bottom graph shows a decrease in non-specific binding as the BSA concentration increased.

AChBP protein (Figure 3.8).

3.7 Functionality of the AChBP

Once conditions for the SPA assay were optimized for binding of [^{3}H]-granisetron, additional binding characteristics of the AChBP protein were explored. For

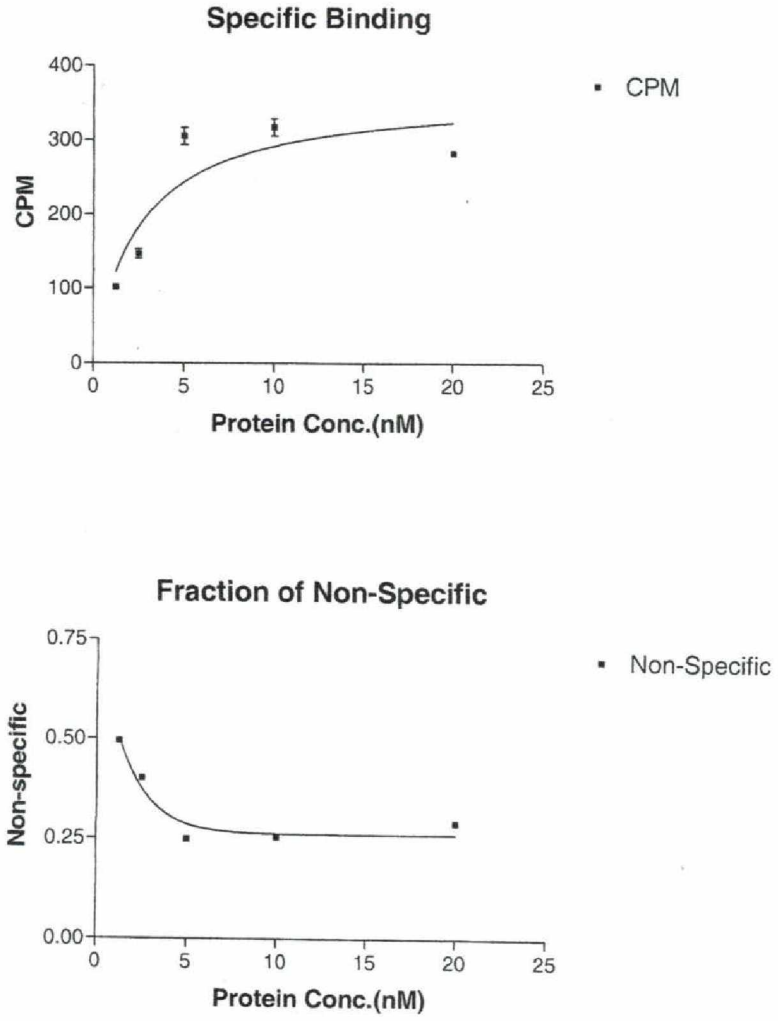

Figure 3.8: The SPA Protein Titration Test. SPA beads, radioligand granisetron, and different concentrations of protein were used for this experiment. Count per minute (CPM) versus protein concentration showed an increase in specific binding as well as a decrease in non-specific binding as the protein concentration increased. The specific binding leveled off at 10nM protein concentration, when all the available beads were utilized.

these assays, the AChBP was immobilized on the SPA beads under optimized conditions as described above (0.2 mg/ml beads, 5 mg/ml BSA and 10 nM AChBP). The 6X His tag on the C-terminal of the AChBP binds to copper on the SPA beads resulting in immobilization of the protein on the bead surface. Different concentrations of radioligand, [^{3}H]-granisetron, were incubated with the protein/bead complex, and the

fraction of bound radioligand was determined by a scintillation counter after a 2 hour incubation period. Nonspecific binding was determined in the presence of 1.0 M acetylcholine, and was subtracted from total binding to give the specific binding of [^{3}H]-granisetron to the AChBP.

To further evaluate the AChBP functionality as a potential biosensor molecule, we explored its ability to interact with other nicotinic ligands in competition with [^{3}H]-granisetron. Since the AChBP is known to bind ligands which also bind to nicotinic acetylcholine (nACh) receptor (100,101,111,112), we tested the nicotinic receptor agonist acetylcholine, as well as the nicotinic receptor antagonist d-tubocurarine (dTC).

The nACh receptor is a cation-selective member of the pentameric ligand-gated ion channel (LGIC) family also commonly referred to as the "Cys-loop" family (4,5). Other members of this family include serotonin type 3 receptors (5-HT$_3$), glycine and GABA receptors (4). Since the primary goal of this Dissertation is to evaluate the AChBP as a potential lead molecule in the development of a soluble biosensor protein that mimics the 5-HT$_3$ receptor, we also evaluated the binding of serotonergic ligands to the AChBP using the SPA assay. Previous data from our laboratory showed that the AChBP protein binds tightly to serotonin antagonists granisetron and dTC, but it binds weakly to serotonin receptor agonists such as serotonin (113). In these experiments, we assayed the following ligands: serotonin (a serotonin receptor agonist); 5-HT$_3$ receptor partial agonists m-chlorophenylbiguanide (mCPBG) and 2-Methyl-serotonin (2-Me-5HT); and the 5-HT$_3$ receptor antagonist granisetron (9,19).

The data in this section is divided into: a) direct binding of the AChBP with [^{3}H]-granisetron, and b) competition binding assays using the nicotinic and serotonergic ligands described above. Both types of binding assays utilized the SPA as the biosensor platform.

3.7.1 The AChBP Binding Assay

For evaluation of [^{3}H]-granisetron binding, 10 nM of the AChBP protein, 5mg/ml of BSA, and 0.2 mg/ml of the SPA beads per sample well were used. [^{3}H]-granisetron concentrations were varied between 0.00-and-100 nM. Similar to conventional binding assays, the equilibrium binding constant or dissociation constant (K_d) for the radioligand

[^{3}H]-granisetron was determined from a plot of radioligand concentration vs. fraction bound. Data was analyzed using GraphPad Prism software. The K_d value was calculated using the simple one-site binding model shown below:

$$Y = B_{max} * X / K_d + X$$

where X is the radioligand [^{3}H]-granisetron concentration, Y is the amount bound in counts per minute (CPM), K_d is the binding affinity, and B_{max} is the calculated maximal binding. The K_d value for the [^{3}H]-granisetron was determined to be 19.4 nM with the standard error of 4.5 (19.4 ± 4.5 nM) (Figure 3.9).

3.7.2 The AChBP Competition Assays

[^{3}H]-granisetron was utilized as the radioligand in competitive binding assays. Competition experiments used the K_d value of the AChBP for [^{3}H]-granisetron concentration in nM; therefore, the concentration of [^{3}H]-granisetron was fixed at 20 nM. In addition, 10 nM of the AChBP protein, 5mg/ml of BSA, and 0.2 mg/ml of the SPA beads were added to each sample well. At least 8 concentrations of competitor ligand in 3-fold increasing concentrations were used to acquire the final data. Competing ligand was added prior to addition of the radioligand, and was incubated with the AChBP protein and the SPA beads for 1-hour at ~21 º C (room temperature). Once radioligand was added, the combined mixture was incubated at room temperature on a shaker (with low speed) for a minimum of 2 hours before the radioactivity level was measured and counted by the scintillation counter.

Competition assays determine the IC_{50} value (in nM or µM), which represents the concentration of a ligand/drug that is required for 50% inhibition. The IC_{50} of cold (non-radioactive) ligands for the inhibition of [^{3}H]-granisetron was determined by using the sigmoidal dose-response equation below and GraphPad Prism software:

$$Y = B_{max} / (1 + 10^{([\log(IC50)-X] * n)})$$

where X is the logarithm of the concentration of cold ligand, Y is the response in count per minute (CPM), and n is the Hill-slope.

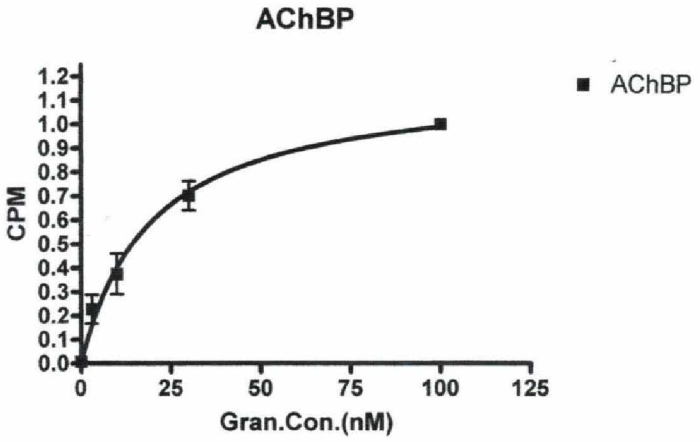

Figure 3.9: Kd for the AChBP. The dissociation constant (K_d) of the AChBP for the radioligand [^{3}H]-granisetron was determined from a plot of radioligand concentration vs. fraction bound. The K_d value was calculated using the simple one-site binding model and GraphPad Prism software, and was determined to be 19.4 ± 4.5 nM.

d-tubocurarine Assay

d-tubocurarine (dTC) is an antagonist for nicotinic ACh, 5-HT$_3$ receptor, and the AChBP (19,21). Nine concentrations of dTC were used to carry out this assay (Figure 3.10A). The IC_{50} of dTC for the inhibition of granisetron was determined to be 14.4 nM. The result is consistent with the previous data from our laboratory indicating that the AChBP binds tightly to serotonin antagonists (113).

Acetylcholine Assay

Acetylcholine (ACh) is an agonist for both nicotinic ACh and the AChBP (19,21). Twelve concentrations of acetylcholine were used for this competition assay (Figure 3.10B). The IC_{50} of acetylcholine for the inhibition of granisetron was 3.16 μM which shows strong interaction and binding between the AChBP and ACh.

Serotonin Assay

Serotonin (5HT) is a serotonin receptor agonist (19,21). Eight concentrations of 5HT were used to carry out this assay (Figure 3.10C). The IC_{50} of 5HT for the inhibition

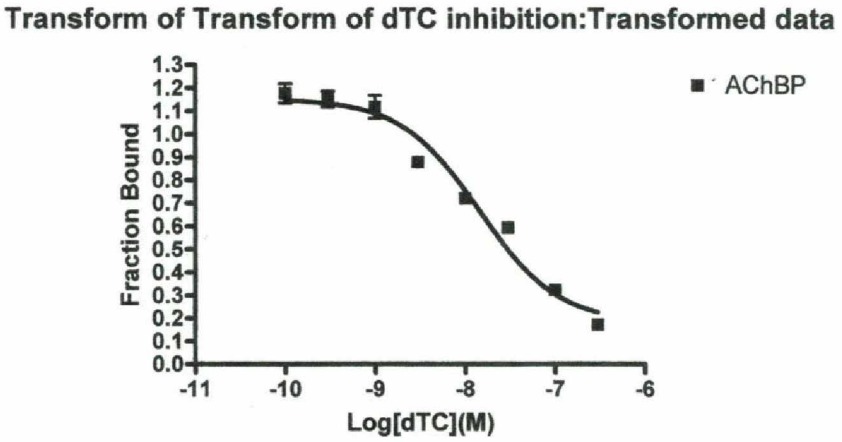

Figure 3.10A: dTC Inhibition Assay. The IC_{50} of dTC, an antagonist for nicotinic ACh, 5-HT_3 receptor, and the AChBP, for the inhibition of granisetron was 14.4 nM.

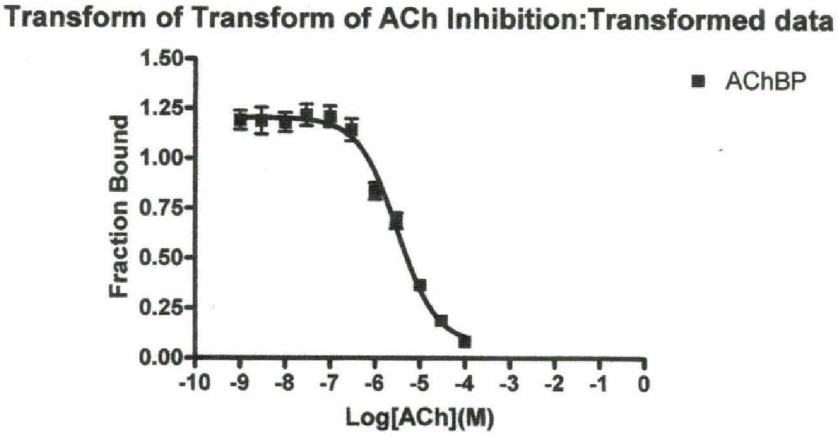

Figure 3.10B: ACh Inhibition Assay. The IC_{50} of ACh, an agonist for both nicotinic ACh and the AChBP, for the inhibition of granisetron was 3.16 µM.

of granisetron was determined to be 640 µM, which is consistent with previous data from our laboratory regarding weak binding of the AChBP to serotonin agonists (113).

m-chlorophenylbiguanide Assay

m-chlorophenylbiguanide (mCPBG) is a partial agonist for serotonin receptor (19,21). Eight concentrations of mCPBG were used for this competition assay (Figure 3.10D). The IC_{50} of mCPBG for the inhibition of granisetron was 344 µM. This data

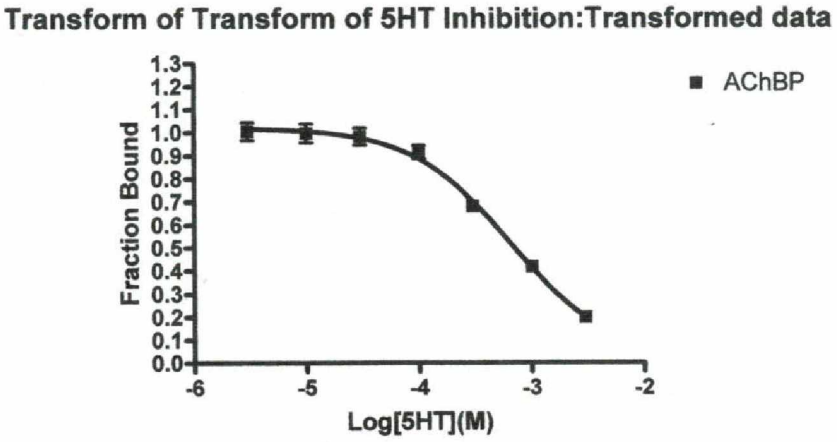

Figure 3.10C: 5HT Inhibition Assay. The IC_{50} of 5HT, a serotonin agonist, for the inhibition of granisetron was 640 μM.

shows a stronger interaction between mCPBG and the AChBP when compare to the data from serotonin competition assay. The result is likely due to structural differences in the binding site which has made mCPBG a partial-agonist for serotonin.

2-Methyl-serotonin Assay

2-Methyl-serotonin (2-Me-5HT) is a serotonin receptor partial agonist (19,21). Eight concentrations of 2-Me-5HT were used to carry out this assay (Figure 3.10E). The IC_{50} of 2-Me-5HT for the inhibition of granisetron was 41 μM. This data shows a very strong interaction between 2-Me-5HT and the AChBP when compared to data from serotonin and mCPBG competition assays. The result is likely due to structural differences in the binding site which has made 2-Me-5HT to behave more like a serotonin antagonist (instead of partial-agonist) when interacting with the AChBP. While the AChBP is not a ligand-gated ion channel, it has been shown that conformational changes occur upon binding of agonists, and that most likely, the AChBP protein shifts from a low affinity to a high affinity agonist binding conformation.

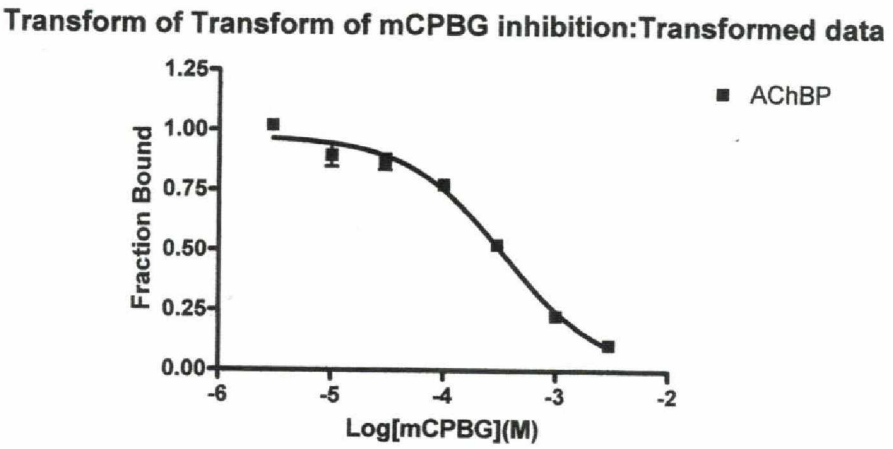

Figure 3.10D: mCPBG Inhibition Assay. The IC_{50} of mCPBG, a partial agonist for serotonin, for the inhibition of granisetron was 344 μM.

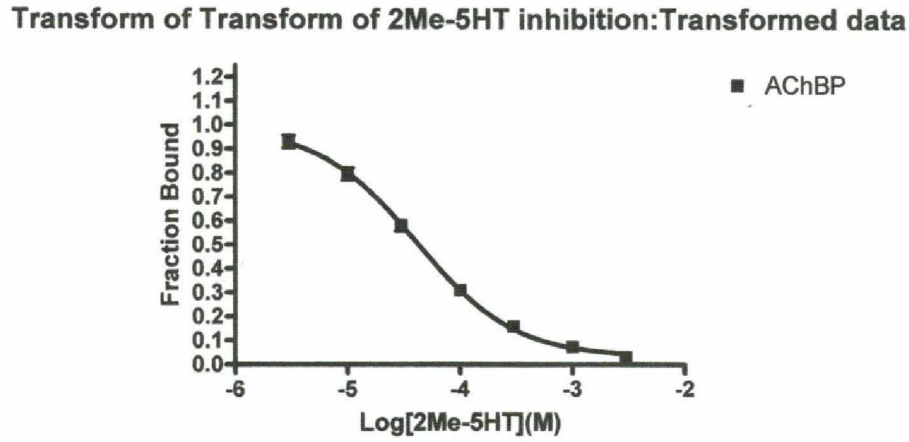

Figure 3.10E: 2-Me-5HT Inhibition Assay. The IC_{50} of 2-Me-5HT, a partial agonist for serotonin, for the inhibition of granisetron was 41 μM.

3.8 Evaluation of the AChBP as a Sensor Protein using a Microcantilever Biosensor Platform

Based on our experience and success with the production and lyophilization of the AChBP protein, a large quantity of dried AChBP was sent to the laboratory of our collaborator, Dr. Hai-Feng Ji, to be tested using the microcantilever biosensor. In that work, microcantilever bending was used for an AChBP-analyte binding study, which has applications in drug screening and drug development. Binding of the AChBP to small

molecules such as acetylcholine (AChBP full agonist), nicotine (AChBP partial agonist), and *d*-tubocurarine (AChBP antagonist) were studied to verify the specificity of microcantilever bending, resulting from binding of ligands to the AChBP receptor, and to identify any variation in binding kinetics for agonists versus antagonists. The data demonstrated that all the ligands produced a deflection of the microcantilever coated with the AChBP, which is the result of binding of ligands with the AChBP. The mechanism responsible for producing deflections of the AChBP-modified microcantilever in response to ligand binding may be due to a slight conformational change of the AChBP on the microcantilever derived from the binding of the ligands to the AChBP. The data showed that the B_{max} for nicotine and *d*-tubocurarine were much less than that for acetylcholine, which reflects a difference in conformational change of the AChBP on the surface. Partial agonists and antagonist, such as nicotine and *d*-tubocurarine, would likely produce smaller conformational changes compare to a full agonist like acetylcholine. Taken together, the results demonstrated that the AChBP binds to different agonists and antagonists, and that the AChBP-modified microcantilever can be used to study the interactions of small molecules with the AChBP. These results were published in a paper entitled "Micromechanical measurement of the AChBP binding for label-free drug discovery"(118). The similarity of data from both the microcantilever and SPA assays validates the use of our synthetic AChBP as a viable sensor molecule.

3.9 Conclusion

The data presented in this chapter demonstrated the successful production of the AChBP protein using HEK-293 cells, as well as the AChBP synthesis, storage, attachment and utilization as a biosensor molecule. The data also validated the scintillation proximity assay (SPA) and the microcantilever assay as fast and effective biosensor platforms for determining the binding properties of different ligands to the AChBP protein. In particular, the ease of use and availability of the SPA platform proved to be very useful for developing a high-throughput analysis of receptor-drug interactions. The limitation of the AChBP is that it has a broader selectivity than the LGIC receptors; hence, modifications will be required to enable its use in drug

development. The goal of developing a soluble biosensor molecule with 5-HT_3 receptor-like selectivity is a primary goal of this thesis. The next chapter explores approaches to modification of the AChBP to mimic the 5-HT_3 receptor.

Chapter 4: Mutations of the AChBP

4.1 Introduction

As described in Chapter 3, the soluble nature of the acetylcholine-binding protein (AChBP), the effective production of the AChBP protein using HEK-293 cells, and its successful purification and subsequent utilization as a biosensor protein makes the AChBP an ideal lead molecule for developing a family of biosensor proteins. In addition, the scintillation proximity assay (SPA) experiments in Chapter 4 demonstrated the potential of SPA for high-throughput screening application, as well as the AChBP as an ideal biosensor molecule for attachment to biosensor surfaces; both of which would be useful tools for drug screening and drug development.

The high sequence homology of the AChBP (15-30%) with the amino terminal domain of ligand-gated ion channel (LGIC) receptors (20,99), and the apparent structural similarity of the AChBP and LGIC binding sites (102,103) raises the possibility that the AChBP could be engineered for use as a biological sensor to mimic LGIC receptors (e.g. Glycine, GABA, Serotonin type 3), and detect LGIC ligands. In order to engineer an AChBP that selectively recognizes different classes of LGIC, the key amino acids in the binding site of the AChBP would need to be mutated to the homologous amino acids of the target LGIC receptor. This is the first step in developing a soluble homolog of a LGIC receptor. Prior to this study, no experiment of this type had been carried out despite the fact that the AChBP has been extensively used as a template to generate ligand-docked computer models of LGIC receptor to study and analyze receptor-ligand interactions (107,119).

Among members of the LGIC family of receptors, the AChBP appears to be most similar to the α7-nACh and serotonin type 3 (5-HT_3) receptors (107,120), and is considered a naturally occurring, soluble homolog of the amino terminal region of these receptors (93,95,101,105). Both the α7-nACh and 5-HT_3 receptors are monomeric pentameric receptors. Domains of these receptors have been shown to be so compatible that the amino terminal of an α7 receptor can be substituted in a 5-HT_3 receptor and produce a functional pentamer (121). This chimeric receptor responds to serotonin but has channel characteristics of the α7 receptor.

Serotonin type 3 receptors are located in both the central and peripheral nervous systems (8,10). The ion channel of this receptor, like the nACh receptor, is cation-selective, and mediates neuronal depolarization and excitation within the nervous systems. The natural ligand of 5-HT_3 receptor is serotonin, which modulates the release of multiple neurotransmitters such as dopamine, glutamate, epinephrine, and GABA (10). 5-HT_3 receptors are involved in multiple nervous system disorders including alcohol and drug dependence, anxiety, depression, schizophrenia, sleep, cognition, memory, and chemotherapy-induced and post-operative nausea and vomiting (13,15,122). Thus, there are multiple drugs to target these disorders including antidepressants, anxiolytics, antiemetics, antipsychotics, and antimigraine, and the ligands that target the 5-HT_3 receptors are considered powerful therapeutic agents (13). As a result, 5-HT_3 receptors have been targets of drug discovery efforts (15,123). The number of available ligands for the 5-HT_3 receptors and the extensive structure-activity relationship (SAR) available for this receptor makes it an excellent model system for the AChBP engineering studies described in this thesis.

Alignment of the AChBP binding domain sequence with the equivalent amino terminal sequence of 5-HT_3 serotonin receptor (Figure 4.1) reveals a significant structural similarity (99,115). While the AChBP has only a 20% sequence homology with the extracellular ligand-binding domain of 5-HT_3 serotonin receptors (20), models of 5-HT_3 receptors have been developed based on the AChBP crystal structure that accurately predict interaction of ligands with the receptor (18,115,124,125). From earlier studies on the nACh receptor, it was hypothesized that 5-HT_3 receptor binding site was composed of six binding loops present in other LGIC receptors; and currently, most of the amino acids comprising the A-F binding loops have been identified (16,93). As a result, it has been noted that with the exception of GABA receptor, all LGIC receptors and the AChBP have a Tryptophan (W) in their aromatic box in the B-loop which is implicated in ligand binding (20,126).

In addition to structural similarity between the AChBP and 5-HT_3 receptor, and the extensive SAR studies of the receptors, a large number of studies have been conducted to understand the binding interactions of 5-HT_3 receptors and ligands (17,120,124,127). Using ligand-docked models, both antagonist and agonist binding

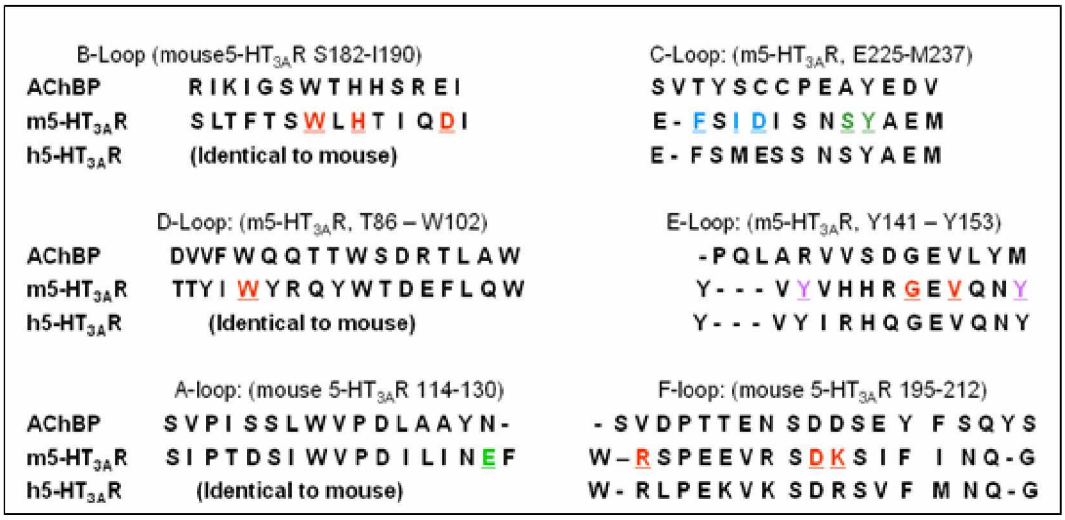

Figure 4.1: Sequence Alignment of Binding Loops in the AChBP and 5-HT$_3$ Receptors. Aligned sequences: *Lymnaea stagnalis* AChBP (AChBP), murine 5-HT$_3$ receptor (m5-HT$_{3A}$R) (115), and human 5-HT$_3$ receptor (h5-HT$_{3A}$R) (99). The underlined amino acid residues indicate their significance (mutations to alanine have a ten-fold or more effect on binding) for binding to 5-HT$_3$ receptor agonist serotonin (blue); 5-HT$_3$ receptor antagonist granisetron (red); 5-HT$_3$ receptor antagonist lerisetron + agonist serotonin (purple); agonist serotonin + antagonist granisetron (green) (113).

models have been proposed for 5-HT$_3$ receptor (16,20,120,125). Extensive site-directed mutagenesis has been used to identify structural and functional features of this receptor. Our laboratory has been particularly active in working with 5-HT$_3$ receptors, and has conducted site-directed mutagenesis on loops A-D of the binding domain (18,20,21,124). Molecular models based on these studies have been developed by previous graduate students to describe the binding of granisetron to the 5-HT$_3$ receptor including all key residues thought to interact with granisetron (20,124). These models lead to the hypothesis that binding of granisetron to the AChBP would be similar to the 5-HT$_3$ receptor, and that the affinity of granisetron for both receptors would be similar based on the conservation of residues that are important for granisetron binding.

A comparison of mutagenesis data from the 5-HT$_3$ serotonin receptor and structural data from the AChBP, as well as the deduced structural similarities between the two, suggests that similarly placed residues perform parallel functions in both the AChBP and 5-HT$_3$ receptor (16,113,124). Taken together, it would seem that construction of a soluble serotonin-binding protein with specificity and sensitivity similar

to the human 5-HT_3 receptors, which in turn could result in development of a molecular biosensor for serotonin, should be possible and would produce a valuable tool to use in drug development. In addition, this method can serve as a template for conducting similar studies on other LGIC receptors.

4.2 Experimental Approach

The structural similarity of the AChBP to other LIGC receptors suggests that the AChBP can be modified and engineered to mimic the selectivity of other receptors. The primary aim of this project is to engineer the AChBP to produce a water-soluble serotonin-binding protein (or biosensor) that precisely mimics the specificity of native 5-HT_3 receptors.

To accomplish this aim, two approaches could be utilized to alter the specificity of the AChBP, namely, a) site-directed mutagenesis of the AChBP binding site, or b) construction of chimeric receptors incorporating regions of the 5-HT_3 receptor into the AChBP. The two approaches are intended to provide two alternative paths to the same goal; however, they require different timeframes and provide distinct types of information. For example, site-directed mutagenesis experiments would take a long time to develop and carry out, but the end results provide valuable information regarding binding sites in both the AChBP and serotonin; whereas chimera experiments do not take as long as mutagenesis, but little data about binding sites would be gained since, if they are non-functional, it is difficult to determine the reason. Non-functional receptors could be the result of poor folding, transport or any number of other issues. We attempted an α7/AChBP chimera to determine if an α7-Binding Protein (α7-BP) could be quickly generated, but as described below, the complex did not appear to assemble correctly and completely. As understanding this lack of assembly clearly would require substantial additional study including site-directed mutagenesis, the studies described in this chapter are primarily focused on more methodical, site-directed mutagenesis.

4.2.1 Chimeric Approach: α7-Binding Protein Studies

Initial attempts to create a modified AChBP were based on the α7 receptor and the premise that the receptor could possibly be truncated prior to the M1

transmembrane (TM1) region, if appropriate changes were made to eliminate hydrophobic pockets on the α7 protein that would be exposed when the receptor was removed from the cell membrane. A chimeric receptor was constructed using the amino terminal region of the α7 receptor combined with regions of the AChBP that are thought to contribute to its ability to express independent of a transmembrane domain. Specifically, the cys-loop region of the N-terminal domain of α7 receptor was replaced by the identical region of the AChBP; and a second substitution replaced the C-terminal end of the α7 receptor with C-terminal from the AChBP. Therefore, regions that had previously been in contact with the hydrophobic TM1-TM2 extracellular loop were replaced with the more hydrophilic regions found in the AChBP. The chimera also contained a signal sequence to enable secretion of the protein into the surrounding media, as well as an N-terminal FLAG epitope tag and a C-terminal His tag to allow for affinity purification.

The chimeric construct, the α7-Binding Protein (α7-BP), was incorporated into a pcDNA3.1 vector, and the vector was transformed into XL-1 blue supercompetent *E.Coli* cells using standard protocol and reagents (Stratagene). DNA was purified from these cells by DNA maxi-prep (Qiagen), and the presence of α7-BP cDNA was verified by restriction digest and agarose gel electrophoresis. The full length α7-BP chimera DNA including the FLAG and His-tagged regions was transfected into HEK-293 cells using the SuperFect reagent kit and standard protocol (Qiagen). Stable cell lines were developed and cultured. Culture medium was collected and any His-tagged proteins purified using Nickel-EDTA His-Select Columns (Sigma). Protein was eluted using imidazole, and then isolated from the eluent by filtration as described in Chapter 2 (Materials and Methods). The protein yield was analyzed by Lowry assay (Sigma) and precast tris-HCl BioRad gels using standard methods.

Gel electrophoresis was performed under denaturing and non-denaturing (or native) conditions (Figure 4.2). The α7-BP protein was identified as about 30kD band under denaturing condition. The native gel showed a very faint band when the same amount of protein as denaturing gel was used (data not shown); therefore, the amount

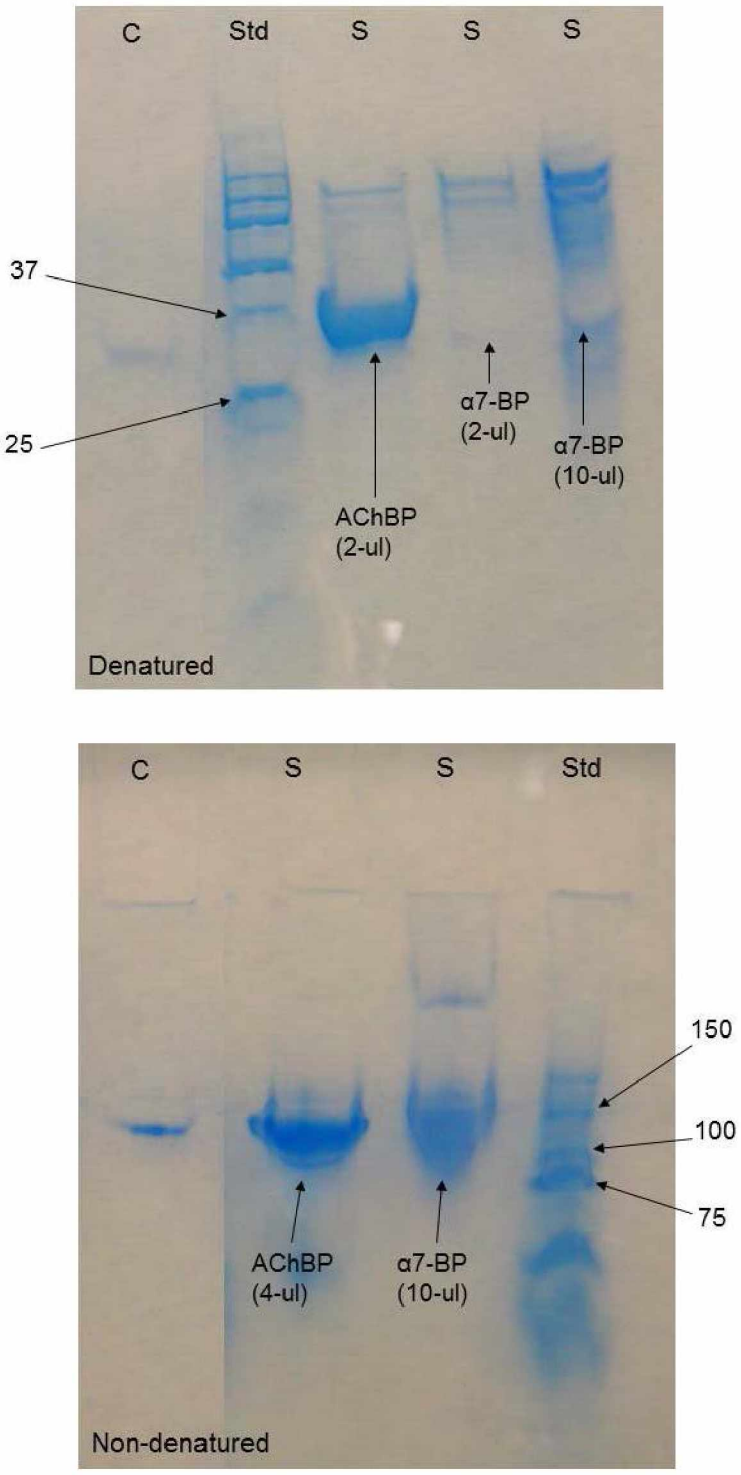

Figure 4.2: 10% Polyacrylamide Gels of α7-Binding Protein. Assembly of α7-Binding Protein (α7-BP) was determined using denaturing and native PAGE. The AChBP protein is added for comparison purposes, and concentrations of both proteins were normalized. The top gel shows the result of SDS PAGE (denaturing conditions) and the bottom gel shows the result of separation under non-denaturing conditions (PAGE). Gels were stained with coomassie blue stain (BioRad) (continued on the next page).

Figure 4.2 (continued): The protein sample lanes are indicated by S, control by C, and the BioRad Kaleidoscope standard by Std. **Denatured** (SDS): Control sample is visualized at 30kD, and the AChBP protein at a region between 25 and 37kD as expected for the monomeric protein. 5X concentration of α7-BP protein (compared to the AChBP) was used for clear visualization. **Non-denatured** (no SDS): The AChBP protein migrated to a region equivalent to 150kD which is consistent with the predicted molecular weight of the pentameric AChBP. 2.5X concentration of α7-BP protein (compared to the AChBP) was used for visualization.

of sample loaded onto the gel was increased by 5-times to better identify the presence of the protein. The data from the denaturing gel indicates the synthesis of individual subunits, but does not indicate if the subunits assemble into a functional protein. The faint band in the native gel at an approximate MW ~ 150kD, likely corresponds to subunit assembly, although the broad diffused band may also suggest incorrect assembly. Possible explanations include: a) substitution of large regions of structure could have decreased the ability of the subunits to form correct contacts, or b) the large substitution might have decreased structural stability of the receptor for proper assembly and chimeric protein expression.

It took several transfections and follow up steps before we were able to see any protein on the gel electrophoresis. On average, Lowry assay showed that concentration of α7-BP protein was $1/5^{th}$ to $1/3^{rd}$ of control, the AChBP protein, which was not sufficient for binding assays. Since concentration of the α7-BP protein never improved after multiple tries, which can signal the failure of construct to produce adequate intact binding proteins, and the fact that chimeric constructs do not provide information regarding the receptor binding site, we decided to utilize the second approach or site-directed mutagenesis to explore the development of a serotonin-binding protein.

4.2.2 Site-directed Mutagenesis Approach

The cys-loop LGIC proteins are composed of five protein subunits that form a pentameric arrangement around a central pore. Each subunit consists of a large extracellular N-terminal domain, four transmembrane regions (M1-M4), and intracellular domain (1). The pore is primarily formed by the M2 helices of five subunits. The agonist binding site is located at the interface between two adjacent subunits in the extracellular domain; therefore, five potential binding sites exist in the pentameric

receptors. Binding sites are composed of six loops of amino acids referred to as A-F (5,6).

Based on modeling and mutagenesis data, it appears that the ligands for LGIC receptors primarily utilize loops B, C, D, and E for their binding (5,126). Loop-A is hypothesized to play a role in initial ligand selection (99,128), and loop-F is suggested to be involved in the binding of all ligands by forming a flexible structure (129,130). While LGIC receptors have different amino acids, similarly positioned amino acids appear to play similar roles in interaction of the receptor with ligands (113,124). These binding loops are also key to transducing binding to conformational changes in LGICs that produce channel opening (3,6). A key receptor region in both binding of agonists and conformational change in the LGIC receptors is the C-loop. C-loop closure on binding of the ligand appears to be required for agonist action, and inhibition of this closing may contribute to the mechanism of competitive antagonists (5,126). The binding loop is highly variable between LGIC receptors that bind different classes of agonists (5,126).

It is known that the AChBP has a high affinity for nicotinic agonists (e.g. acetylcholine, nicotine, epibatidine), and antagonists (e.g. d-tubocurarine, bungarotoxin, conotoxin) (17,126). Previous data from our laboratory showed that the AChBP has a high affinity for serotonin antagonists (e.g. granisetron, d-tubocurarine, tropisetron, lerisetron, epibatidine), due to highly conserved residues in the B-and-D binding loops of both the AChBP and 5-HT_3 receptor (113). On the other hand, the AChBP displays low affinity for serotonin agonists (e.g. serotonin, 2-Me-5HT, PBG, mCPBG) due to large sequence differences between the AChBP and 5-HT_3 receptor in regions critical for agonist binding, particularly the C-and-E loops (113).

To convert the AChBP to a 5-HT_3 binding protein, we systematically mutated those amino acids in the A, C and E loop that were known to be critical for recognition and binding of serotonin ligands to the appropriate 5-HT_3 residues (113,124) using site-directed mutagenesis. Mutations were made as single and multiple site mutations with the goal of changing the selectivity of the AChBP to favor 5-HT_3 ligands over nicotinic ligands.

To determine if the binding characteristics of the mutated proteins were intact, we utilized scintillation proximity assay (SPA) as our standard method of evaluating binding interactions for the AChBP and AChBP-derivatives. This technique enables rapid evaluation of radioligand binding characteristics with minimal amounts of protein (113,117). SPA does not have a filtration step, which makes it easier to automate this technique and develop high-throughput assays. Since the receptor is covalently linked to the beads using an approach common to other biosensor surfaces, this approach also facilitates use of other surfaces including microcantilever (MC) (78,81) and surface plasmon resonance (SPR) sensors (77,80). [^{3}H]-granisetron was selected as the radioligand for SPA since it binds to both the AChBP and 5-HT$_3$ receptor (21,113). By monitoring changes in granisetron binding, the general structural impact of mutations on the binding site can be monitored. Previous modeling data from our laboratory predicted that the affinity of both the AChBP and 5-HT$_3$ receptor for [^{3}H]-granisetron would be similar since amino acid residues that are important in granisetron binding are conserved in both the AChBP and 5-HT$_3$ models (19,20,113,124).

It should be noted that the current project drew heavily on our laboratory's experience and a wealth of prior structure and functional studies with: a) LGICs, b) extensive site-directed mutagenesis studies, c) biosensor experiences, and d) previous work and data collected for 5-HT$_3$ receptors (19-21,113,124,131). This project is a highly ambitious protein engineering project since it is the first time that the AChBP has been investigated as a potential biosensor molecule for development of a soluble homolog of a non-nicotinic LGIC receptor. No binding protein has yet been developed with the ligand specificity of the 5-HT$_3$ receptor despite the fact that the AChBP has been used extensively as a template to generate models of LGIC receptors, including the 5-HT$_3$ receptor (9,93,115,124).

4.3 Selection of the AChBP Amino Acid Mutation

Alignment of the amino terminal sequence of the 5-HT$_3$ receptor with the AChBP reveals significant sequence similarity (Figure 4.1). This similarity has been used for the development of several homology models of the 5-HT$_3$ receptor biding site (16,18,124). From homology models, ligand-docked models have been developed, and

both agonist and antagonist binding models have been proposed (8,115,127). Agonist models have focused on the full agonist serotonin (5-HT), and the partial-agonist m-chlorophenylbiguanide (mCPBG) (16,103,106,124,127). Antagonist models have focused on the classical antagonist granisetron which has one aromatic group and the non-classical antagonist Lerisetron with two aromatic groups (10,19,20,125,129).

Homology models of the 5-HT_3 receptor show the binding site for agonist and antagonist is located at the interface between two adjacent subunits in the N-terminal, extracellular domain of 5-HT_3 receptor (16,17). Therefore, five potential binding sites exist in the pentameric 5-HT_3 receptors. Binding sites are composed of six loops of amino acids referred to as A-F. Each subunit contributes three loops on each of its two interfaces with loops A-C located on one interface (the ' + ' face), and D-F located on the opposing interface (the ' – ' face) (8,16). Key residues in these loops of the homomeric 5-HT_3 receptor, as well as the AChBP mutants are described below and summarized in Table 4.1.

Loop-A

Residue N128 of the 5-HT_3 receptor A-loop (equivalent to Y89 of the AChBP) has been proposed to be in the binding pocket (103,125). This residue is identified as a critical residue in ligand binding in the AChBP (99,128); however, data suggest that this residue is not a critical binding residue in the 5-HT_3 receptor as N128 mutations do not significantly alter the binding efficacy of antagonists (129). It has been proposed that the A-loop might be involved in receptor assembly in 5-HT_3 receptors since mutation of W121 and P123 results in receptors that do not reach the cell surface (132-134). It has also been suggested that the most critical A-loop residue is E129 (highlighted in Green in Loop-A, Figure 4.1), as it can modify both binding and function of the 5-HT_3 receptor (22,134). The importance of E129 supports a role for loop-A binding and selectivity of ligands. For this study, N90 in loop-A of the AChBP was mutated to its equivalent E129 residue in the 5-HT_3 receptor. The mutation produces the N90E mutant, replacing asparagine (N) which has an uncharged R-group (side chain) with glutamate (E) which has a negatively charged R-group.

Table 4.1: Mutants. The left-hand column shows the corresponding 5-HT_3 receptor amino acids in murine (m) or human (h), and the right-hand column shows the AChBP mutants.

Loop, m-or-h, 5-HT_3 receptor amino acid	AChBP residue, Mutation
Loop A (m), E129	N90E
Loop E (m), Y143	R104Y
Loop E (m), Y153	M114Y
Loop C (m), F226	T184F
Loop C (m), I228	S186I
Loop C (h), M228	S186M
Loop C (m), S233	A191S
Loop C (m), D229 / I230	C187D / C188I
Loop C (h), E229 / S230	C187E / C188S
Loop C (m), I230 /S231	C187I / C188S
Loop C (h), S230 /S231	C187S / C188S

Loop-B

The primary binding site for all LGIC and the AChBP ligands is the aromatic pocket of loop-B (16). The most important loop-B residue in the 5-HT_3 receptor is W183 (highlighted in Red in Loop-B, Figure 4.1). W183 has been extensively studied, and data has shown the critical nature of W183 for both ligand binding and function (130,135). In the AChBP, this residue is conserved as a tryptophan (W143). Tryptophan is conserved in this position in all LGIC receptors except the GABA receptor which has a tyrosine (Y) in this position (128,136,137). Any mutation of W183 in the B-loop results in loss of ligand binding (130,135). Previous mutagenesis studies have shown that W183 forms a cation- π bind with the primary amine (positive nitrogen) of LGIC ligands such as serotonin (124,130,138). Additional residues previously identified in this loop of the 5-HT_3 receptor are H185, and D190 (16,138). The H185 residue is conserved in both the 5-HT_3 receptor and the AChBP (H145). However, D190 (aspartate) in the 5-HT_3 receptor is equivalent to E149 (glutamate) in the AChBP (20,127). Since both residues have hydrophilic amino acids and carry a negatively charged R-group, the properties of amino acids are conserved while the size is altered. The similarity of the B-loop in both the 5-HT_3 and the AChBP indicate the importance of this loop for general ligand interactions, although it may play a less important role in ligand selectivity other than the preference of the receptor for a positively charged nitrogen group (127,138).

Loop-C

This loop has been investigated intensely since little sequence homology is observed in loop-C between LGIC receptors that bind different classes of agonists (18,124). In addition, this loop differs more substantially between species than any other loop of the 5-HT_3 receptor (13,15,18). This suggests the C-loop may play a key role in ligand selectivity. Earlier studies attempted to find the residues responsible for the difference in the pharmacology of 5-HT_3 receptor in murine and human using point mutations, but the results suggested that multiple regions of the binding site were involved (18,139). Since this is a highly variable region with little sequence homology between the AChBP and 5-HT_3 receptor, the C-loop sequence of these receptors are difficult to align. A number of studies point to Y234 (highlighted in Green in Loop-C, Figure 4.1) in the 5-HT_3 receptor as the most important residue involved in both ligand binding and function (124,140,141). It is suggested that upon binding of an agonist, the C-loop closes over the agonist, bringing Y234 into close contact with tryptophan residue 183 (W183) in the aromatic pocket of B-loop (124,140). This tryptophan appears to produce one part of an aromatic binding domain that forms a key component of the ligand-binding domain in LGICs (5,6). The interactions of agonist with the C-loop are hypothesized to promote stability of this new conformation, thus providing energy for channel opening (6,126). Y234 of the 5-HT_3 receptor appears equivalent to a tyrosine amino acid in the AChBP (Y192), which we used to loosely align the amino acid sequence of the AChBP and 5-HT_3 receptor (18,113). An interesting feature of this loop is the existence of proximal cysteines in the AChBP at positions 187/188 (C187/C188) that is missing in all the LGIC receptors except nACh receptor (98,99). These proximal cysteines produce a slight bulge in the C-loop, and are thought to confer the structural orientation that produce correct positioning of other residues (94,95,104).

It has been hypothesized that loop-C is also involved in the functional effects of binding of agonist versus antagonist, and may play a critical role in mediating the conformational change to the receptor in response to agonist (18,140). For agonist binding, the C-loop is thought to close more completely over the ligand compared to antagonists (18,130,140). The degree of C-loop closure may determine if a particular ligand is an antagonist, agonist or partial-agonist. Previous data from our laboratory

showed that the AChBP has a low affinity for serotonin agonists and a high affinity for its antagonists (113). By mutating certain amino acids in the C-loop of the AChBP to appropriate 5-HT_3 receptor residues, we hope to change the selectivity of the AChBP to closely resemble that of the serotonin receptor. This loop in particular may help explain why serotonin antagonists, but not agonists, generally bind to the AChBP. We chose to construct both single and double mutations to investigate if: a) our alignment of C-loop was correct, and b) to study the effect of removing the proximal cysteines of the AChBP on ligand binding.

Single mutations of C-loop amino acids are highlighted in blue or green in Figure 4.1, and include F226, I228, D229, S233, and Y234:

a) F226 and S233 of the serotonin receptor are involved in agonist binding (18,124); therefore, we mutated the equivalent AChBP amino acid (T184 and A191) to the homologous serotonin residue to produce the T184F and A191S mutations.
b) As mentioned, Y234 of the 5-HT_3 receptor has an equivalent tyrosine amino acid in the AChBP (Y192), and these tyrosines were used to loosely align the amino acid sequence of the AChBP and 5-HT_3 receptor. The AChBP proximal cysteines were aligned with D229 and I230 of the 5-HT_3 receptor. Given the likely structural importance of this region of the C-loop and presence of a proline (P189) adjacent to the proximal cysteines of the AChBP, we decided to mutate the amino acids on each side of the proximal cysteines (AChBP amino acids S186 and P189) to their equivalent residues in the m5-HT_3 receptor (I228 and S231 respectively). The resulting S186I and P189S mutations should produce alterations in the C-loop structure similar to that observed in the 5-HT_3 C-loop. The C-loop of the 5-HT_3 receptors from human and mouse differ in one position (I228), thus a human equivalent to the S186I mutation was also constructed to produce the S186M mutation.

Double amino acid mutations of the C-loop were also constructed. Since the C-loop contains structural differences (proximal cysteines/proline), deletion (one less residue in the 5-HT_3 receptor), and several non-conserved residues, it presents a challenging engineering target. In addition, it is thought that all ligands (agonist or antagonist) bind

to the C-loop, making it an important component of the binding site (18,124). In engineering this region, the following were considered key observations:

a) It has been suggested that the low affinity of the AChBP for serotonin agonists might be due to the presence of proximal cysteines (104,113,142); therefore, we decided to mutate those cysteine residues to their equivalent amino acids in the 5-HT_3 receptor to make the AChBP more like serotonin receptor and study the effect of cysteine removal on the AChBP affinity for serotonin agonist. Since 5-HT_3 receptor residues equivalent to the C187 and C188 of the AChBP are also different between murine and human receptors, we also mutated the AChBP proximal cysteines to their equivalent in human receptor. The end result was production of C187D / C188I (mouse equivalent) and C187E / C188S (human equivalent) mutants.

b) The amino acid sequences of the AChBP and 5-HT_3 receptors were loosely aligned, using tyrosine residues, which are hydrophobic amino acids. To verify this alignment, an alternate alignment was tested by aligning Y192 of the AChBP with A235 of the murine receptor, effectively shifting the alignment of the C-loop region by one residue. Based on this new alignment, the proximal cysteines of the AChBP were mutated to the alternate equivalent residues for the 5-HT_3 receptor in both murine and human receptors. These mutations correspond to C187I / C188S (murine) and C187S / C188S (human) mutants.

c) A third option which was not constructed was the potential deletion of V183 in the C-loop of the AChBP. Given other substantial structural and sequence differences, this would be unlikely to produce positive effects; however, it is possible this deletion could produce improvements if combined with the other mutations described above. This deletion mutation was thus considered premature until the effect of other mutations was considered.

Loop-D

Two aromatic residues have been shown to be important for agonist and antagonist interactions in the loop-D of 5-HT_3 receptor, namely W90 and W95. W90 is critical for ligand binding, while W95 affects cell surface expression (129,130). Both of

these residues have an equivalent tryptophan amino acid in the AChBP (W53 and W58) that are also important in binding (101,143), indicating that this position is functionally similar in both receptors. The D-loop of 5-HT_3 receptor and the AChBP are highly homologous in this region, with only small differences observed and critical residues identical between the two proteins (101,130,144).

Loop-E

A homologous glycine (G148) was used to align the residues of 5-HT_3 receptors and the AChBP since glycine likely produces a sharp and very tight β-turn in the middle of the loop. A glycine residue cannot be replaced as any mutation of this amino acid would typically produce structural changes. Different studies of the 5-HT_3 receptor have shown that Y143, G148, V150, and Y153 are likely important for granisetron binding to serotonin receptor, and mutation of G148 and V150 completely abolished granisetron binding (21). Both of these residues have an equivalent glycine and valine amino acid in the AChBP (G109 and V111). Two tyrosine residues of 5-HT_3 receptor, Y143 and Y153, have been shown to be involved in receptor function (140), and Y153 also has a role in ligand binding (141). It is suggested that as the C-loop closes over the agonist, these tyrosines, especially Y153, interacts directly with the ligand and stabilizes the new position of the ligand (21,140). We decided to mutate the R104 and M114 residues from loop-E of the AChBP to its equivalent Y143 and Y153 residues in 5-HT_3 receptor, resulting in R104Y and M114Y mutants.

Loop-F

In the AChBP crystal structure, the F-loop region was poorly resolved (99). Early functional studies suggested loop-F had two distinct regions: the upper region that lines the binding pocket and the lower region that acts as a link between ligand binding and channel opening (115). Several studies suggested loop-F may play a role in locking the agonist molecule into the binding site, and thus resulting in a local structural rearrangement (111). To date, mutational information suggests that loop-F is the most flexible region in the receptor during activation, and that it is involved in ligand binding and activation (98,111).

4.4 Methods

Once the AChBP amino acids for single-site and double-site mutations were determined as explained above, oligonucleotides were created to generate mutations, and mutant receptors constructed as described in the Materials and Methods, Chapter 2. Oligonucleotides were designed using the DNA Strider program, and custom designed DNA oligonucleotides corresponding to the desired mutations were ordered through The Midland Certified Reagent Co., Inc. Using these oligonucleotides, mutations were constructed with the QuickChange II Site-Directed Mutagenesis kit (Stratagene) using the standard methods with the following modifications: 50 ng of the AChBP DNA and a pair of designed oligonucleotides for a specific mutation were used for each Polymerase Chain Reaction (PCR). The PCR machine was programmed for 18 cycles of denaturation for 1-minute at 95 ºC, annealing for 1-minute at 60-65 ºC (it was always 10 ºC less than oligo's temperature), and extension for 9-minutes at 68 ºC. PCR products were treated with 1- µl of DpnI restriction enzyme (20,000 units/ml), and incubated for 1-hour at 37 ºC to digest methylated parental DNA.

XL-1 blue supercompetent *E.Coli* cells were transformed with 4- µl of DpnI-treated mutant DNA using standard protocol and reagents (Stratagene). DNA was purified using Mini-prep and Maxi-prep DNA purification systems (Qiagen). The presence of the coding region (insert) was verified by restriction digest and agarose gel electrophoresis. The verified mutant DNA was sent to Sequetech Corp. Mountain View, CA (http://datasytem.sequetech.com) for commercial sequencing to verify only desired mutations had been incorporated into the coding region.

Once it was verified that the AChBP residues were correctly mutated, mutant DNA was transfected into HEK-293 cells to develop stably transfected cell lines that secrete mutated AChBP protein into the extracellular medium. The mutant DNA was then purified, and analyzed by Lowry assay and polyacrylamide gel electrophoresis. The mutant protein was identified as the 150kD band under non-denatured conditions, and it was concluded that the mutant protein was expressed as a pentamer (data not shown). The mutant DNA was then stored, and pharmacologically characterized using SPA as explained in Chapters 2-and-3.

4.5 Functionality of the AChBP Mutants

To explore the binding characteristics of the AChBP mutants, mutant proteins were immobilized on the SPA beads under optimized conditions as described in Chapter 3 (0.2 mg/ml beads, 5 mg/ml BSA and 10 nM AChBP). The 6X His tag on the C-terminal of the mutated protein binds to copper on the SPA beads resulting in immobilization of the mutated protein on the bead surface. Different concentrations of radioligand, [^{3}H]-granisetron, were incubated with the protein/bead complex, and the fraction of bound radioligand was determined by a scintillation counter after a 2-hour incubation period. Nonspecific binding was determined in the presence of 1.0 M acetylcholine, and was subtracted from total binding to give the specific binding of [^{3}H]-granisetron to the AChBP.

To test the functionality of mutated proteins and evaluate them for development of a soluble biosensor protein that mimics the 5-HT$_3$ receptor, we explored the ability of mutated proteins to interact with nicotinic and serotonergic ligands in competition with [^{3}H]-granisetron using SPA assay. In these experiments, we assayed the following ligands: nicotinic receptor agonist acetylcholine; nicotinic receptor antagonist d-tubocurarine (dTC); serotonin agonist, seroton; 5-HT$_3$ receptor partial-agonists m-chlorophenylbiguanide (mCPBG) and 2-Methyl-serotonin (2-Me-5HT); and the 5-HT$_3$ receptor antagonist granisetron.

The data in this section is divided into: a) direct binding of the AChBP mutants with [^{3}H]-granisetron, and b) competition binding assays using the nicotinic and serotonergic ligands described above. Both assays utilized SPA as the biosensor platform, and data for both assays are listed on Table 4.2.

4.5.1 The AChBP Mutant Binding Assay

For evaluation of [^{3}H]-granisetron binding, 10 nM of mutant protein, 5mg/ml of BSA, and 0.2 mg/ml of SPA beads per sample well were used. [^{3}H]-granisetron concentrations were varied between 0.00-and-300 nM. Similar to conventional binding assays, the equilibrium binding constant or dissociation constant (K_d) for the radioligand [^{3}H]-granisetron was determined from a plot of radioligand concentration vs. fraction

bound. Data was analyzed using GraphPad Prism software. The K_d value was calculated using the simple one-site binding model:

$$Y = B_{max} * X / K_d + X$$

where X is the radioligand concentration, Y is the amount bound in counts per minute (CPM), Kd is the binding affinity, and Bmax is the calculated maximal binding.

4.5.2 The AChBP Mutant Competition Assay

The radioligand [^{3}H]-granisetron was utilized as the radioligand in competitive binding assays. For competition experiments, the [^{3}H]-granisetron concentration was fixed at a concentration equal to the K_d for granisetron. In addition, 10 nM of mutant protein, 5mg/ml of BSA, and 0.2 mg/ml of SPA beads were added to each sample well. At least 8 concentrations of competitor ligand in 3-fold increasing concentrations were used to acquire the final data. Competing ligand was added prior to addition of the radioligand, and was incubated with mutant protein and SPA beads for 1-hour at ~21 º C (room temperature). Once radioligand was added, the combined mixture was incubated at room temperature on a shaker (with low speed) for a minimum of 2-hours before the radioactivity level was measured and counted by the scintillation counter.

Competition assays determine the IC_{50} value (in nM or µM), which represents the concentration of a ligand/drug that is required for 50% inhibition. The IC_{50} of cold ligands for the inhibition of granisetron was determined by using the sigmoidal dose-response equation and GraphPad Prism software:

$$Y = B_{max} / (1 + 10^{([\log(IC50)-X] * n)})$$

where X is the logarithm of the concentration of cold ligand, Y is the response in counts per minute (CPM), and n is the Hill-slope.

4.6 Results

The equilibrium binding constant or dissociation constant (K_d) for the radioligand [^{3}H]-granisetron was first determined for all the mutants. The K_d value determined for each mutant binding protein was then used as the fixed [^{3}H]-granisetron concentration for competition / inhibition assays. This section is divided into two major subsections: a) mutants that did not interact with granisetron, and b) mutants that interacted with

granisetron and different ligands. Each subsection will review the data presented, propose possible explanation and an overall conclusion. Data for all the assays are listed in Table 4.2 and Figure 4.3.

4.6.1 Mutants that Did Not Interact with Granisetron

Although it is ideal to have positive results in any type of experiment, especially mutagenesis studies, negative results are equally important since they demonstrate involvement and/or role of certain residues in an interaction. In general, mutagenesis data that shows a decrease in affinity suggests that the mutated residue is involved in the interaction of the receptor with the ligand.

A-loop Mutation (N90E):

As mentioned before, A-loop is considered a rigid loop which contains conserved residues. In the A-loop, the E129 residue of the 5-HT_3 receptor (5-HT_3R-E129) is involved in binding of both agonists and antagonists (124,134). Under normal conditions, serotonin does not bind to the nACh receptor; however, mutation of E129 residue of 5-HT_3 receptor to its equivalent in the nACh receptor leads to binding of serotonin to the nACh receptor. This suggests that E129 is important for ligand selectivity. Mutation of the AChBP-**N**90, which is the counterpart to 5-HT_3R-E129 (in both mouse and human), was intended to increase selectivity of the AChBP for serotonin ligands. Asparagine (**N**) is a hydrophilic residue with an uncharged R group, and glutamate (E) is also a hydrophilic residue but with a negatively charged R group. Binding data for [^{3}H]-granisetron showed a significant decrease in Kd for granisetron (>300 nM), thus preventing analysis of other compounds using competition assays (Table 4.2). This result signals importance of this A-loop residue for binding of granisetron to the AChBP. We did not test this mutant with the remaining ligands as without [^{3}H]-granisetron binding we would not have been able to monitor any change or compare results of ligand interaction in mutant receptors versus wild type. Previous data from our lab proposed that A-loop in 5-HT_3 receptor might serves as a pre-binding site to facilitate ligand entry by allowing antagonists to bind to A-loop, followed by a shift

Table 4.2: Mutant Data. The AChBP and mutants are listed on the left-hand column, and ligands used are listed on the top row. The result for 95% Confidence Interval (Conf.Inter.) is the top number, and K_d or IC_{50} in nM or μM is the second number in the result section. The abbreviations used in this table and their meaning are as follow: SE (standard error); Kd > 300 nM (maximum granisetron used for this experiment was 300 nM, and B_{max} could not be calculated to calculate the K_d); ND (not determined due to high K_d for granisetron); NI (inhibition did not reach 50% using the highest concentration of ligand); ** (inhibition reached 50% or more using the highest concentration of ligand; however, the available data was insufficient. Estimated value reported here was obtained by constraining top and bottom of the curve between 0-and-1). Second table shows literature values reported by Schulte et al. (21), which lists K_d and IC_{50} in nM or μM for 5-HT_3 receptor.

Name	Granisetron 95% Conf.Inter. K_d ± SE (nM)	dTC 95% Conf.Inter. (IC_{50}) nM	ACh 95% Conf.Inter. (IC_{50}) μM	5HT 95% Conf.Inter. (IC_{50}) μM	mCPBG 95% Conf.Inter. (IC_{50}) μM	2-Me-5HT 95% Conf.Inter. (IC_{50}) μM
AChBP	10.0 – 28.8 19.4 ± 4.5	9.95 - 20.9 (14.4)	2.30 - 4.32 (3.16)	442 - 927 (640)	253 - 469 (344)	33.7 - 49.8 (41.0)
N90E (A)	> 300 nM	ND	ND	ND	ND	ND
R104Y (E)	> 300 nM	ND	ND	ND	ND	ND
M114Y (E)	> 300 nM	ND	ND	ND	ND	ND
T184F (C)	12.1 – 39.5 25.8 ± 6.5	NI (> 300)	1.21 - 4.54 (2.34)	NI (> 3000)	NI (> 3000)	1498-3701 (2355) **
S186I (C)	56.2 - 106 81 ± 12	NI (> 300)	9.31 - 19.2 (13.4)	623 - 1093 (825)	536 - 1071 (758)	54.2 – 87.0 (68.7)
S186M (C)	15.0 – 45.2 30.1 ± 7.2	NI (> 300)	3.85 – 7.41 (5.34)	NI (> 3000)	NI (> 3000)	1656-4204 (2638) **
P189S (C)	63.4 - 101 82.3 ± 9.1	88.6 - 224 (141)	4.89 – 12.7 (7.90)	1614-2678 (2079) **	1445-2252 (1804) **	327 - 518 (412)
A191S (C)	> 300 nM	ND	ND	ND	ND	ND
C187D/C188I	> 300 nM	ND	ND	ND	ND	ND
C187E/C188S	48.2 – 93.0 70.6 ± 11	34.5 – 54.6 (43.4)	25.6 – 68.1 (41.7)	1648-2792 (2145) **	321 - 514 (407)	83.8 - 145 (110)
C187I/C188S	8.85 – 15.9 12.4 ± 1.8	57.6 - 153 (93.8)	5.26 – 11.6 (7.82)	146 - 510 (273)	136 - 328 (211)	90.1 - 173 (125)
C187S/C188S	45.8 – 72.3 59 ± 6.4	56.3 - 132 (86.2)	15.9 – 50.8 (28.4)	1350-2335 (1775) **	455 - 880 (633)	141 - 256 (190)

5-HT_3	0.98 ± 0.12	(12)	Not available	(0.148)	(0.006)	(0.3)

of ligand to D-loop, and its final association with the B-loop (113,124). It is possible that mutation of A-loop in the AChBP blocked ligand entry since the glutamate (E) residue is large in size and it might not have left enough space for the ligand to bind, or the structural change of the receptor due to the mutation affected or prevented residue interactions.

E-loop Mutations (R104Y and M114Y):

In the E-loop, Y143 of 5-HT_3 receptor is involved in agonist binding, and Y153 is selective for binding of agonist over partial-agonist, mCPBG (21). The R104Y and M114Y mutations produce the AChBPs that are equivalent to 5-HT_3R-Y143 and Y153 respectively (in both mouse and human). These mutations were intended to increase selectivity of the AChBP for the serotonin agonist. Arginine (R) is a hydrophilic residue with a positively charged R group, methionine (M) is a hydrophobic residue with a nonpolar R group, and tyrosine (Y) is a hydrophobic residue with an aromatic R group. Binding data showed a significant decrease in granisetron affinity (>300 nM) for both mutated AChBPs, thus preventing analysis of other compounds using competition assays (Table 4.2). The results indicate that the original residues in the E-loop are important for binding of granisetron to the AChBP. It is possible that mutation of E-loop in the AChBP blocked ligand entry since the tyrosine residue contains an aromatic ring which is large in size and it might not have left enough space for the ligand to bind, or the structural change of the receptor due to the mutation affected or prevented residue interactions. We did not test these mutants with the remaining ligands as without [^{3}H]-granisetron binding we would not have been able to monitor any change or compare results of ligand interaction in mutant receptors versus wild type.

C-loop Mutations (A191S and C187D/C188I):

The C-loop is proposed to be involved in ligand selectivity (18). This loop has the most variable residues and is very different between the AChBP and serotonin receptor (18,124). In addition, proximal cysteines are present in the C-loop of the AChBP, but not in the serotonin receptor (18,113). In the C-loop, the S233 residue of the 5-HT_3 receptor (5-HT_3R-S233) is involved in binding of both agonists and antagonists. The AChBP-A191S mutation, which is equivalent to 5-HT_3R-S233 (in both mouse and human), was intended to increase selectivity of the AChBP for serotonin ligands. In addition, the double mutation of AChBP-C187 and AChBP-C188 to their equivalent in the serotonin receptor (C187D/C188I in mouse, or C187E/C188S in human) was intended to remove the proximal cysteines to study their effect on the function of the C-loop. Alanine (A) and isoleucine (I) are hydrophobic residues with a nonpolar R group;

serine (S) and cysteine (C) are hydrophilic residues with an uncharged R group; and aspartate (D) is also a hydrophilic residue, but with a negatively charged R group. Binding data for [^{3}H]-granisetron showed a significant decrease in Kd for granisetron (>300 nM), in both the single mutation (A191S), and double mutations (C187D/C188I), thus preventing analysis of other compounds using competition assays (Table 4.2). The results signal importance of the original residues for binding of granisetron to the AChBP. In addition, since the C-loop is the most variable loop between the AChBP and 5-HT$_3$ receptor, the results might indicate that these mutations have shifted the C-loop alignment, or that the C-loop alignment is not correct. We did not test these mutants with the remaining ligands as without [^{3}H]-granisetron binding we would not have been able to monitor any change or compare results of ligand interactions in mutant receptors versus wild type. Since granisetron did bind to the C187E/C188S mutation, the result of this mutant will be discussed in the next section.

Conclusion:

All of our mutants produced protein which were tested and identified as assembled protein. However, the five mutants mentioned above did not result in binding of granisetron to the AChBP which signals importance of those residues in binding of granisetron to the AChBP. As mentioned previously, we did not test these mutants with the remaining ligands as without [^{3}H]-granisetron binding we would not have been able to monitor any change or compare results of ligand interactions in mutant receptors versus wild type.

Based on previous results from our lab, serotonin antagonists bind tightly to the AChBP, whereas the opposite is true for serotonin agonists (21,113). Since all of the mutations in this study are 'substitution' mutations, a decrease in affinity means the ligand does not interact similarly with the wild-type as it does with the mutant receptor. The results could be due to the size of substituted residue, meaning the new residue did not leave enough space for the ligand to bind, or that it completely blocked ligand entry. It is also possible that a structural change of the receptor due to the mutation affected or prevented residue interactions.

4.6.2 Mutants that Interacted with Granisetron and Different Ligands

All the mutants that interacted with granisetron were in the C-loop (Table 4.2 and Figure 4.3). Mutations were selected to try to increase binding affinity of the serotonin agonist and partial-agonists for the receptor. In general, mutations result in a change of affinity. Since all the mutations in this study were 'substitution' mutations, a positive result can mean a substantial, small or no affinity increase when a mutant data is compared with the wild-type. In addition, small improvements or no change in the affinity of the mutated receptor for a serotonin ligand signals proper alignment of the C-loop between the AChBP and serotonin receptors.

C-loop Mutation T184F:

This mutation replaced a threonine (T) residue that contains a hydrogen bond with phenylalanine (F) which has an aromatic ring and is a larger residue compared to T. Results show that the mutation did not affect granisetron and ACh binding; however, it decreased the binding affinity of the antagonist dTC as well as serotonin agonist 5-HTand partial-agonists mCPBG, for the mutated receptor. Results for the T184F mutation indicate that the T residue is involved in binding of dTC, 5-HT and mCPBG to the AChBP (Figure 4.3). It is possible that the large size of the substituted residue (F) makes it impossible for certain ligands to interact with the mutated receptor, or that a structural change of the receptor due to the mutation affected or prevented residue interactions. Data might also indicate that the T residue is involved in selective interaction of 2-Me-5HT with the AChBP since the other partial-agonist did not interact with the receptor. This discrepancy might be due to a structural alteration in the binding site caused by the mutation. The 95% confidence interval of the AChBP for 2-Me-5HT did not overlap with the mutated receptor, signaling a significant difference between the mutated receptor and the AChBP (Table 4.2). This data is verified by decreased affinity of the 2-Me-5HT ligand for the receptor due to the mutation.

In addition, results indicate that antagonists dTC and granisetron might interact differently with this region since the affinity of granisetron had decreased for the mutated receptor, but binding of granisetron was not altered by this mutation. The difference in the binding site interaction between these two antagonists cold be the

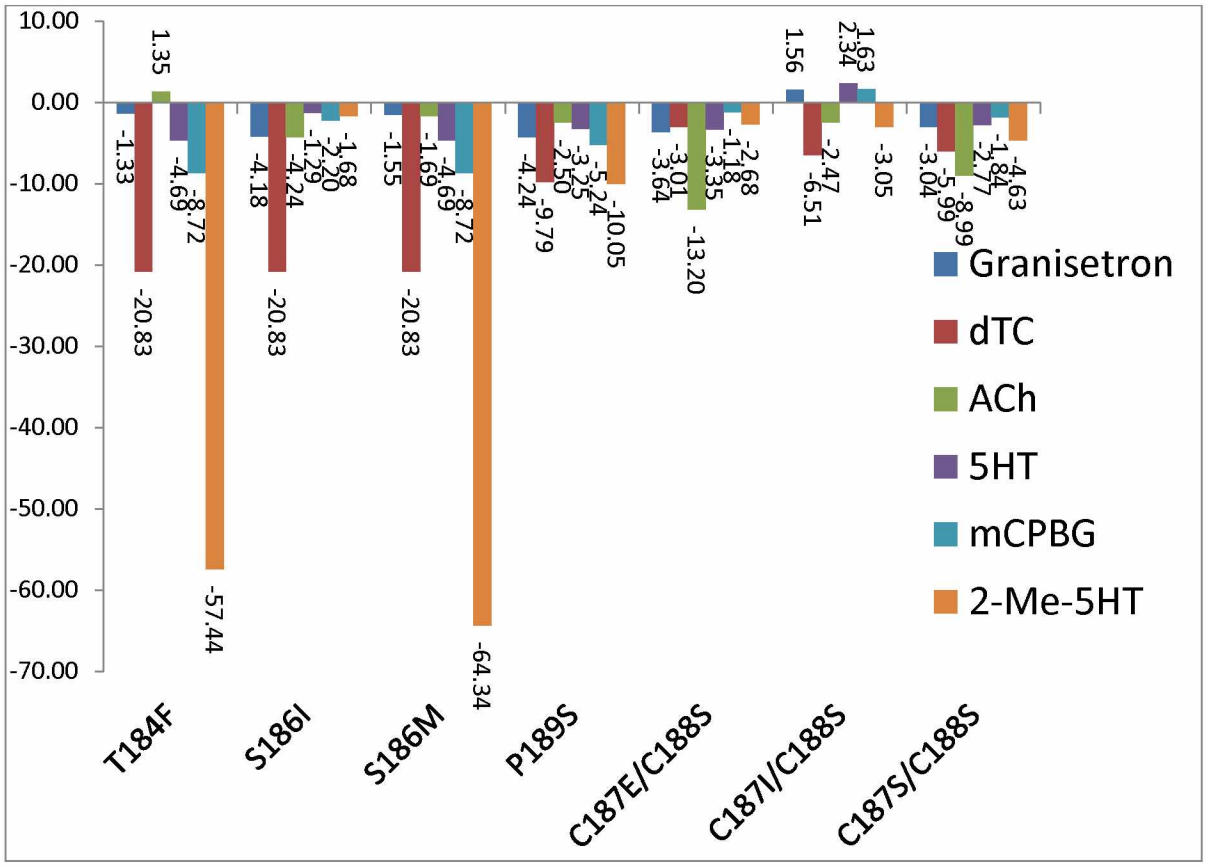

Figure 4.3: Results of Binding Assays for Different Mutants. This figure was developed using original data from Table 4.2. All the mutant data were normalized using the AChBP results.

result of a different positioning of dTC in the binding site, resulting in a lack of interaction between dTC and the mutated receptor. Data also show that ACh binding is present, which indicates that the basic structure of the C-loop is not affected by the mutation. In order to have a functional receptor, hydrogen bonding properties are needed. An option to improve the results of this mutation might be a substitution of the serine (S) residue of the 5-HT_3 receptor (5-HT_3R-S227), which is capable of hydrogen bonding, instead of F226. This would mean that the residues have to shift one position to align the AChBP-T184 with 5-HT_3R-S227, which would indicate that the current alignment used to design the mutants might not be correct.

C-loop Mutation S186I (mouse equivalent):

This mutation replaced serine (S) which is hydrophilic and capable of forming a hydrogen bond with isoleucine (I), which is hydrophobic and larger in size when compared to S. Results show that the mutation decreased the binding affinity of the antagonist dTC for the mutated receptor, which indicates that the S residue is involved in binding of dTC to the AChBP (Figure 4.3). However, binding of granisetron was not altered by this mutation which indicates antagonists dTC and granisetron might interact differently with this region. The difference in binding site interaction between the two antagonists could be the result of a different positioning of dTC in the binding site.

The 95% confidence interval of the mutated receptor for granisetron, ACh, mCPBG and 2-Me-5HT did not overlap with the wild-type receptor, signaling significant difference between the mutated receptor and the AChBP (Table 4.2). This data is verified by decreased affinity of above mentioned ligands for the receptor due to the mutation. In addition, results show that ACh binding is present, although the mutation has decreased affinity of ACh for the receptor, which indicates the basic structure of the C-loop was not affected by the mutation. Taken together, these effects seem to suggest that this residue (S) is not very important to binding as the mutation itself is a substantial change (from hydrogen bond to lack of hydrogen bond); however, the mutation did not alter the binding affinity of either nicotinic or serotonergic ligands drastically. This could possibly be another alignment problem.

C-loop Mutation S186M (human equivalent):

This mutation replaced serine (S) which is hydrophilic and contains a hydrogen bond with methionine (M) which is hydrophobic and larger in size compared to S. Results show that the mutation did not affect granisetron and ACh binding; however, it decreased the binding affinity of the antagonist dTC as well as the serotonin agonist 5-HT and partial-agonists mCPBG, for the mutated receptor (Figure 4.3). Results for the S186M mutation indicate that the S residue is involved in binding of dTC, 5-HT and mCPBG to the AChBP. It is possible that the mutation blocked ligand entry since the substituted M residue is large in size and it might not have left enough space for the ligand to bind, or that the structural change of the receptor due to the mutation affected

or prevented residue interactions. Data might also indicate that the S residue is involved in a selective interaction of 2-Me-5HT with the AChBP since the other partial-agonist did not interact with the receptor. This discrepancy might be due to a structural alteration in the binding site caused by the mutation. The 95% confidence interval of the AChBP for 2-Me-5HT did not overlap with the mutated receptor, signaling a significant difference between the mutated receptor and the AChBP (Table 4.2). This data is verified by a decreased affinity of the 2-Me-5HT ligand for the receptor due to the mutation.

In addition, results indicate that antagonists dTC and granisetron might interact differently with this region since the affinity of granisetron had decreased for the mutated receptor, but binding of granisetron was not altered by this mutation. The difference in the binding site interaction between the two antagonists could be the result of a different positioning of dTC in the binding site. Since ACh binding is present, although the mutation decreased affinity of ACh for the receptor very little, it indicates that the basic structure of the C-loop was not affected by the mutation. Comparison of results for S186I and S186M indicate similar effects for both receptors which might suggest an alignment problem.

C-loop Mutation P189S:

This mutation replaced proline (P) which is hydrophobic with serine (S) which is hydrophilic and is capable of forming a hydrogen bond. Proline has a distinctive cyclic structure that causes it to have an exceptional conformational rigidity compared to other amino acids (1). P is commonly found in protein turns where the polypeptide chain reverses its overall direction. Results show that the mutation did not affect binding and interaction of the antagonist dTC, which indicates that the P residue is not involved in binding of dTC to the AChBP. In addition, data also show that this mutation resulted in the highest affinity decrease of any mutant for both antagonists at the same time (Figure 4.3). Since the general goal of the mutation was to decrease affinity of serotonin antagonists and ACh, and increase affinity of serotonin agonists for the receptor, these results indicate involvement of the S residue in decreasing affinity of serotonin antagonists for the AChBP.

The 95% confidence interval of the mutated receptor for none of the ligands overlapped with the wild-type receptor, signaling a significant difference between the mutated receptor and the AChBP (Table 4.2). This data was verified by decreased affinity of all the ligands for the receptor. In addition, although P changed the structure of C-loop profoundly, data shows that ACh binding was present, and that the mutation had decreased affinity of ACh for the receptor. This result indicates that the basic structure of C-loop was not affected by the mutation.

C-loop Mutations C187E/C188S (human equivalent):

This mutation replaced cysteine (C) which is a hydrophilic residue and contains an uncharged R group, with serine (S) which is from the same group as C, as well as glutamate (E) which is also hydrophilic but contains a negatively charged R group. The main goal of this mutation was to replace the proximal cysteines of the AChBP (which is absent in serotonin receptor) with its equivalent residues in the human 5-HT_3 receptor, and study its effect on the structure of the receptor as well as binding and interaction of the mutated receptor with different ligands.

Results show that mutation did not affect binding and interactions of antagonists granisetron or dTC with the receptor, although it decreased affinity of both ligands for the mutated receptor, which indicates proximal cysteines were not involved in binding of granisetron or dTC to the AChBP (Figure 4.3). This is the first time it was shown that the proximal cysteines could be substituted with other residues and result in a functioning receptor.

The 95% confidence interval of the mutated receptor for the ligands did not overlap with the wild-type receptor, signaling a significant difference between the mutated receptor and the AChBP (Table 4.2). This data was verified by decreased affinity of all ligands for the receptor. Results also showed that ACh binding was present, and that the mutation decreased affinity of ACh for the receptor, indicating that the basic structure of the C-loop was not affected by the mutation.

The general goal of the mutation was to decrease affinity of serotonin antagonists and ACh, and increase affinity of serotonin agonists for the receptor. Both C187E/C188S and P189S mutations showed a decrease in affinity of ligands for the

receptor, which might suggest that the S residue was involved in this process. In addition, the C187D/C188I mutation (mouse equivalent) did not yield any result; however, ligands interacted with the C187E/C188S mutant (human equivalent). Comparing the results of two double mutants might indicate that at position 188, the C-to-S mutation did less damage than the C-to-I mutation since the C-to-E and C-to-D at position 187 were similar (both are hydrophilic and have a negatively charged R group). This would support the idea that the original alignment might be wrong.

C-loop Mutations C187I/C188S (mouse equivalent, alternate alignment):

Results of single mutations indicated that in order to have a functional receptor, hydrogen bonding properties were needed, and that the S residue was involved in increasing the affinity of ligands for the receptor. And results of double mutations showed that proximal cysteines could be substituted with other residues and yield a functional receptor, and that most likely, the original alignment used to design the mutants might be wrong. We decided to shift the alignment one residue (position) so the proximal cysteines could be substituted with new residues capable of hydrogen bonding. This new alignment produced a C187I/C188S double mutation which is explained in this section. The mutation replaced the cysteine (C) with serine (S), both of which are from the same group of hydrophilic residues that contain an uncharged R group and can form a hydrogen bond. The other substituted residue was isoleucine (I) which is hydrophobic and nonpolar (Table 4.3).

Results showed that the mutation did not affect binding and interaction of antagonists granisetron or dTC with the receptor, which indicates proximal cysteines were not involved in binding of granisetron or dTC to the AChBP (Figure 4.3). Data indicates a decreased affinity of dTC for mutated receptor when compared to the AChBP, and the 95% confidence interval of mutant did not overlap with the AChBP indicating a significant difference between them (Table 4.2). Results might indicate a difference in binding site interaction between the two antagonists, which most likely could be the result of a different positioning of granisetron and dTC in the binding site. Since ACh binding was present, although the mutation has decreased affinity of ACh for

Table 4.3: Alternative Sequence Alignment of the C-loop for the AChBP and 5-HT_3 Receptors. Aligned sequences in the C-loop: *Lymnaea stagnalis* AChBP (AChBP), murine 5-HT_3 receptor (m5-HT_{3A}R), human 5-HT_3 receptor (h5-HT_{3A}R), and suggested alternative alignment (Alt).

AChBP	S	V	T	Y	S	C	C	P	E	A	Y	E	D	V
m5-HT_3	E	-	F	S	I	D	I	S	N	S	Y	A	E	M
h5-HT_3	E	-	F	S	M	E	S	S	N	S	Y	A	E	M
Alt: m5-HT_3	E	F	S	I	D	I	S	N	S	Y	A	E	M	-
Alt: h5-HT_3	E	F	S	M	E	S	S	N	S	Y	A	E	M	-

the receptor, it indicates that the basic structure of the C-loop was not affected by the mutation.

The general goal was to decrease affinity of serotonin antagonists and acetylcholine for the receptor through mutation. The 95% confidence interval of the mutated receptor for dTC and ACh did not overlap with the wild-type receptor, signaling a significant difference between the mutated receptor and the AChBP (Table 4.2). This data was verified by the decreased affinity of the ligands for the mutated receptor. It was also a general goal to increase receptor affinity for serotonin agonists and partial-agonists. IC_{50} data verifies increased affinity of 5-HT and mCPBG for the mutated receptor, when compared to other receptors; however, data shows a decreased affinity of partial-agonist mCPBG for the receptor when compared to the wild-type. The 95% confidence interval of the mutated receptor for 2-Me-5HT ligands did not overlap with the wild-type receptor, signaling significant difference between the two (Table 4.2). Since the structural make up of partial-agonists are different, it is possible that the structural change of the receptor due to the mutation affected residue interactions, resulting in a low affinity of the 2-Me-5HT ligand for the mutated receptor when compared to the AChBP. It is interesting to note that the highest affinity for this ligand was observed in the S186I mutant, and although the IC_{50} data for C187I/C188S showed a lower affinity for 2-Me-5HT ligand when compared to the wild-type receptor, in reality, it was the third highest affinity after S186I and C187E/C188S. Taken together, data showed the proximal cysteines were not involved in ligand binding and could be substituted to yield a fully functional receptor, which indicates that the new alignment might be an improved alignment.

C-loop Mutations C187S/C188S (human equivalent, alternate alignment):

Both original (C) and mutated (S) amino acids belong to the same group whose members have hydrophilic residues that contain an uncharged R group. Data for this mutant was very similar to the first functional double mutation C187E/C188S. Results showed that the mutation did not affect binding and interaction of antagonists granisetron or dTC with the receptor, although it decreased affinity of both ligands for the mutated receptor, which indicates that the proximal cysteines were not involved in binding of granisetron or dTC to the AChBP (Figure 4.3). Data also showed that ACh binding was present, although the mutation decreased affinity of ACh for the receptor, indicating that the basic structure of the C-loop was not affected by the mutation.

Except for mCPBG, the 95% confidence interval of the mutated receptor for none of the ligands overlapped with the wild-type receptor, signaling a significant difference between the mutated receptor and the AChBP (Table 4.2). This data was verified by decreased affinity of the ligands for the mutated receptor.

Conclusion A: Antagonist Binding Site

Granisetron and d-Tubocurarine (dTC) are antagonists for both the AChBP and 5-HT_3 receptors, and the goal of the mutations was to decrease the affinity of the mutants for serotonin antagonists. N90E (loop-A), R104Y and M114Y (loop-E), and A191S (loop-C) did not show any binding to antagonist granisetron, indicating that amino acids N, R, M and A were involved in binding of the AChBP to granisetron. It is possible that the structural change of the receptor due to the mutation affected residue interactions, resulting in lack of interaction between granisetron and the mutated receptors. Data for mutants that were tested showed a general decrease in affinity of granisetron for the mutated receptors, and the majority of mutants did not show any overlap in their 95% confidence intervals with the AChBP, signaling a significant difference between these mutant receptors and the wild-type (Table 4.2).

Mutants that showed the least affinity for granisetron, P189S and S186I, were the two residues on either side of the AChBP proximal cysteines. In addition, the third mutant with the least affinity was C187E/C188S, which was a mutant with no proximal cysteines. Taken together, it seems that the AChBP proximal cysteines might be

involved in high affinity of the AChBP for serotonin antagonist, granisetron. And that substitution of proximal cysteines in the AChBP with its corresponding residues in the 5-HT_3 receptor, as well as mutation of one residue on either side of the proximal cysteines might result in decreased affinity of granisetron for the AChBP.

The only mutation that showed increased affinity of granisetron for the receptor, C187I/C188S, was designed by using a new alignment, and the Kd value of this mutant was close to the AChBP. This data suggests: a) possibility and probable validity of a new alignment between the AChBP and 5-HT_3 receptor since the mutation produced an active protein with similar functional characteristic as the AChBP, and b) proximal cysteines can be replaced with different residues, namely isoleucine (I) and serine (S), without inactivating the receptor protein. This is the first time it has been shown that the proximal cysteines can be substituted with other residues and result in a functioning receptor.

In the C-loop, mutants T184F, S186I and S186M did not show any binding to antagonist dTC, indicating that amino acids T and S are involved in binding of the AChBP to dTC. It appears antagonists dTC and granisetron interact differently with this region since binding of granisetron was not altered by this mutation. The difference in binding site interaction between the two antagonists could be the result of a different positioning of dTC in the binding site.

The general result for the rest of mutations showed decreased affinity of mutated receptors for dTC. None of the mutations showed any overlap in their 95% confidence intervals for dTC with the AChBP, signaling a significant difference between these mutant receptors and the wild-type (Table 4.2). Among these mutants, the highest affinity decrease for dTC was 8.8 fold (displayed by P189S), which was considered moving in the right direction; however, the difference was not very significant from the AChBP. The lack of any large change in binding affinity showed that there was little structural change at the binding site due to the mutation, and that the substituted residues were important in the interaction of the ligand, dTC, with the 5-HT_3 receptor.

Conclusion B: Agonist Binding Site

Acetylcholine (ACh) is an agonist for the AChBP, and the goal of the mutations was to decrease affinity of ACh for the mutant receptors. In the C-loop, mutants T184F, S186I and S186M did not show any binding to antagonist dTC; however, the mutations did not affect ACh binding which indicates the basic structure of the C-loop was not disturbed by the mutation.

Except for T184F, which showed a slight increase in affinity of ACh for the receptor, data indicated a general decrease in affinity of acetylcholine for mutated receptors. These results demonstrate the importance of substituted residues in binding of ACh to the 5-HT_3 receptor, as well as decreased affinity of the ligand for receptors. S186I, P189S, and the three double mutations did not show any overlap in their 95% confidence intervals with the AChBP, signaling significant difference between these mutant receptors and the wild-type (Table 4.2). Since the general goal was to decrease affinity of acetylcholine for receptor through mutation, results showed that double mutations had the largest affinity decrease which might indicate that removal of the proximal cysteines was necessary to decrease affinity of the ACh ligand for the receptor.

In addition, the goal of mutation was to increase affinity of the serotonin agonist, serotonin (5-HT), and partial-agonists, m-chlorophenylbiguanide (mCPBG) and 2-Methyl-serotonin (2-Me-5HT) for the receptors. Data showed that the serotonin agonist, 5-HT, did not bind to T184F and S186M mutants, indicating that amino acids T and S were involved in binding of the serotonin ligand to the AChBP. In both cases, the substituted amino acid was much larger than the original residue, which might not have left enough space for the ligand to bind. Since the mutation reduced affinity, it might also indicate that it decreased an interaction or altered the structure of the binding loop. Except for C187I/C188S, data for mutants that were tested showed a general decrease in affinity of 5-HT for the mutated receptors, and their 95% confidence intervals did not overlap with the AChBP, signaling significant differences between the mutant receptors and the wild-type (Table 4.2). The 5-HT ligand showed an increased affinity for the C187I/C188S mutant, which supported the new and alternate alignment of the C-loop residues.

The result of 5-HT inhibition indicated that: a) removal of proximal cysteines is needed to increase affinity of the mutated receptor for the serotonin ligand since the highest affinity was seen in double mutations, b) depending on the original or substituted residue, the mutated receptor showed increased or decreased affinity for the ligand; therefore, mutation of the AChBP proximal cysteines to E-and-S or S-and-S did not increase affinity of mutated receptor for serotonin ligand, but I-and-S residue mutation could result in a receptor resembling the 5-HT_3 receptor, and c) a new alignment between the AChBP and 5-HT_3 receptor was needed.

Similar to data from 5-HT inhibition, the partial-agonist mCPBG did not show any binding to T184F and S186M mutants, indicating that amino acids T and S were involved in binding of the mCPBG ligand to the AChBP. In both cases, the substituted amino acid was much larger than the original residue, which might not have left enough space for the ligand to bind. Since mutation reduced affinity, it might also indicate that it decreased an interaction or altered the structure of the binding loop. Except for C187I/C188S, data for the mutants that were tested showed a general decrease in affinity of mCPBG for the mutated receptors, and their 95% confidence intervals did not overlap with the AChBP, signaling significant differences between the mutant receptors and the wild-type (Table 4.2). The mCPBG ligand showed an increased affinity for the C187I/C188S mutant, which supports the new and alternate alignment of the C-loop residues.

Data for 2-Me-5HT showed a general decrease in affinity of the 2-Me-5HT ligand for the mutated receptors. The 95% confidence intervals for none of the mutants overlapped with the AChBP, signaling significant differences between the mutant receptors and wild-type (Table 4.2). The 2-Me-5HT inhibition results showed that the original residues in T184F and S186M mutations might be involved in a selective interaction of 2-Me-5HT ligand with the AChBP. These same receptors also did not interact with the other serotonin partial-agonist, mCPBG, which might be due to the large size of the substituted residue that made it impossible for the ligand to interact with the mutated receptor, or the structural differences in the 2-Me-5HT binding site by the mutation prevented the interaction.

Taken together, data indicates that the C187I/C188S double mutant showed almost no change in granisetron binding affinity, a decrease in dTC and ACh affinities, and an increase in serotonin agonist 5-HT and partial-agonists mCPBG and 2-Me-5HT affinities. It should be noted that the affinity changes were small when compared to the affinity of the wild-type receptor for different ligands. These small differences showed that the new amino acids could be substituted for the original ones in the AChBP, which also supported the alternate alignment of the C-loop between the AChBP and 5-HT_3 receptors.

4.7 Summary

The goal of our study was to decrease affinity of acetylcholine (ACh) and serotonin antagonist, and increase affinity of serotonin agonist and partial-agonist for the AChBP using site-directed mutagenesis, since previous data from our laboratory showed that the AChBP had high affinity for serotonin antagonist and low affinity for serotonin agonists (113).

Data indicated that the most significant changes occurred in the C-loop. Results for mutants showed a general decrease in affinity of ACh and serotonin antagonists, granisetron and d-tubocurarine (dTC) for the mutated receptors; however, no large changes (>10 folds) in binding was observed when compared to the wild-type AChBP, which indicates that there was little structural perturbation of the C-loop and binding site due to each individual mutation. The largest affinity decrease for the ACh was observed in double mutations which might indicate removal of the proximal cysteines will be necessary for a successful conversion of the AChBP to the 5-HT_3 receptor. This is the first time it was shown that the proximal cysteines could be substituted with other residues and result in a functioning receptor.

In addition, mutation of certain AChBP residues to its equivalent in serotonin receptor resulted in an increased affinity of serotonin agonists and partial-agonists for the AChBP. Data indicated that individual mutations were not capable of increasing affinity of serotonin agonists for the AChBP very much; however, each individual mutation increased the affinity to a certain degree. The highest affinity increase was observed in double mutants, C187I/C188S, which indicates that removal of proximal

cysteines was involved in increasing the affinity of serotonin ligands for the mutated receptor. The best residues to substitute for the proximal cysteines were 'IS' which preserved the structure of the C-loop. Therefore, based on these data, we propose a new alignment for the C-loop between the AChBP and the serotonin receptor.

Chapter 5: Discussion

5.1 Introduction

The overarching goal of this thesis was to explore acetylcholine-binding protein (AChBP) as a potential biosensor molecule by using it as a template for development of a soluble binding protein analog of the serotonin type 3 (5-HT_3) receptor that would be suitable for use in high-throughput biosensor devices. The 5-HT_3 receptor is an important central nervous system (CNS) receptor that is the target for anti-emetic (145) and other potential CNS-acting therapeutic agents (15).

The specific aim of this thesis was to engineer a soluble serotonin-binding protein using the *Lymnaea* AChBP that would mimic the specificity of native human 5-HT_3 ligand-gated ion channel (LGIC) receptor. The aim of this project was approached in a sequential manner to achieve the following objectives:

Objective 1: *Development of stable expression of the Lymnaea AChBP in mammalian cell lines, evaluation of its application to scintillation proximity assay (SPA) and microcantilever assay (MC), and its subsequent pharmacological evaluation (Chapter 3).*

Objective 2: *Design and development of mutations of the AChBP consistent with the 5-HT_3 receptor-ligand interactions, designed to improve interactions of the AChBP with serotonin ligands and decrease interactions with nicotinic receptor ligands (Chapter 4).*

Objective 3: *Design and development of double mutations to determine if the selectivity for serotonin ligands could be enhanced (Chapter 4).*

Objective 4: *Using the data from objectives 2-and-3 to suggest new mutations and produce a new model to further enhance selectivity for serotonin ligands (Chapter 5).*

Objective 1 was addressed in Chapter 3, which focused on developing the AChBP as a sensor protein and evaluating the structure, stability and functionality of this protein. SPA was used to determine how different ligands interact with the AChBP.

This data is of value since the AChBP has been used as a template in computer modeling studies of the 5-HT_3 receptor (9,103,115). In addition, the AChBP protein produced in these studies was evaluated to determine if it could be used on a high-throughput microcantilever system.

Objectives 2 and 3 were addressed in Chapter 4, which focused on mutation of the AChBP using single and double amino acid substitutions of residues previously determined to be critical to interaction of the 5-HT_3 receptor with serotonin ligands. All the mutations were expressed in stably transfected mammalian cell lines designed to secrete the modified AChBP proteins into the cellular medium. Mutated proteins were characterized by gel electrophoresis and subsequently tested for their interaction with different ligands.

5.2 The AChBP Mutant Data

Previous data from our laboratory identified specific amino acids that are important for agonist and/or antagonist binding to the 5-HT_3 receptor (113). Our laboratory also constructed homology models of the 5-HT_3 receptor that aligned binding loops (A-F) between the AChBP and serotonin receptor (20,21). The alignment showed conservation of amino acids in all key binding loops with the exception of the A, C and E loops. The C-loop has been identified as a key region responsible for ligand selectivity (18,125), thus we designed a number of single and double mutants in this more variable region. A single potentially important mutation was also made in the A-loop along with two mutations in the E-loop (Figure 4.1). All three regions have been implicated in ligand binding by prior studies (18,124). The AChBP residues were individually mutated to 5-HT_3 receptor equivalent residues with the goal of increasing ligand selectivity and specificity of the AChBP for serotonin receptor ligands.

Previous data from our laboratory showed that the AChBP binds strongly to serotonin receptor antagonists, and weakly to serotonin receptor agonists (113). Since the serotonin antagonists already bind to the AChBP with high affinity, little change was expected for these ligands on the modified AChBP. In contrast, for agonists we expected to see improved interaction as indicated by increases in affinity of the modified receptor. Thus, the expected outcome of these studies was to increase the affinity of

AChBP for serotonin agonists, and decrease or have no effect on its affinity for serotonin antagonists.

Representative members of major structural classes of 5-HT_3 receptor ligands were chosen to test effects of different mutations on binding of ligands to the AChBP. Acetylcholine (ACh) was used as control to monitor the effect of mutations on a nicotinic ligand. In this case, the goal was to decrease the affinity of the AChBP for ACh when making serotonin receptor equivalent mutations. Granisetron and *d*-tubocurarine (dTC) were selected as antagonists since they bind to both the AChBP and serotonin receptor (21). Since granisetron is available in a radioligand form, it was also ideal for use in the SPA assays. Thus, our studies used [^{3}H]-granisetron for binding and completion assays. While epibatidine is a common radioligand for use in the AChBP binding assays (21), we chose not to use this ligand since it is not an antagonist to both the AChBP and serotonin receptor, and it was anticipated that it would bind less tightly to the modified receptors and would not permit easy comparison across all receptors (native AChBP and modified AChBP) in competition assays. Serotonin (5-HT), 2-Methyl-serotonin (2 -Me-5HT), and m-chlorophenylbiguanide (mCPBG) ligands were chosen as representatives of common agonist and partial-agonists. The choice of multiple ligands with different structure is considered important to fully assess changes in selectivity (21,124) as the receptor is systematically altered by mutation of the AChBP. In a receptor, different degrees of C-loop closure are considered critical to interaction of the receptor with agonists, partial-agonists and antagonists (corresponding to complete closure, partial closure and no closure of the C-loop) (124,125), and thus modification of the C-loop can potentially produce substantially different effects on different ligand classes.

Data in Chapter 4 indicated that the most significant differences in amino acid sequence, and presumably structure, appear to be in the C-loop. C-loop mutations produced a general decrease in affinity of mutated receptors for ACh and serotonin antagonists. However, individual mutations were not adequate to significantly increase affinity of the AChBP for serotonin agonist and partial-agonist; multiple mutations were necessary.

5.3 New Mutant Constructs

A key determination of the data presented in Chapter 4 is the discovery that the proximal cysteines of the C-loop can be substituted with 5-HT_3 receptor equivalent amino acids and still produce a functioning receptor, presumably with a preserved C-loop structure. Based on these data, we proposed a new alignment for the C-loop between the AChBP and serotonin receptor. Aligning the AChBP proximal cysteines (C187/C188) with the I-and-S amino acids of 5-HT_3 receptor (I230/S231) shift the C-loop alignment between the two receptors by one residue. Since Y234 of the 5-HT_3 receptor and Y192 of the AChBP were used to align the amino acid sequence of the two receptors, the difference between the old and new alignment is a total of three residues in the AChBP, of which one residue has to be eliminated to keep the tyrosines in their original position and in alignment with each other. The three AChBP residues for consideration were proline (P189), glutamate (E190) and alanine (A191). We decided to eliminate alanine rather than proline since prolines are typically found in tight turns and its presence in this loop is likely critical to the structural integrity and stability of the protein. Since glutamate (E190) is a hydrophilic residue, it aligns well with serine (another hydrophilic residue) in the 5-HT_3 receptor sequence. Removal of an amino acid, or residue deletion, is generally expected to cause a large conformational change in the receptor and its binding properties.

We constructed two modified AChBPs: one with only the A191 deletion (A-deletion), and the other with a C187I/C188S mutation along with the A191 deletion (IS + A-deletion). Stable cell lines were produced for both binding proteins; however, we were unable to detect any protein which suggests the A-residue is important in protein assembly and expression. Since expressed protein should have been purified via the His tag added to each subunit of the receptor that bind to the nickel column and is pulled out the media (even in unassembled receptors), it appears that the protein was either not produced or was not secreted. It is possible that A-deletion altered protein structure, preventing protein secretion into the cellular medium. Absence of mutated protein could also be the result of a structural change of protein that buried the His tag in a misfolded protein, making it unavailable to bind to the nickel column.

5.4 Future Directions

The goal of this section is to explore and suggest possibilities for future directions of this protein engineering project. While this project did not succeed in producing a viable analog of the 5-HT_3 receptor that met the goals of the project, an engineered soluble receptor analog suitable for biosensor use would allow screening of wide range of natural products and synthetic drugs in a much shorter period of time and is still a valuable goal. As the cost of drug discovery is about 1/3 of the cost of developing a drug (https://www.fda.gov/drugs/developmentapprovalprocess/), this would represent a large cost savings. In addition, such proteins would find important uses in detection of bioweapons or bedside drug screenings as these receptors are important receptors for toxic compounds as well (109). Other important outcomes did result from this study, demonstrating the value of the mutagenesis approach presented here. Understanding of the similarities and differences between the AChBP and the 5-HT_3 receptor provides new information about both proteins and ligand selectivity, and provides a starting point for the next series of experiments.

5.4.1 Mutations

In this project, we substituted residues of one receptor (AChBP) to its equivalent in the other receptor (5-HT_3) so it could bind to certain ligands. Therefore, it was expected to see small changes which would mean either the substituted residue was not involved or the changes were so small that the substitution did not matter. Data showed the unique feature of the AChBP, namely the proximal cysteines which is important in the structure of the C-loop, could be substituted and was in fact necessary to increase affinity of the modified receptors for the serotonin agonist and partial-agonist. The C-loop is the most variable loop which is also involved in binding of ligands (124). The degree of C-loop closure determines whether a ligand is a full or partial agonist (124,125), and thus, mutation will affect the degree of C-loop closure. Data from double mutations suggested a new alignment for the C-loop, and using this new alignment, we can make multiple mutations within this group. For example:

1. *Use the new alignment (IS substitution) and delete proline (P189) in the AChBP*. In homology structures of the 5-HT_3 receptor and x-ray structures of

the AChBP protein, differences in fundamental C-loop structure are clearly evident (18,20). This observation and data from previous studies (113,124) indicate that the C-loop is critical to ligand selectivity, and the fundamental nature of agonists and antagonists suggest this should be a key focus of any further studies. The proximal cysteines (C187/C188) in the AChBP introduce a kink in the C-loop, and presence of proline after the proximal cysteines introduces another kink (1) in the same loop. Mutation of C187/C188 to IS would remove the first kink, and perhaps deletion of P will remove the second kink of C-loop, leading to a more direct interaction of the mutated receptor with serotonin ligands.

2. *Use the new IS alignment and eliminate glutamate (E190) in the AChBP.* This mutation would align P189 residue of the AChBP which is hydrophobic with asparagine (N232) of serotonin receptor which is hydrophilic and capable of hydrogen bonding; a feature that can stabilize the AChBP-ligand complex.

As mentioned earlier in this chapter, we designed and produced a mutant that carried the IS substitution plus A-deletion; however, the mutant was incapable of protein production. This raises the question of whether the result was due to deletion of alanine (A191) residue in the AChBP, alignment of P189 (AChBP) with N232 (5-HT_3), or alignment of E190 (AChBP) with S233 (5-HT_3). To answer these questions, we can:

1. *Construct a single mutation in the AChBP to substitute P189 with an N residue.* This mutation will replace proline which exists in tight turns (1), and thus introduces a special kind of kink in a protein, with asparagine; a residue that can form hydrogen bond.
2. *Substitute E190 in the AChBP with serine (S) residue.* Both amino acids are hydrophilic and capable of hydrogen bonding that leads to receptor-ligand stabilization.

5.4.2 Optimizing Results

The next natural step in this process would be production of mutant AChBPs based on the data from these studies, along with new molecular modeling and site-

directed mutagenesis studies. Mutant data could be used as a starting point to develop models, in which molecular determinants of interactions can be predicted from structures of agonists and antagonists. Modeling studies can also be aimed at deciphering the structural features that drive the binding affinity of the serotonin ligands, and in improving interpretation of the results presented in Chapter 4.

Critical information can also be obtained via determination of crystal structures for modified AChBPs. The production of modified, soluble AChBPs allows for more detailed structural analysis of the effects of mutations in the AChBP and the effects of these structural changes in ways that are typically not available in mutagenesis studied of the ligand-gated ion channel (LGIC) receptors. This will contribute towards a better understanding of not only the mutagenesis of these receptors, but also the effects of mutations on protein structures in general. These data could provide a more comprehensive understanding of the molecular basis for receptor and ligand interactions, which may aid in designing better drug candidates. Crystalized complexes with different agonists and antagonists could also lead to identification of structural features in the ligands that confer differences in their behavior. Thus, the mutant and associated co-crystal structures with serotonin receptor ligands provide a rich starting point for understanding interactions for the various LGIC receptor subtypes.

And yet another approach to optimizing results would be to consider contributions of other loops and different amino acids from those loops to ligand selectivity. Data provided by this approach will not only be the first study of its kind, but in general, a great contribution to this area of research. Advances in protein and DNA manipulation now permit mutations to be constructed using commercial mutagenesis services to facilitate rapid production of mutations and save time. Mutant receptors could then be expressed and characterized, and mutant binding proteins would be evaluated via attachment to a sensor platform (e.g. SPA).

5.4.3 Acetylcholine-binding Protein from Other Species

This project utilized acetylcholine-binding protein (AChBP), a protein thought to be secreted into the synapse by the glia of certain snails (96) and the homolog of extracellular domain of nicotinic acetylcholine (nACh) receptors, from the great pond

snail *Lymnaea Stagnalis* (99). At the time of this project, two additional homologs of this protein had already been identified in the freshwater snail *Bulinus truncates (98)*, and sea hare *Aplysia californica* (111). Since that time, another mollusk, the abalone *Haliotis discus hannai* was shown to have a functional homologue of the AChBP (146), and a homologue of the AChBP from the pearl oyster *Pinctada fucat* was found to bind to calcium carbonate (147). Taken together, this trend raised the assumption that the AChBP was limited to the aquatic mollusks and phylum Mollusca. However, recent identification of the AChBP in other phyla has provided more information toward understanding this protein and its function. For example, the AChBP has been identified in the marine segmented worm *Capitella teleta* (148) from the phylum Annelid, and in spider (149), from the phylum Arthropoda. The amino acid sequence for the newly found AChBPs is approximately 30% identical with those of known molluscan AChBPs (148,149). These discoveries show the AChBP exists in different phyla, and that it has variation in the sequence, structure and function, which raises the question of whether the AChBP has phylum-specific amino acid sequence or structure. It will be of interest to compare the C-loop of both spider and segmented worm with the *L. Stagnalis* used in this project to find if they align better with the C-loop of the serotonin receptor. Furthermore, the entire amino acid sequence of the AChBP for spider and segmented worm could be compared with different LGIC receptors to ascertain if they offer a better alignment than the AChBPs in mollusks. The identification of AChBP in other phyla and analysis of their sequence and structure will provide additional information about critical residues for agonist and antagonist binding.

5.4.4 Development of other LGIC Binding Proteins

Members of the cys-loop LGICs, namely nicotinic acetylcholine (nACh), glycine, γ-aminobutyric acid (GABA), and 5-hydroxytryptamine type 3 (5-HT_3) receptors have been modeled based on the AChBP (9,93,113). These models have provided a wealth of useful information regarding binding site structure of the LGIC receptor family. Development, production and stability of the mutant cells in this project could be expanded to enable development of binding proteins for other cys-loop receptors. A long-term goal of this project could be to use the AChBP to develop soluble binding

protein by mutating the key amino acids involved in ligand selectivity in different LGIC receptors. This would be a focused project and the first of its kind, since such mutant constructs can serve to enhance the use of the soluble AChBP in the template-guided therapeutic design of novel agents for LGIC disorders (24-28,32), as well as allow for fast evaluation of new drugs that might interact with these receptors.

5.4.5 Biosensor Platforms

This project utilized the scintillation proximity assay (SPA) as its preferred method for evaluation of competitive ligands. SPA offers a low price assay that requires low quantity of protein and does not have any molecular weight limitations. The primary disadvantage of this method was use of a radioligand, as well as the requirement of the competing ligand to alter the binding affinity of the radioligand. This requirement prohibits discovery of novel compounds that may alter receptor function by non-competing mechanism. Nevertheless, the SPA experiments demonstrated its potential for high-throughput screening.

The ability of radioligand-free detection, sensitivity of the detection range, and scalability to allow multiple parallel detections are some of the important requirements for a future generation of biosensors. Two biosensor platforms that possess these criteria are surface plasmon resonance (SPR) and microcantilever (MC). The SPR and MC assays are chip-based assays have the advantage of not requiring a radioligand, requiring only small amounts of test compounds, and scalability to multiwall systems to speed analysis, and allowing the detection of binding to both orthosteric and allosteric binding sites (78,81). The SPR assay can obtain rate constants for both on-and-off rates, and older SPR approach could not determine kinetics for low molecular weight compounds due to its reliance on molecular weight detection, which was considered a major disadvantage of SPR ; however, current SPR approaches are sensitive to ligands with molecular weights as low as 90 kD (77,80).

Microcantilever-based biosensors have attracted much attention. They consist of a chip-based, label-free, real-time and highly sensitive approach to the detection of biomolecules. While not yet commercially available, much progress has been made in this field in recent years (81,118). Data shown in Chapter 3 demonstrates the viability

of using the AChBP to produce an active microcantilever sensor that can detect interaction of ligands with great sensitivity. Further development of this assay would permit rapid screening of multiple receptors at one time using a micro sensor array. The microcantilever system can be used to produce sensor arrays on a microchip containing in excess of 96 independent, addressable flow channels, and detection of microcantilever bending could be accomplished as integrated detection in the microchip. A significant finding of the microcantilever study is that the sensor detects conformational change in the binding protein, thus producing a larger bending for agonist ligands versus antagonists (118). This may provide a new way to obtain functional data. It seems likely that the modified AChBP proteins can be added to the detection arrays to permit evaluation of a single drug molecule on multiple receptors at the same time.

5.4.6 Protein Expression

As mentioned in previous chapters, some of the mutants in this project did not express any protein, and some like the chimera had a low yield that was too low to permit further experimentation. More recently, the important role of molecular chaperone proteins in LGIC assembly has become evident (150). Chaperone proteins, or molecular chaperones, are proteins that reversibly bind to the hydrophobic area of an unfolded, misfolded, or aggregated protein, and through cycles of binding and release help the protein attain its native and active conformation (151). In addition, since chaperone proteins are present in all cells, tissues and organs, they are also implicated in assisting proteins to translocate to their final destination (151). A new approach to the expression of chimeric AChBPs would be to use these molecular chaperone proteins to enhance expression of the AChBP constructs. Use of chaperone proteins could lead to increased production of the chimeric proteins, thus enabling purification, evaluation, and characterization of target protein.

Acetylcholine (ACh) receptor folding, assembly and trafficking in muscle and neurons are influenced by several chaperone proteins. The RIC-3 protein, a transmembrane protein resistant to inhibitors of cholinesterase is a much more selective chaperone for the α7-ACh receptor, which is the most abundant ACh receptor subtype

in the mammalian central nervous system (152). The RIC-3 protein was first identified in the nematode, *C.elegans*, as a protein necessary for synaptic transmission mediated by neuronal ACh receptors, but not by other LGICs (153). Homologs of the gene ric-3 have been identified, cloned and characterized in other species (e.g. insects (154), amphibians (155), mammalians (150)), and human RIC-3 is expressed in neurons and muscles (152,156), thus enabling its interactions with ACh receptors.

Co-immunoprecipitation studies have demonstrated the interaction between RIC-3 and the α7-ACh receptor subunit (157,158). It has been reported that RIC-3 increases α7 expression in HEK-293 and other mammalian cell lines (152,154,158,159), and that difficulties in the efficient expression of α7 in some cultured mammalian cell lines may be due to a requirement for the RIC-3 protein (157,160). Findings of Osman et al. (161) supported the view that RIC-3 regulates ACh receptor trafficking by increasing the number of mature or correctly folded receptor subunits reaching the cell surface. In addition, it has been shown that RIC-3 enhances functional expression of 5-HT_3 receptors in a human kidney cell line (159,162-164). It seems that with the exception of the 5-HT_3 receptor, RIC-3 appears to have little or no effect upon other LGICs, including those activated by GABA and glutamate (150,157,162,163). More recently, Kuryatov et al. (156) reported that RIC-3 alone is insufficient for optimal expression of functional α7; however, chemical chaperones (cholinergic ligands that can act as a pharmacological chaperone) can greatly increase the assembly, and upgrade the amount of functional α7 in a HEK-293 cell line that expressed both α7 and RIC-3.

Taken together, all collected data suggests that RIC-3 chaperone protein, and possibly some pharmacological chaperone, are required for the correct folding and expression of the α7-ACh and 5-HT_3 receptors. Therefore, it is possible that transfection of HEK-293 cells with both the AChBP DNA and RIC-3 protein might optimize protein expression of the wild-type protein in the stable cell line. The amount of protein produced from this experiment can be compared to the original protein concentration. If the results are positive, the same protocol could be extended to all the mutated DNAs, as well as the chimera to investigate effect of molecular chaperones on protein expression.

5.4.7 Protein Expression Systems

There are various protein expression systems such as bacterial (E. coli), yeast (S. cerevisiae), insect / baculovirus, or mammalian cells. This project utilized the HEK-293 cell line (human embryonic kidney cells), which is a mammalian cell expression system to generate mature protein (165) to be used with different biosensor platforms. The mammalian expression system allows post-translational modifications that can be important for the solubility and activity of the expressed protein (166) such as the AChBP; however, these expression systems are typically costly, time-consuming and more complex when compared to the other expression systems such as *E. coli* (167).

Bacterial protein expression systems are popular as bacteria are easy to culture and grow fast, but they are not capable of post-translational modifications (e.g. glycosylation) or molecular folding of the eukaryotic proteins (167). However, it was shown glycosylation was not important for binding properties of the AChBP (168), and that de-glycosylation was required to facilitate crystallization of the protein (101,111). With advances in the cell lines, fusion proteins and expression vectors, the *E. coli* expression systems have become an attractive option for the production of recombinant proteins (167,169), and most recently, an *E. coli* recombinant expression system capable of expressing the AChBPs in the soluble fractions was developed (170). Considering the AChBPs are routinely used for biophysical and structural studies, the recombinant expression system in *E. coli* offers a simpler, faster, cost-effective and high-throughput source of protein production when milligram quantities of soluble, stable and functional proteins are required.

The baculovirus-insect cell expression system is widely and routinely used for the production of recombinant proteins with modifications similar to mammalian cells (171,172). This expression system is based on the use of recombinant baculoviruses (insect viruses) and their ability to produce proteins in cultured insect cells or insect larvae. The genes in insect viruses can be replaced with foreign genes, thus converting the viruses into expression vectors which are then transfected into insect cells to produce recombinant proteins (173). Lin et al. (174) reported use of the baculovirus-insect cell expression system for high yield production of the AChBP proteins to be used for structural and functional studies. This expression system can be easily scaled up for

a more convenient and high-throughput expression of proteins that are more functionally similar to native mammalian proteins.

5.5 General Summary and Closing Remarks

Ligand-gated ion channels (LGICs) are crucial to the function of the peripheral and central nervous system, and have been implicated in learning and memory, fluid balance, appetite control, regulation of blood flow, and pain (22). Malfunctions of cys-loop LGICs, like the serotonin receptor (5-HT_3), are linked to various diseases and disorders including muscular dystrophies (23), central neurological disorders (e.g. autism, attention deficit hyperactivity) (24,25), neurodegenerative diseases (e.g. Alzheimer, Parkinson) (26-29), neuropsychiatric disorders (e.g. anxiety, depression, schizophrenia, epilepsy) (30,31), and nicotine, drug and alcohol addiction (32,33).

The specific goal of this project was to develop a molecular biosensor for serotonin through engineering a soluble, serotonin-binding protein that would mimic the serotonin protein. To accomplish this goal, we used a soluble acetylcholine-binding protein (AChBP) that is similar in sequence and structure to the membrane-bound LGIC family. Our approach used site-directed mutagenesis of the AChBP biding site, with the goal of increasing the affinity of the AChBP for serotonin ligands. Chapter 3 explored and confirmed the potential of the AChBP as a viable biosensor option, and Chapter 4 presented the results of select mutations of the AChBP and our success in this approach.

This project was a highly ambitious protein engineering project, since it was the first time the AChBP was being investigated as a potential biosensor molecule for development of a soluble homolog of a non-nicotinic LGIC receptor. Consequently, this project was unique and one of its kind, high risk and very difficult, but with potentially a high return as it focused on the development of biosensor proteins to be used in drug development. It provided valuable information regarding pharmacology of the AChBP as a potential biosensor molecule, as well as its interactions with 5-HT_3 receptor ligands, which was not previously available. By applying suggested strategies mentioned earlier in this chapter, we will be able to further identify key amino acids that are involved in selectivity, and reach the point of a viable serotonin biosensor. Once the

nature of selectivity in the serotonin receptor is discovered, this knowledge can be applied to other receptors, leading to the development of soluble LGIC biosensors. These soluble biosensors can be easily attached to biosensor surfaces and be utilized in high-throughput drug screening, drug development, ligand detection, and synthesis of new ligands which will contribute to human health. In addition, sensors of this type could be used for in-vitro, in-vivo, and environmental biosensor applications.

References

1. Nelson, D., and Cox, M. (2005) Lehninger Principles of Biochemistry, 4th ed. New York: W.H. Freeman and Company.
2. Cockcroft, V. B., Osguthorpe, D. J., Barnard, E. A., Friday, A. E., and Lunt, G. G. (1990) Ligand-gated ion channels. Homology and diversity. *Molecular neurobiology* **4**, 129-169
3. Barry, P. H., and Lynch, J. W. (2005) Ligand-gated channels. *IEEE transactions on nanobioscience* **4**, 70-80
4. Connolly, C. N., and Wafford, K. A. (2004) The Cys-loop superfamily of ligand-gated ion channels: the impact of receptor structure on function. *Biochemical Society transactions* **32**, 529-534
5. Nys, M., Kesters, D., and Ulens, C. (2013) Structural insights into Cys-loop receptor function and ligand recognition. *Biochemical pharmacology* **86**, 1042-1053
6. Maksay, G. (2009) Ligand-gated pentameric ion channels, from binding to gating. *Current molecular pharmacology* **2**, 253-262
7. Derkach, V., Surprenant, A., and North, R. A. (1989) 5-HT3 receptors are membrane ion channels. *Nature* **339**, 706-709
8. Barnes, N. M., Hales, T. G., Lummis, S. C., and Peters, J. A. (2009) The 5-HT3 receptor--the relationship between structure and function. *Neuropharmacology* **56**, 273-284
9. Reeves, D. C., and Lummis, S. C. (2002) The molecular basis of the structure and function of the 5-HT3 receptor: a model ligand-gated ion channel (review). *Molecular membrane biology* **19**, 11-26
10. Thompson, A. J., and Lummis, S. C. (2006) 5-HT3 receptors. *Current pharmaceutical design* **12**, 3615-3630
11. Gholipour, T., Ghasemi, M., Riazi, K., Ghaffarpour, M., and Dehpour, A. R. (2010) Seizure susceptibility alteration through 5-HT(3) receptor: modulation by nitric oxide. *Seizure* **19**, 17-22
12. Sanger, G. J. (2008) 5-hydroxytryptamine and the gastrointestinal tract: where next? *Trends in pharmacological sciences* **29**, 465-471
13. Thompson, A. J., and Lummis, S. C. (2007) The 5-HT3 receptor as a therapeutic target. *Expert opinion on therapeutic targets* **11**, 527-540
14. Bonhaus, D. W., Wong, E. H., Stefanich, E., Kunysz, E. A., and Eglen, R. M. (1993) Pharmacological characterization of 5-hydroxytryptamine3 receptors in murine brain and ileum using the novel radioligand [3H]RS-42358-197: evidence for receptor heterogeneity. *Journal of neurochemistry* **61**, 1927-1932
15. Walstab, J., Rappold, G., and Niesler, B. (2010) *5-HT(3) receptors: role in disease and target of drugs.* 128
16. Lummis, S. C. (2012) 5-HT(3) receptors. *The Journal of biological chemistry* **287**, 40239-40245
17. Wu, Z. S., Cheng, H., Jiang, Y., Melcher, K., and Xu, H. E. (2015) Ion channels gated by acetylcholine and serotonin: structures, biology, and drug discovery. *Acta Pharmacol Sin* **36**, 895-907

18. Suryanarayanan, A., Joshi, P. R., Bikadi, Z., Mani, M., Kulkarni, T. R., Gaines, C., and Schulte, M. K. (2005) The loop C region of the murine 5-HT3A receptor contributes to the differential actions of 5-hydroxytryptamine and m-chlorophenylbiguanide. *Biochemistry* **44**, 9140-9149
19. Venkataraman, P., Joshi, P., Venkatachalan, S. P., Muthalagi, M., Parihar, H. S., Kirschbaum, K. S., and Schulte, M. K. (2002) Functional group interactions of a 5-HT3R antagonist. *BMC biochemistry* **3**, 16
20. Joshi, P. R., Suryanarayanan, A., Hazai, E., Schulte, M. K., Maksay, G., and Bikadi, Z. (2006) Interactions of granisetron with an agonist-free 5-HT3A receptor model. *Biochemistry* **45**, 1099-1105
21. Venkataraman, P., Venkatachalan, S. P., Joshi, P. R., Muthalagi, M., and Schulte, M. K. (2002) Identification of critical residues in loop E in the 5-HT3ASR binding site. *BMC biochemistry* **3**, 15
22. Arias HR, E. (2006) *Biological and Biophysical Aspects of Ligand-Gated Ion Channel Receptor Superfamilies.*, Research Signpost, Kerela, India
23. Leite, P. E., Gandia, L., de Pascual, R., Nanclares, C., Colmena, I., Santos, W. C., Lagrota-Candido, J., and Quirico-Santos, T. (2014) Selective activation of alpha7 nicotinic acetylcholine receptor (nAChRalpha7) inhibits muscular degeneration in mdx dystrophic mice. *Brain research* **1573**, 27-36
24. Lippiello, P. M. (2006) Nicotinic cholinergic antagonists: a novel approach for the treatment of autism. *Medical hypotheses* **66**, 985-990
25. Levin, E. D., and Rezvani, A. H. (2002) Nicotinic treatment for cognitive dysfunction. *Current drug targets. CNS and neurological disorders* **1**, 423-431
26. Maelicke, A., Schrattenholz, A., Samochocki, M., Radina, M., and Albuquerque, E. X. (2000) Allosterically potentiating ligands of nicotinic receptors as a treatment strategy for Alzheimer's disease. *Behavioural brain research* **113**, 199-206
27. Guan, Z. Z., Zhang, X., Ravid, R., and Nordberg, A. (2000) Decreased protein levels of nicotinic receptor subunits in the hippocampus and temporal cortex of patients with Alzheimer's disease. *Journal of neurochemistry* **74**, 237-243
28. Rusted, J. M., Newhouse, P. A., and Levin, E. D. (2000) Nicotinic treatment for degenerative neuropsychiatric disorders such as Alzheimer's disease and Parkinson's disease. *Behavioural brain research* **113**, 121-129
29. Geldenhuys, W. J., and Van der Schyf, C. J. (2011) Role of serotonin in Alzheimer's disease: a new therapeutic target? *CNS drugs* **25**, 765-781
30. Mineur, Y. S., and Picciotto, M. R. (2010) Nicotine receptors and depression: revisiting and revising the cholinergic hypothesis. *Trends in pharmacological sciences* **31**, 580-586
31. Dukat, M., Alix, K., Worsham, J., Khatri, S., and Schulte, M. K. (2013) 2-Amino-6-chloro-3,4-dihydroquinazoline: A novel 5-HT3 receptor antagonist with antidepressant character. *Bioorganic & medicinal chemistry letters* **23**, 5945-5948
32. Diehl, A., Nakovics, H., Croissant, B., Smolka, M. N., Batra, A., and Mann, K. (2006) Galantamine reduces smoking in alcohol-dependent patients: a randomized, placebo-controlled trial. *International journal of clinical pharmacology and therapeutics* **44**, 614-622

33. Rahman, S., Engleman, E. A., and Bell, R. L. (2016) Recent Advances in Nicotinic Receptor Signaling in Alcohol Abuse and Alcoholism. *Progress in molecular biology and translational science* **137**, 183-201
34. Hughes, J. P., Rees, S., Kalindjian, S. B., and Philpott, K. L. (2011) Principles of early drug discovery. *Br J Pharmacol* **162**, 1239-1249
35. Warren, J. (2011) Drug discovery: lessons from evolution. *British journal of clinical pharmacology* **71**, 497-503
36. Swinney, D. C., and Anthony, J. (2011) How were new medicines discovered? *Nature reviews. Drug discovery* **10**, 507-519
37. Rask-Andersen, M., Almen, M. S., and Schioth, H. B. (2011) Trends in the exploitation of novel drug targets. *Nature reviews. Drug discovery* **10**, 579-590
38. Li, J. W., and Vederas, J. C. (2009) Drug discovery and natural products: end of an era or an endless frontier? *Science (New York, N.Y.)* **325**, 161-165
39. Baker, M. (2017) Deceptive curcumin offers cautionary tale for chemists. *Nature* **541**, 144-145
40. Chen, Y., de Bruyn Kops, C., and Kirchmair, J. (2017) Data Resources for the Computer-Guided Discovery of Bioactive Natural Products. *Journal of chemical information and modeling* **57**, 2099-2111
41. Schuster, D., and Wolber, G. (2010) Identification of bioactive natural products by pharmacophore-based virtual screening. *Current pharmaceutical design* **16**, 1666-1681
42. Newman, D. J., and Cragg, G. M. (2007) Natural products as sources of new drugs over the last 25 years. *Journal of natural products* **70**, 461-477
43. Feher, M., and Schmidt, J. M. (2003) Property distributions: differences between drugs, natural products, and molecules from combinatorial chemistry. *Journal of chemical information and computer sciences* **43**, 218-227
44. Gordeeva, E. V., Lushniknov, D. E., and Zefirov, N. S. (1992) COMPASS Program - An Original Semi-Emperical Approach To Computer-Assisted Synthesis. *Tetrahedron* **48**, 3789-3804
45. Rollinger, J. M., Stuppner, H., and Langer, T. (2008) Virtual screening for the discovery of bioactive natural products. *Progress in drug research. Fortschritte der Arzneimittelforschung. Progres des recherches pharmaceutiques* **65**, 211, 213-249
46. Hopkins, A. L., Groom, C. R., and Alex, A. (2004) Ligand efficiency: a useful metric for lead selection. *Drug Discovery Today* **9**, 430-431
47. Rester, U. (2008) From virtuality to reality - Virtual screening in lead discovery and lead optimization: a medicinal chemistry perspective. *Current opinion in drug discovery & development* **11**, 559-568
48. Silverman, E. (20 November 2014) What Does It Cost to Develop a New Drug? Latest Study Says $2.6 Billion., Wall Street Journal
49. DiMasi, J. A., Grabowski, H. G., and Hansen, R. W. (2016) Innovation in the pharmaceutical industry: New estimates of R&D costs. *Journal of health economics* **47**, 20-33
50. DiMasi, J. A., Grabowski, H. G., and Hansen, R. W. (2016) Innovation in the pharmaceutical industry: New estimates of R&D costs. *Journal of health economics* **47**, 20-33

51. Association, B. R. (2016) New Drug Development Process. California Biomedical Research Association
52. Zhu, T., Cao, S., Su, P. C., Patel, R., Shah, D., Chokshi, H. B., Szukala, R., Johnson, M. E., and Hevener, K. E. (2013) Hit identification and optimization in virtual screening: practical recommendations based on a critical literature analysis. *J Med Chem* **56**, 6560-6572
53. Research. (2017) Center for Drug Evaluation and Research. www.fda.gov
54. Caraus, I., Alsuwailem, A. A., Nadon, R., and Makarenkov, V. (2015) Detecting and overcoming systematic bias in high-throughput screening technologies: a comprehensive review of practical issues and methodological solutions. *Briefings in bioinformatics* **16**, 974-986
55. Szymanski, P., Markowicz, M., and Mikiciuk-Olasik, E. (2012) Adaptation of high-throughput screening in drug discovery-toxicological screening tests. *International journal of molecular sciences* **13**, 427-452
56. Dandapani, S., Rosse, G., Southall, N., Salvino, J. M., and Thomas, C. J. (2012) Selecting, Acquiring, and Using Small Molecule Libraries for High-Throughput Screening. *Current protocols in chemical biology* **4**, 177-191
57. Erlanson, D. A. (2012) Introduction to fragment-based drug discovery. *Topics in current chemistry* **317**, 1-32
58. Alex, A. A., and Flocco, M. M. (2007) Fragment-based drug discovery: what has it achieved so far? *Current topics in medicinal chemistry* **7**, 1544-1567
59. Huang, R., and Leung, I. K. (2016) Protein-Directed Dynamic Combinatorial Chemistry: A Guide to Protein Ligand and Inhibitor Discovery. *Molecules (Basel, Switzerland)* **21**
60. Mondal, M., and Hirsch, A. K. (2015) Dynamic combinatorial chemistry: a tool to facilitate the identification of inhibitors for protein targets. *Chemical Society reviews* **44**, 2455-2488
61. Caliandro, R., Belviso, D. B., Aresta, B. M., de Candia, M., and Altomare, C. D. (2013) Protein crystallography and fragment-based drug design. *Future medicinal chemistry* **5**, 1121-1140
62. Chilingaryan, Z., Yin, Z., and Oakley, A. J. (2012) Fragment-based screening by protein crystallography: successes and pitfalls. *International journal of molecular sciences* **13**, 12857-12879
63. Ferreira, L. G., and Andricopulo, A. D. (2017) From Protein Structure to Small-Molecules: Recent Advances and Applications to Fragment-Based Drug Discovery. *Current topics in medicinal chemistry* **17**, 2260-2270
64. Price, A. J., Howard, S., and Cons, B. D. (2017) Fragment-based drug discovery and its application to challenging drug targets. *Essays in biochemistry* **61**, 475-484
65. Herrmann, A. (2014) Dynamic combinatorial/covalent chemistry: a tool to read, generate and modulate the bioactivity of compounds and compound mixtures. *Chemical Society reviews* **43**, 1899-1933
66. Reddy, A. S., Pati, S. P., Kumar, P. P., Pradeep, H. N., and Sastry, G. N. (2007) Virtual screening in drug discovery -- a computational perspective. *Current protein & peptide science* **8**, 329-351

67. de Azevedo, W. F., Jr., and Dias, R. (2008) Computational methods for calculation of ligand-binding affinity. *Current drug targets* **9**, 1031-1039
68. Heck, G. S., Pintro, V. O., Pereira, R. R., de Avila, M. B., Levin, N. M. B., and de Azevedo, W. F. (2017) Supervised Machine Learning Methods Applied to Predict Ligand- Binding Affinity. *Current medicinal chemistry* **24**, 2459-2470
69. Barcellos, G. B., Pauli, I., Caceres, R. A., Timmers, L. F., Dias, R., and de Azevedo, W. F., Jr. (2008) Molecular modeling as a tool for drug discovery. *Current drug targets* **9**, 1084-1091
70. Durrant, J. D., and McCammon, J. A. (2011) Molecular dynamics simulations and drug discovery. *BMC biology* **9**, 71
71. Borhani, D. W., and Shaw, D. E. (2012) The future of molecular dynamics simulations in drug discovery. *Journal of computer-aided molecular design* **26**, 15-26
72. de Jong, L. A., Uges, D. R., Franke, J. P., and Bischoff, R. (2005) Receptor-ligand binding assays: technologies and applications. *Journal of chromatography. B, Analytical technologies in the biomedical and life sciences* **829**, 1-25
73. Auld, D. S., Farmen, M. W., Kahl, S. D., Kriauciunas, A., McKnight, K. L., Montrose, C., and Weidner, J. R. (2004) Receptor Binding Assays for HTS and Drug Discovery. in *Assay Guidance Manual* (Sittampalam, G. S., Coussens, N. P., Brimacombe, K., Grossman, A., Arkin, M., Auld, D., Austin, C., Baell, J., Bejcek, B., Chung, T. D. Y., Dahlin, J. L., Devanaryan, V., Foley, T. L., Glicksman, M., Hall, M. D., Hass, J. V., Inglese, J., Iversen, P. W., Kahl, S. D., Kales, S. C., Lal-Nag, M., Li, Z., McGee, J., McManus, O., Riss, T., Trask, O. J., Jr., Weidner, J. R., Xia, M., and Xu, X. eds.), Eli Lilly & Company and the National Center for Advancing Translational Sciences, Bethesda (MD). pp
74. Sittampalam, G. S., Kahl, S. D., and Janzen, W. P. (1997) High-throughput screening: advances in assay technologies. *Current opinion in chemical biology* **1**, 384-391
75. Rabinovitch, P. S., and Robinson, J. P. (2002) Overview of functional cell assays. *Current protocols in cytometry* **Chapter 9**, Unit 9.1
76. Papke, R. L., and Smith-Maxwell, C. (2009) High throughput electrophysiology with Xenopus oocytes. *Combinatorial chemistry & high throughput screening* **12**, 38-50
77. Olaru, A., Bala, C., Jaffrezic-Renault, N., and Aboul-Enein, H. Y. (2015) Surface plasmon resonance (SPR) biosensors in pharmaceutical analysis. *Critical reviews in analytical chemistry* **45**, 97-105
78. Hansen, K. M., and Thundat, T. (2005) Microcantilever biosensors. *Methods (San Diego, Calif.)* **37**, 57-64
79. Wu, S., and Liu, B. (2005) Application of scintillation proximity assay in drug discovery. *BioDrugs : clinical immunotherapeutics, biopharmaceuticals and gene therapy* **19**, 383-392
80. Maynard, J. A., Lindquist, N. C., Sutherland, J. N., Lesuffleur, A., Warrington, A. E., Rodriguez, M., and Oh, S. H. (2009) Surface plasmon resonance for high-throughput ligand screening of membrane-bound proteins. *Biotechnology journal* **4**, 1542-1558

81. Ji, H. F., Gao, H., Buchapudi, K. R., Yang, X., Xu, X., and Schulte, M. K. (2008) Microcantilever biosensors based on conformational change of proteins. *The Analyst* **133**, 434-443
82. Hirose, S. (2004) [Radioluminography and scintillation proximity assay for high-throughput screening]. *Tanpakushitsu kakusan koso. Protein, nucleic acid, enzyme* **49**, 1572-1575
83. Matias, V. R., and Beveridge, T. J. (2005) Cryo-electron microscopy reveals native polymeric cell wall structure in Bacillus subtilis 168 and the existence of a periplasmic space. *Mol Microbiol* **56**, 240-251
84. Zuber, B., Haenni, M., Ribeiro, T., Minnig, K., Lopes, F., Moreillon, P., and Dubochet, J. (2006) Granular layer in the periplasmic space of gram-positive bacteria and fine structures of Enterococcus gallinarum and Streptococcus gordonii septa revealed by cryo-electron microscopy of vitreous sections. *Journal of bacteriology* **188**, 6652-6660
85. Encyclopedia. (2003) Periplasm. in *World of Microbiology and Immunology*, Encyclopedia.com
86. Wulfing, C., and Pluckthun, A. (1994) Protein folding in the periplasm of Escherichia coli. *Mol Microbiol* **12**, 685-692
87. Mulligan, C., Fischer, M., and Thomas, G. H. (2011) Tripartite ATP-independent periplasmic (TRAP) transporters in bacteria and archaea. *FEMS microbiology reviews* **35**, 68-86
88. Ausili, A., Staiano, M., Dattelbaum, J., Varriale, A., Capo, A., and D'Auria, S. (2013) Periplasmic Binding Proteins in Thermophiles: Characterization and Potential Application of an Arginine-Binding Protein from Thermotoga maritima: A Brief Thermo-Story. *Life (Basel, Switzerland)* **3**, 149-160
89. Wiech, E. M., Cheng, H. P., and Singh, S. M. (2015) Molecular modeling and computational analyses suggests that the Sinorhizobium meliloti periplasmic regulator protein ExoR adopts a superhelical fold and is controlled by a unique mechanism of proteolysis. *Protein science : a publication of the Protein Society* **24**, 319-327
90. Schubert, T., and Romer, W. (2015) How synthetic membrane systems contribute to the understanding of lipid-driven endocytosis. *Biochimica et biophysica acta* **1853**, 2992-3005
91. Serebryany, E., Zhu, G. A., and Yan, E. C. Y. (2012) Artificial membrane-like environments for in vitro studies of purified G-protein coupled receptors. *Biochimica et Biophysica Acta (BBA) - Biomembranes* **1818**, 225-233
92. Rajesh, S., Knowles, T., and Overduin, M. (2011) Production of membrane proteins without cells or detergents. *New Biotechnology* **28**, 250-254
93. Sixma, T. K., and Smit, A. B. (2003) Acetylcholine binding protein (AChBP): a secreted glial protein that provides a high-resolution model for the extracellular domain of pentameric ligand-gated ion channels. *Annual review of biophysics and biomolecular structure* **32**, 311-334
94. Karlin, A. (2001) The acetylcholine-binding protein: 'What's in a name?'. *The pharmacogenomics journal* **1**, 221-223

95. Smit, A. B., Brejc, K., Syed, N., and Sixma, T. K. (2003) Structure and function of AChBP, homologue of the ligand-binding domain of the nicotinic acetylcholine receptor. *Annals of the New York Academy of Sciences* **998**, 81-92
96. Smit, A. B., Syed, N. I., Schaap, D., van Minnen, J., Klumperman, J., Kits, K. S., Lodder, H., van der Schors, R. C., van Elk, R., Sorgedrager, B., Brejc, K., Sixma, T. K., and Geraerts, W. P. (2001) A glia-derived acetylcholine-binding protein that modulates synaptic transmission. *Nature* **411**, 261-268
97. Hansen, S. B., Talley, T. T., Radic, Z., and Taylor, P. (2004) Structural and ligand recognition characteristics of an acetylcholine-binding protein from Aplysia californica. *The Journal of biological chemistry* **279**, 24197-24202
98. Celie, P. H., Klaassen, R. V., van Rossum-Fikkert, S. E., van Elk, R., van Nierop, P., Smit, A. B., and Sixma, T. K. (2005) Crystal structure of acetylcholine-binding protein from Bulinus truncatus reveals the conserved structural scaffold and sites of variation in nicotinic acetylcholine receptors. *The Journal of biological chemistry* **280**, 26457-26466
99. Brejc, K., van Dijk, W. J., Klaassen, R. V., Schuurmans, M., van Der Oost, J., Smit, A. B., and Sixma, T. K. (2001) Crystal structure of an ACh-binding protein reveals the ligand-binding domain of nicotinic receptors. *Nature* **411**, 269-276
100. Harel, M., Kasher, R., Nicolas, A., Guss, J. M., Balass, M., Fridkin, M., Smit, A. B., Brejc, K., Sixma, T. K., Katchalski-Katzir, E., Sussman, J. L., and Fuchs, S. (2001) The binding site of acetylcholine receptor as visualized in the X-Ray structure of a complex between alpha-bungarotoxin and a mimotope peptide. *Neuron* **32**, 265-275
101. Celie, P. H., van Rossum-Fikkert, S. E., van Dijk, W. J., Brejc, K., Smit, A. B., and Sixma, T. K. (2004) Nicotine and carbamylcholine binding to nicotinic acetylcholine receptors as studied in AChBP crystal structures. *Neuron* **41**, 907-914
102. Harrison, N. J., and Lummis, S. C. (2006) Molecular modeling of the GABA(C) receptor ligand-binding domain. *Journal of molecular modeling* **12**, 317-324
103. Reeves, D. C., Sayed, M. F., Chau, P. L., Price, K. L., and Lummis, S. C. (2003) Prediction of 5-HT3 receptor agonist-binding residues using homology modeling. *Biophysical journal* **84**, 2338-2344
104. Smit, A. B., Celie, P. H., Kasheverov, I. E., Mordvintsev, D. Y., van Nierop, P., Bertrand, D., Tsetlin, V., and Sixma, T. K. (2006) Acetylcholine-binding proteins: functional and structural homologs of nicotinic acetylcholine receptors. *Journal of molecular neuroscience : MN* **30**, 9-10
105. Costa, V., Nistri, A., Cavalli, A., and Carloni, P. (2003) A structural model of agonist binding to the alpha3beta4 neuronal nicotinic receptor. *Br J Pharmacol* **140**, 921-931
106. Bouzat, C., Gumilar, F., Spitzmaul, G., Wang, H. L., Rayes, D., Hansen, S. B., Taylor, P., and Sine, S. M. (2004) Coupling of agonist binding to channel gating in an ACh-binding protein linked to an ion channel. *Nature* **430**, 896-900
107. Nemecz, A., and Taylor, P. (2011) Creating an alpha7 nicotinic acetylcholine recognition domain from the acetylcholine-binding protein: crystallographic and ligand selectivity analyses. *The Journal of biological chemistry* **286**, 42555-42565

108. Li, S. X., Huang, S., Bren, N., Noridomi, K., Dellisanti, C. D., Sine, S. M., and Chen, L. (2011) Ligand-binding domain of an alpha7-nicotinic receptor chimera and its complex with agonist. *Nature neuroscience* **14**, 1253-1259
109. Araoz, R., Vilarino, N., Botana, L. M., and Molgo, J. (2010) Ligand-binding assays for cyanobacterial neurotoxins targeting cholinergic receptors. *Analytical and bioanalytical chemistry* **397**, 1695-1704
110. Julie Evans, M. L., Gerard Brophy, Maxine Beveridge, Albert Santos. (2009) Use of Copper-loaded His-tag Beads in the Scintillation Proximity Assay. Amersham England, www.perkinelmer.com
111. Hansen, S. B., Sulzenbacher, G., Huxford, T., Marchot, P., Taylor, P., and Bourne, Y. (2005) Structures of Aplysia AChBP complexes with nicotinic agonists and antagonists reveal distinctive binding interfaces and conformations. *The EMBO journal* **24**, 3635-3646
112. Olsen, J. A., Balle, T., Gajhede, M., Ahring, P. K., and Kastrup, J. S. (2014) Molecular recognition of the neurotransmitter acetylcholine by an acetylcholine binding protein reveals determinants of binding to nicotinic acetylcholine receptors. *PloS one* **9**, e91232
113. Harms-Smyth, A. (2008) *The Acetylcholine Binding Protein of Lymnaea Stagnalis as a Biosensor and Model for Ligand Gated Ion Channel Proteins.* Master's Thesis, University of Alaska Fairbanks
114. Taylor, P., Talley, T. T., Radic, Z., Hansen, S. B., Hibbs, R. E., and Shi, J. (2007) Structure-guided drug design: conferring selectivity among neuronal nicotinic receptor and acetylcholine-binding protein subtypes. *Biochemical pharmacology* **74**, 1164-1171
115. Thompson, A. J., Padgett, C. L., and Lummis, S. C. (2006) Mutagenesis and molecular modeling reveal the importance of the 5-HT3 receptor F-loop. *The Journal of biological chemistry* **281**, 16576-16582
116. Hansen, S. B., Radic, Z., Talley, T. T., Molles, B. E., Deerinck, T., Tsigelny, I., and Taylor, P. (2002) Tryptophan fluorescence reveals conformational changes in the acetylcholine binding protein. *The Journal of biological chemistry* **277**, 41299-41302
117. Berry, J., Price-Jones, M., and Killian, B. (2012) Use of scintillation proximity assay to measure radioligand binding to immobilized receptors without separation of bound from free ligand. *Methods in molecular biology (Clifton, N.J.)* **897**, 79-94
118. Buchapudi, K., Xu, X., Ataian, Y., Ji, H. F., and Schulte, M. (2012) Micromechanical measurement of AChBP binding for label-free drug discovery. *The Analyst* **137**, 263-268
119. Hibbs, R. E., Sulzenbacher, G., Shi, J., Talley, T. T., Conrod, S., Kem, W. R., Taylor, P., Marchot, P., and Bourne, Y. (2009) Structural determinants for interaction of partial agonists with acetylcholine binding protein and neuronal alpha7 nicotinic acetylcholine receptor. *The EMBO journal* **28**, 3040-3051
120. Kesters, D., Thompson, A. J., Brams, M., van Elk, R., Spurny, R., Geitmann, M., Villalgordo, J. M., Guskov, A., Danielson, U. H., Lummis, S. C., Smit, A. B., and Ulens, C. (2013) Structural basis of ligand recognition in 5-HT3 receptors. *EMBO reports* **14**, 49-56

121. Gee, V. J., Kracun, S., Cooper, S. T., Gibb, A. J., and Millar, N. S. (2007) Identification of domains influencing assembly and ion channel properties in alpha 7 nicotinic receptor and 5-HT3 receptor subunit chimaeras. *Br J Pharmacol* **152**, 501-512
122. Van Ryckeghem, F., and Van Belle, S. (2010) Management of chemotherapy-induced nausea and vomiting. *Acta clinica Belgica* **65**, 305-310
123. Stahl, S. M., Lee-Zimmerman, C., Cartwright, S., and Morrissette, D. A. (2013) Serotonergic drugs for depression and beyond. *Current drug targets* **14**, 578-585
124. Joshi, P. (2005) *Structure-function studies of the serotonin type-3 receptor ligand-binding domain*, University of Alaska, Fairbanks
125. Maksay, G., Bikadi, Z., and Simonyi, M. (2003) Binding interactions of antagonists with 5-hydroxytryptamine3A receptor models. *Journal of receptor and signal transduction research* **23**, 255-270
126. Van Arnam, E. B., and Dougherty, D. A. (2014) Functional probes of drug-receptor interactions implicated by structural studies: Cys-loop receptors provide a fertile testing ground. *J Med Chem* **57**, 6289-6300
127. Hazai, E., Joshi, P., Skoviak, E. C., Suryanarayanan, A., Schulte, M. K., and Bikadi, Z. (2009) A comprehensive study on the 5-hydroxytryptamine(3A) receptor binding of agonists serotonin and m-chlorophenylbiguanidine. *Bioorganic & medicinal chemistry* **17**, 5796-5805
128. Akk, G. (2001) Aromatics at the murine nicotinic receptor agonist binding site: mutational analysis of the alphaY93 and alphaW149 residues. *The Journal of physiology* **535**, 729-740
129. Thompson, A. J., Price, K. L., Reeves, D. C., Chan, S. L., Chau, P. L., and Lummis, S. C. (2005) Locating an antagonist in the 5-HT3 receptor binding site using modeling and radioligand binding. *The Journal of biological chemistry* **280**, 20476-20482
130. Spier, A. D., and Lummis, S. C. (2000) The role of tryptophan residues in the 5-Hydroxytryptamine(3) receptor ligand binding domain. *The Journal of biological chemistry* **275**, 5620-5625
131. Yan, D., Schulte, M. K., Bloom, K. E., and White, M. M. (1999) Structural features of the ligand-binding domain of the serotonin 5HT3 receptor. *The Journal of biological chemistry* **274**, 5537-5541
132. Spier, A. D., and Lummis, S. C. (2002) Immunological characterization of 5-HT3 receptor transmembrane topology. *Journal of molecular neuroscience : MN* **18**, 169-178
133. Deane, C. M., and Lummis, S. C. (2001) The role and predicted propensity of conserved proline residues in the 5-HT3 receptor. *The Journal of biological chemistry* **276**, 37962-37966
134. Price, K. L., Bower, K. S., Thompson, A. J., Lester, H. A., Dougherty, D. A., and Lummis, S. C. (2008) A hydrogen bond in loop A is critical for the binding and function of the 5-HT3 receptor. *Biochemistry* **47**, 6370-6377
135. Beene, D. L., Brandt, G. S., Zhong, W., Zacharias, N. M., Lester, H. A., and Dougherty, D. A. (2002) Cation-pi interactions in ligand recognition by serotonergic (5-HT3A) and nicotinic acetylcholine receptors: the anomalous binding properties of nicotine. *Biochemistry* **41**, 10262-10269

136. Amin, J., and Weiss, D. S. (1993) GABAA receptor needs two homologous domains of the beta-subunit for activation by GABA but not by pentobarbital. *Nature* **366**, 565-569
137. Schmieden, V., Kuhse, J., and Betz, H. (1993) Mutation of glycine receptor subunit creates beta-alanine receptor responsive to GABA. *Science (New York, N.Y.)* **262**, 256-258
138. Thompson, A. J., Lochner, M., and Lummis, S. C. (2008) Loop B is a major structural component of the 5-HT3 receptor. *Biophysical journal* **95**, 5728-5736
139. Mochizuki, S., Miyake, A., and Furuichi, K. (1999) Ion permeation properties of a cloned human 5-HT3 receptor transiently expressed in HEK 293 cells. *Amino acids* **17**, 243-255
140. Beene, D. L., Price, K. L., Lester, H. A., Dougherty, D. A., and Lummis, S. C. (2004) Tyrosine residues that control binding and gating in the 5-hydroxytryptamine3 receptor revealed by unnatural amino acid mutagenesis. *The Journal of neuroscience : the official journal of the Society for Neuroscience* **24**, 9097-9104
141. Price, K. L., and Lummis, S. C. (2004) The role of tyrosine residues in the extracellular domain of the 5-hydroxytryptamine3 receptor. *The Journal of biological chemistry* **279**, 23294-23301
142. Xu, M., Zhu, X., Yu, J., Yu, J., Luo, S., and Wang, X. (2017) The crystal structure of Ac-AChBP in complex with alpha-conotoxin LvIA reveals the mechanism of its selectivity towards different nAChR subtypes. *Protein & cell* **8**, 675-685
143. Xie, Y., and Cohen, J. B. (2001) Contributions of Torpedo nicotinic acetylcholine receptor gamma Trp-55 and delta Trp-57 to agonist and competitive antagonist function. *The Journal of biological chemistry* **276**, 2417-2426
144. Akk, G. (2002) Contributions of the non-alpha subunit residues (loop D) to agonist binding and channel gating in the muscle nicotinic acetylcholine receptor. *The Journal of physiology* **544**, 695-705
145. Kovac, A. L. (2016) Comparative Pharmacology and Guide to the Use of the Serotonin 5-HT3 Receptor Antagonists for Postoperative Nausea and Vomiting. *Drugs* **76**, 1719-1735
146. Huang, J., Wang, H., Cui, Y., Zhang, G., Zheng, G., Liu, S., Xie, L., and Zhang, R. (2009) Identification and comparison of amorphous calcium carbonate-binding protein and acetylcholine-binding protein in the abalone, Haliotis discus hannai. *Marine biotechnology (New York, N.Y.)* **11**, 596-607
147. Ma, Z., Huang, J., Sun, J., Wang, G., Li, C., Xie, L., and Zhang, R. (2007) A novel extrapallial fluid protein controls the morphology of nacre lamellae in the pearl oyster, Pinctada fucata. *The Journal of biological chemistry* **282**, 23253-23263
148. McCormack, T., Petrovich, R. M., Mercier, K. A., DeRose, E. F., Cuneo, M. J., Williams, J., Johnson, K. L., Lamb, P. W., London, R. E., and Yakel, J. L. (2010) Identification and functional characterization of a novel acetylcholine-binding protein from the marine annelid Capitella teleta. *Biochemistry* **49**, 2279-2287
149. Liu, H., French, A. S., and Torkkeli, P. H. (2017) Expression of Cys-loop receptor subunits and acetylcholine binding protein in the mechanosensory neurons, glial

cells, and muscle tissue of the spider Cupiennius salei. *The Journal of comparative neurology* **525**, 1139-1154
150. Halevi, S., Yassin, L., Eshel, M., Sala, F., Sala, S., Criado, M., and Treinin, M. (2003) Conservation within the RIC-3 gene family. Effectors of mammalian nicotinic acetylcholine receptor expression. *The Journal of biological chemistry* **278**, 34411-34417
151. Schonfelder, J., Alonso-Caballero, A., De Sancho, D., and Perez-Jimenez, R. (2018) The life of proteins under mechanical force. *Chemical Society reviews*
152. Millar, N. S. (2008) RIC-3: a nicotinic acetylcholine receptor chaperone. *Br J Pharmacol* **153 Suppl 1**, S177-183
153. Halevi, S., McKay, J., Palfreyman, M., Yassin, L., Eshel, M., Jorgensen, E., and Treinin, M. (2002) The C. elegans ric-3 gene is required for maturation of nicotinic acetylcholine receptors. *The EMBO journal* **21**, 1012-1020
154. Lansdell, S. J., Collins, T., Yabe, A., Gee, V. J., Gibb, A. J., and Millar, N. S. (2008) Host-cell specific effects of the nicotinic acetylcholine receptor chaperone RIC-3 revealed by a comparison of human and Drosophila RIC-3 homologues. *Journal of neurochemistry* **105**, 1573-1581
155. Bennett, H. M., Lees, K., Harper, K. M., Jones, A. K., Sattelle, D. B., Wonnacott, S., and Wolstenholme, A. J. (2012) Xenopus laevis RIC-3 enhances the functional expression of the C. elegans homomeric nicotinic receptor, ACR-16, in Xenopus oocytes. *Journal of neurochemistry* **123**, 911-918
156. Kuryatov, A., Mukherjee, J., and Lindstrom, J. (2013) Chemical chaperones exceed the chaperone effects of RIC-3 in promoting assembly of functional alpha7 AChRs. *PloS one* **8**, e62246
157. Lansdell, S. J., Gee, V. J., Harkness, P. C., Doward, A. I., Baker, E. R., Gibb, A. J., and Millar, N. S. (2005) RIC-3 enhances functional expression of multiple nicotinic acetylcholine receptor subtypes in mammalian cells. *Molecular pharmacology* **68**, 1431-1438
158. Williams, M. E., Burton, B., Urrutia, A., Shcherbatko, A., Chavez-Noriega, L. E., Cohen, C. J., and Aiyar, J. (2005) Ric-3 promotes functional expression of the nicotinic acetylcholine receptor alpha7 subunit in mammalian cells. *The Journal of biological chemistry* **280**, 1257-1263
159. Roncarati, R., Seredenina, T., Jow, B., Jow, F., Papini, S., Kramer, A., Bothmann, H., Dunlop, J., and Terstappen, G. C. (2008) Functional properties of alpha7 nicotinic acetylcholine receptors co-expressed with RIC-3 in a stable recombinant CHO-K1 cell line. *Assay and drug development technologies* **6**, 181-193
160. Castillo, M., Mulet, J., Gutierrez, L. M., Ortiz, J. A., Castelan, F., Gerber, S., Sala, S., Sala, F., and Criado, M. (2005) Dual role of the RIC-3 protein in trafficking of serotonin and nicotinic acetylcholine receptors. *The Journal of biological chemistry* **280**, 27062-27068
161. Osman, A. A., Schrader, A. D., Hawkes, A. J., Akil, O., Bergeron, A., Lustig, L. R., and Simmons, D. D. (2008) Muscle-like nicotinic receptor accessory molecules in sensory hair cells of the inner ear. *Molecular and cellular neurosciences* **38**, 153-169

162. Cheng, A., McDonald, N. A., and Connolly, C. N. (2005) Cell surface expression of 5-hydroxytryptamine type 3 receptors is promoted by RIC-3. *The Journal of biological chemistry* **280**, 22502-22507
163. Cheng, A., Bollan, K. A., Greenwood, S. M., Irving, A. J., and Connolly, C. N. (2007) Differential subcellular localization of RIC-3 isoforms and their role in determining 5-HT3 receptor composition. *The Journal of biological chemistry* **282**, 26158-26166
164. Walstab, J., Hammer, C., Lasitschka, F., Moller, D., Connolly, C. N., Rappold, G., Bruss, M., Bonisch, H., and Niesler, B. (2010) RIC-3 exclusively enhances the surface expression of human homomeric 5-hydroxytryptamine type 3A (5-HT3A) receptors despite direct interactions with 5-HT3A, -C, -D, and -E subunits. *The Journal of biological chemistry* **285**, 26956-26965
165. Thomas, P., and Smart, T. G. (2005) HEK293 cell line: a vehicle for the expression of recombinant proteins. *Journal of pharmacological and toxicological methods* **51**, 187-200
166. Mitra, N., Sinha, S., Ramya, T. N., and Surolia, A. (2006) N-linked oligosaccharides as outfitters for glycoprotein folding, form and function. *Trends in biochemical sciences* **31**, 156-163
167. Rosano, G. L., and Ceccarelli, E. A. (2014) Recombinant protein expression in Escherichia coli: advances and challenges. *Frontiers in microbiology* **5**, 172
168. Dyson, M. R., Shadbolt, S. P., Vincent, K. J., Perera, R. L., and McCafferty, J. (2004) Production of soluble mammalian proteins in Escherichia coli: identification of protein features that correlate with successful expression. *BMC biotechnology* **4**, 32
169. Chen, R. (2012) Bacterial expression systems for recombinant protein production: E. coli and beyond. *Biotechnology advances* **30**, 1102-1107
170. Abraham, N., Paul, B., Ragnarsson, L., and Lewis, R. J. (2016) Escherichia coli Protein Expression System for Acetylcholine Binding Proteins (AChBPs). *PloS one* **11**, e0157363
171. Contreras-Gomez, A., Sanchez-Miron, A., Garcia-Camacho, F., Molina-Grima, E., and Chisti, Y. (2014) Protein production using the baculovirus-insect cell expression system. *Biotechnology progress* **30**, 1-18
172. Jarvis, D. L. (2009) Baculovirus-insect cell expression systems. *Methods in enzymology* **463**, 191-222
173. van Oers, M. M., Pijlman, G. P., and Vlak, J. M. (2015) Thirty years of baculovirus-insect cell protein expression: from dark horse to mainstream technology. *The Journal of general virology* **96**, 6-23
174. Lin, B., Meng, H., Bing, H., Zhangsun, D., and Luo, S. (2014) Efficient expression of acetylcholine-binding protein from Aplysia californica in Bac-to-Bac system. *BioMed research international* **2014**, 691480